CHARACTERIZATION OF WELDABILITY OF SCANDIUM INOCULATED Al-Zn-Mg ALLOY

A DISSERTATION

Submitted in partial fulfillment of the requirements for the award of the degree of

MASTER OF TECHNOLOGY

in

METALLURGICAL AND MATERIALS ENGINEERING

(With Specialization in Corrosion Engineering)

By

AMIT MUKE

DEPARTMENT OF METALLURGICAL AND MATERIALS ENGINEERING

INDIAN INSTITUTE OF TECHNOLOGY ROORKEE

ROORKEE - 247 667 (INDIA)

JUNE, 2011

INDIAN INSTITUTE OF TECHNOLOGY ROORKEE

CANDIDATE'S DECLARATION

I hereby declare that the work carried out in this dissertation entitled **"CHARACTERIZATION OF WELDABILITY OF SCANDIUM INOCULATED Al-Zn-Mg ALLOY"** is presented on behalf of partial fulfillment of the requirements for the award of the degree of **Master of Technology in Corrosion Engineering** and is submitted to the **Department of Metallurgical & Materials Engineering, Indian Institute of Technology Roorkee, India** under the supervision of Dr.P.K.Ghosh, Professor, Dr. V.Pancholi, Assistant Professor, Department of Metallurgical & Materials Engineering, Indian Institute of Technology Roorkee, India.

The matter embodied in this dissertation has not been submitted by me for the award of any other degree of this institute or any other institute.

Dated: 30th June 2011

Place: IIT Roorkee **(AMIT MUKE)**

CERTIFICATION

This is to certify that the above statement made by the candidate is correct to the best of my knowledge.

Dr. P.K.Ghosh
Professor

Dr.V.Pancholi
Assistant Professor

Department of Metallurgical and Materials Engineering
Indian Institute of Technology Roorkee
Roorkee – 247667

ACKNOWLEDGEMENT

On successful completion of my dissertation, I Amit Muke, hereby, take this opportunity to express my gratitude towards all the generous people involved directly or indirectly in this accomplishment.

I cannot express in few words gratitude towards **Dr.P.K. Ghosh**, Professor and **Dr. V.Pancholi**, Assistant Professor at MMED, IIT Roorkee who provided valuable guidance and direction by keeping time aside for me from his highly engaged schedule. I am thankful for their guidance and fruitful discussions, as and when I needed from the inception of the dissertation to its successful completion.

I am greatful to Dr. Mukesh Bharadwaj who not only encouraged me to take up this dissertation work but also motivated me during the course of this work.

I would also like to thank head **Institute Instrumentation Centre (IIC)** to allow me to avail the facilities needed for the completion of this project work.

I can't forget Mr.P. Mondol, research scholar MMED, IIT Roorkee for his kind support, motivation and extremely useful suggestions during the course of this dissertation work.

My special thanks is to the laboratory incharge and assistants of **Metallography lab, Materials Testing Lab, Metal forming lab and Materials Joining Lab** for providing me the facilities as and when I needed.

Last but not the least I would like to thank all my friends and colleagues and my family for their support and timely help.

Muke

AMIT MUKE

Place: Roorkee

Date: 30/06/2011

ABSTRACT

The high strength aluminum alloys hold significant share in the worldwide usage of light alloys. The Al-Zn-Mg alloys in particular which come under the 7xxx series of aluminum alloys have special high strength characteristics. Their usage in construction of light armored vehicles, light weight bridges, and other components like fuselage in fighter crafts which demand for high strength to weight ratio, have earned these alloys a special recognition among the light alloys. Although, they have the highest mechanical properties among all the aluminum alloys and provide superior ballistic protection, they suffer few drawbacks especially in terms of welding. The material has stress corrosion cracking issues in both parent metal and weld joint.

Most of the industries prefer cost effective conventional welding processes like GTAW and GMAW for the purpose of welding these alloys. The variant of the GMAW process in which pulse current is used, also called Pulse GMAW process, have been reported to successfully weld these alloys.

In the present work, the characterization of the weldability of Al-Zn-Mg alloys by making alloy modification i.e. Scandium inoculation and controlling the pulse parameters of the pulse GMAW process was attempted in order to improve the properties in terms of metallurgical and mechanical context, especially in the weld zone and the adjacent HAZ. Different parameters like voltage, peak current, pulse on time, frequency, heat input etc were suitably chosen and then executed on the forged cum heat treated material. The metallurgical as well as mechanical properties were studied by analyzing the weld specimens through standard testing and measurement solutions viz. microstructure analysis, weld geometry analysis, weld dilution analysis, porosity analysis, hardness measurement, etc. Critical reasoning and analysis of the results was done in order to achieve the objective of characterization of weldability of Sc inoculated Al-Zn-Mg alloy.

LIST OF TABLES

LIST OF FIGURES

TABLE OF CONTENTS

Chapter 1: Introduction

Aluminum & its alloys are one of the most widely used non-ferrous materials for structural as well as for non-structural applications with most of its applications being aerospace , automotive, canning centric, just next to ferrous alloys, mainly due to its variety of properties viz. low density, high strength to weight ratio, electrical conductivity, thermal conductivity, malleability, ductility, corrosion resistance, etc. that can be achieved through various economical processing routes like die casting , sand casting, forging & rolling, age hardening, mechanical alloying, solutionising heat treatment, precipitation heat treatment etc.

Among these Al-alloys, 7xxx series Al-alloys have special place due to their high strength to weight ratio characteristics. These series of alloys contain zinc in the range of 1-8 % along with a small addition of magnesium, which gives them characteristic heat treatability resulting in moderate to high strength breed of Al-alloys. Other alloying elements like copper, lithium, scandium, zirconium etc. impart different characteristic properties based on their weight percentage addition. These alloys are mainly used in the following forms: Flat-rolled products (sheets & plates); Shapes; Forgings; Tubular products.

These 7xxx series alloys not only show significant rise in strength with increase in magnesium content but it also results in increase in brittleness. Also, there are lot of metallurgical issues pertaining to the control of weldability of these aluminum alloys.

Many researchers have developed different alloys suited for specific applications e.g. Alclad 7178 for aircraft & its structures, etc. A small addition of Scandium enhances the mechanical & metallurgical properties of the Al-alloys due to its strong inoculation characteristics of the cast grain structure. Also, Sc has significant recrystallization suppression property along with age hardening characteristics [12-15]. Welding can be effectively used to fabricate the aircraft structures made out of these alloys provided the technology used is up to certain optimum standards to guarantee the weld quality.

Welded structures are preferred over mechanical fastened structures due to weight saving along with the absence of the gap between the joining members, thereby reducing the problems associated with the entrapped media. In order to produce sound weld there is a need to find & develop synergy point between different welding variables (bead width, filler & joint configuration) to certify the soundness of the weld along with desired micro- structural & mechanical properties.

MIG (Metal Inet Gas) welding is used for joining various ferrous & non-ferrous materials. During continuous current GMAW (Gas Metal Arc Welding), it has been observed that weldment properties are highly sensitive to the welding parameters. Welding becomes difficult when the heat input exceeds beyond or falls below a certain critical value. By using pulsed current GMAW process, welding can be performed at much lower currents & also at high rate as compared to continuous current welding at the same current level. In pulsed current GMAW, the control of parameters such as the mean current, peak current, background current, pulse off & on time & frequency are very important as they can significantly affect the weld quality measured in terms of weld geometry, porosity content, microstructure, mechanical properties etc. The weldability issues and various welding procedures and the related data have been documented and studied for various conventional Al-alloys but data regarding pulse GMAW on experimental alloys of 7xxx series with scandium inoculation is scant.

In this study, an attempt has been made to characterize the weldability of experimentally developed scandium inoculated Al-Zn-Mg alloy, using pulse GMAW process. The welding of the different alloy compositions was performed at different welding parameters. The effect of heat input on the mechanical properties like hardness has been noted. Study has been carried out to analyze the influence of the heat input on metallurgical properties viz. weld bead geometry, dilution, porosity content & microstructure, on welded samples by continuous current GMAW & pulsed current GMAW processes. Based on the results, the study revealed that a significant amount of strengthening has been achieved in the HAZ region based on the different welding parameters & scandium weight % used in experimental alloys which is otherwise a very weak section & is responsible for most of the failure in welded structures.

Chapter 2: Literature Review

2.1 Light Alloys:

Light alloys fundamentally refer to characteristic high strength to weight ratio feature which makes them attractive for automobile and aerospace applications. Titanium, aluminum and magnesium and their alloys come under the purview of light alloys. Among them, titanium is expensive to extract and also possess the oxidation characteristic at low temperature, while aluminum and its alloys have limited temperature capability. Magnesium and its alloys have low strength, low stiffness, poor corrosion resistance, poor formability and formation of strong texture. Among aluminum and its alloys some are vital for aerospace application due to their fundamental properties like high thermal conductivity, high ductility(with some exceptions in 7xxx series Al-Alloys), moderate machinability, excellent corrosion resistance etc. makes them one of the most sought after materials for industrial application and center of attraction for researchers to enhance their properties and there by enlarge their usage in various applications.

2.2 Al-Zn-Mg alloys and effect of scandium inoculation:

2.2.1 Introduction:

- Aluminum alloys in which zinc and magnesium are the key alloying elements (7xxx series) are striking amongst the commercially available aluminum alloys due to their ability to get age hardened to the strengths that cannot be produced in other aluminum alloys (Table 1).
- Two key classes of the 7xxx series Al alloys have been in use for some time. The lofty mechanical properties have been extensively used in the aircraft industry wherever high strength to weight ratio is of significance. The range of high strength aircraft alloys normally contains major alloying elements viz. 4.3-6.8% zinc, 2.5-3.3% magnesium, 0.5-2.0% copper, and minor additions (less than 1%), of chromium, manganese, and zirconium. The weldable alloys have restricted alloying contents like zinc 4.0-5.0%, magnesium 1.4-2.0% and copper 0.2% maximum. Minor alloy additions of chromium, manganese or zirconium may be permitted. As the amount of alloy addition

decreases in the weldable alloys, this results into the reduction in maximum strength attainable otherwise. Hence, they are normally referred to as medium strength 7xxx series Al alloys.

- Recently, there has been increased demand in the military wings for materials with high strength to weight ratio properties as their usage will significantly reduce the cost pertaining to transportation and manpower mobilization like in case of the light armored trucks used by US military- code named Humvee.
- High strength Al alloys have advantage over the high strength steels in respect that for the equal strength, a member is thicker, stiffer and more robust.
- 7xxx series alloys have excellent ballistic defense against all types of attacks compared to other aluminum alloys and have inherent advantage of high strength to weight ratio over the steel armor of same strength.
- The distinctive feature of weldable medium strength 7xxx series alloy is its ability of the HAZ region and the weld zone to age naturally with almost recovery of 80% strength of the base metal.

2.2.2 Physical metallurgical aspects:

a) Strengthening mechanisms:

The physical metallurgy concerned with the 7xxx series has been discussed and reviewed[3] in depth since the initial work reported by Eger[4], Sander and Meissener [5]. A necessary property of a precipitation hardening alloy system is a temperature dependent equilibrium solid solubility characterized by increasing solubility with increasing temperatures. Above the solvus temperatures, the alloying elements are completely dragged into solid solution. Below the solvus line, a supersaturated sold solution exists and precipitation takes place by solid state precipitation mechanism. The nature and dispersion of the second phase precipitates determines the degree of hardenability.

b) The different precipitation reactions which may occur during the decomposition of this supersaturated solid solution have been looked into by Ryum [6]:

1. **Solid solution → η ($MgZn_2$) precipitates:**
   The equilibrium phase existing in the alloys with composition containing Zn from 4 to 6 % and Mg from 1 to 3 % is η ($MgZn_2$). The equilibrium phase just above 200 °C is T(Al, $Zn_{48}Mg_{32}$). The activation energy for this reaction is high and results into homogenous nucleation

with low precipitate density which takes place after long aging periods, eg. 12 days, at 150 °C. At temperatures above 145 °C, the heterogeneous precipitation takes place on the grain boundaries and small intermetallic particles.

2. **Solid solution → nuclei → η':**
   Here, nuclei participating in the reaction is assumed to involve vacancy clusters. This reaction occurrs prominently in materials quenched upto room temperatures and aged at least for a period of 5 sec. and then further aged at 150 °C. The nuclei formed during the quenching to room temperature are independent of nucleation and growth of Guiner Preston (G.P.) zone. The η' phase can nucleate consistently throughout after an incubation period observed after quenching the material at temperature in between 125 °C and 145 °C.
3. **Solid solution → G.P. zones → η'→ η:**
   This reaction explains the complete decomposition process of the supersaturated solid solution. The G.P. zone formation occurs predominantly in the temperature range of 20 °C to 125 °C. The transformation of G.P. zone to η precipitates takes place when subjected to prolonged aging. The peak strength is attained by optimal distribution of G.P. zones and η' precipitates throughout the material while the incoherent equilibrium stage attained by η particles contribute negligibly to the hardening of these alloys [7].

c) Effect of material processing:

i. In case of 7xxx series alloys, there is subtle relationship between the processing parameters and microstructure which is complicated enough to understand. The process and production variables have strong bearing on the aging characteristics of these alloys.

ii. Insoluble compounds formed out of Fe, Si and other impurity elements formed during casting process further split up during working on the material to form stringers which appear in the final product along the grain boundaries. These stringers disturb the homogeneity of the material thereby degrading its properties [8]. Operations like forging and rolling helps in breaking of these insoluble compounds which add extra cost to final product.

iii. Toughness can be improved by reducing the contents of iron, silicon and other

impurity elements but with a limitation of investment and availability of high purity materials [9].

iv. Precipitation of η particles ($MgZn_2$) during the cooling period after solution heat treatment yield lower strength due to coarsening of these particles in large quantity. Hence, careful control of quenching process without any interruption would yield a supersaturated solid solution which would decay further to form G.P.zones and η' particles. Hence proper control or minimization of transfer time from furnace to quenching medium must be low enough coupled with high quenching rate to avoid slow cooling or reheating in the temperature range of 400 °C to 290 °C where rapid precipitation can occur [11].

v. The formation tendency of the η particles during cooling after the solution heat treatment process is referred to as quench sensitivity. The Additives like Cr and Mn increases the quench sensitivity by forming intermetallics precipitates which provide heterogeneous nucleation site for η particles. Only the intermetallic precipitates with incoherent interfaces were found to be favorable for nucleation. Zr forms Al_3Zr intermetallic compound which is coherent in nature and hence unfavorable for nucleation. Hence, Zr addition is favored only when the grain growth and recrystallization control are required along with the tolerance to slow quenching rates.

vi. The size and distribution of intermetallics is governed by the temperature and time factors involved in heating processes like homogenization or high temperature heat treatments. Coarsening of intermetallics adversely affects the mechanical properties of the alloy. After solution heat treatment and quenching, 7xxx series alloy shows natural aging property. 7xxx series alloy changes significantly in terms of the mechanical properties over the number of years. Normally, 7xxx alloys are artificially aged (T7x) condition in which corrosion resistance is improved at the cost of some strength.

d) Effect of Sc on the structure and properties of Aluminum alloys from physical metallurgy point of view:

1) Scandium is the most powerful inoculants of grain structure in Al alloys. It gives rise to fine grain structure i.e. dendrite free structure in ingots of Al and its alloys, due to the presence of Al_3Sc particles which act as centers for nucleation of grains in aluminum solid solution. In the pre-crystallization period, the primary Al_3Sc particles with $L1_2$ crystal structure which is unique in size and corresponds to the Aluminum crystal lattice serves as a grain nucleation site. This might be the reason behind the powerful inoculation characteristics of Sc on Al and its alloys.[12-15]
2) The Sc content crosses over the eutectic solubility level, where in the appearance of the Al_3Sc particles cause the grains to disintegrate to the finest possible size. Research in this field indicates that transition point where the dendritic stage crosses over to non dendritic stage occurs at Sc % exceeding a certain critical value exceeding the by 0.01-0.15 %. [16]
3) When the melt reaches the eutectic temperature at which the crystallization process in Aluminum solid solution begins, a volume of melt equivalent to volume of post solidification grains contains many Al_3Sc particles. In spite of that, the crystallization begins with one Al_3Sc particle which at later stage becomes the center of grain nucleation while other particles get sandwiched in between the solidifying/crystallization front and the grain boundary.[17]
4) After a certain limiting value of Sc , the disintegration of the grains and their sizes comes to saturation and the cooling rate of the ingot in the crystallization temperature range becomes the deciding factor.[15]
5) Commercially, Sc is introduced in Al alloys along with zirconium due to the Zr element's ability to increase the inoculation power of Sc at very low Sc% say from 0.18 onwards. In this case, $Al_3(Sc_{1-x}, Zr_x)$ particles are formed which has the same $L1_2$ crystal lattice as the Al_3Sc particle thereby saving in capacity to serve as active grain nucleation sites in Al solid solution.[18]
6) In case of deformed semiproducts obtained from Sc inoculated Al alloys by the continuous casting process, the supersaturated solid solution of Sc in

aluminum is formed. This gives a lot of advantage over the deformed semiproducts obtained from conventional Al alloys. In a controlled process, 90% of Sc introduced enters in solid solution while the remaining 10% segregates to form Al_3Sc particle in the pre-crystallization period which is the starting point for Sc inoculation process of the grain structure of the ingots.[18]

7) The presence of Zirconium does not affect the solubility of the Scandium in aluminum and vice versa. The maximum joint solubility of Sc and Zr in aluminum under metastable equilibrium occurs at the ratio Sc to Zr equal to unity.[19]

8) Super saturated solid solution of Sc in aluminum show special features during the decomposition process, which yields Al_3Sc or $Al_3(Sc_{1-x}, Zr_x)$ particle that actually governs the operating characteristics of the deformed semiproducts of Sc bearing Al alloys. The kinetics of decomposition and the morphology of the decomposition products become the key to get desired operating characteristics or properties thereby makes it a necessity to control the temperature and time parameters of the manufacturing process.[18]

9) The brisk decomposition of solid solution of Sc with aluminum occurs at temperatures above 250 °C, only due to its instability.[19,20]

10) The decomposition of the solid solution of Sc in Aluminum results into strong rise in hardness due to the presence of highly dispersed Al_3Sc particles. But this hardening effect is temperature dependent. With increasing time, the coarsening of Al_3Sc particles takes place resulting into loss of hardness. Although, Zr does not change the kinetics or the intensity of hardening, but it decelerates the softening rate prominently. The coarsening of Al_3Sc particles occurs more prominently compared to or $Al_3(Sc_{1-x}, Zr_x)$ particles.[21]

11) Sc inoculation to Al alloys markedly increases the recrystalliztion temperature of deformed semi-products [22,23,24]. Other anti- recrystalliztion promoters are Zr, Mg, Cr. But amongst them, effect of Sc is highest. This effect of Sc is applicable to both hot and cold deformed semi-products. The highly dispersed Al_3Sc particles in suspension formed during decomposition of Sc bearing Al alloys, hinders the recrystallization. In presence of Zr, the anti- recrystalliztion

effect from the Sc gets accelerated as Zr boycotts the tendency of coagulation of secondary particles during in-process heating. Depending upon the base system pertaining to Al alloys under consideration, their recrystalliztion resistance varies widely.

12) The commercial alloy 1970 (Al-Zn-Mg-Sc-Zr system) has a very high recrystallization temperature and it retains the non recrystallized structure without the slightest indication of recrystalliztion after heating for hardening in any kind of semiproducts including strongly deformed sheets of 1 mm thickness.

13) Alloys of Al-Mg-Sc-Zr class show lower recrystallization temperature due to its dependence upon the Mg content. With increase in Mg content, the recrystallization temperature decreases and when Mg content of 6% is reached in commercial Al-Mg-Sc-Zr alloys, it becomes hard to fabricate thin cold rolled sheets with a thermally stable nonrecrystallized structure from the latter. This target is achieved by increasing Sc and Zr content along with a control on decomposition process in between the heating operations. The selection of proper deformation and temperature values in rolling decreases the deformation energy accumulation in the metal which acts as governing force of the recrystallization.

14) Hardening effect is prominent in deformed semiproducts of Sc bearing Al alloys compared to one without Sc inoculation. In case of deformed semi-products, the strength comes from the two factors viz. the dispersed particles of Al_3Sc type and by sub-structural hardening due to the preservation of the nonrecrystallized structure. In case of forged semi-products say of Al – 6% Mg without Sc and Al – 6% Mg with scandium (1570), the strength differences comes in picture due to the two reasons viz. the subgrain hardening in 1570 alloy along with the hardening effect of $Al_3(Sc_{1-x}, Zr_x)$ particles. It is hard to express the contribution of above two factors towards the hardening effect. In this case, a conservative approach is observed by considering 50% contribution of each factor. While on the other hand, overestimation implies that hardening due to particles in s insignificant. The subgrain hardening is low solely due to the large size of the subgrains in

forged semiproducts. The hardening due to coarse Al_3Sc particles is insignificant and depends lesser upon the kind of semiproduct. While the substructural hardening actually depends upon the kid of semiproduct and the method of its manufacturing. The increment in degree and rate of deformation along with decrease in deformation temperature coupled with the use of pressure treatment, the substructural hardening increases due to disintegration of the subgrains in heat treated semiproducts.

15) Commercially available Al-Zn-Mg alloys have some inherent advantages like probability to achieve high strength without deterioration of ductility, a high corrosion resistance , a good weldability coupled with its high ability to undergo metallurgical processes like pressing. Their usage is limited due to their high stress corrosion susceptibility, This tendency can be reduced by adding low amount of copper but this addition gives rise to other problems like the increase in weld crack susceptibility, thereby reducing its weldability. The positive effects of Sc addition can overcome these disadvantages. The Sc addition shows its talent in terms of disintegration of grains in the weld zone which markedly decreases the susceptibility of the alloy to hot cracking. Scandium was added as alloying element to the 1970 weldable alloy based on Al-Zn-Mg-Cu[25,26]. The 1970 alloy is the best high strength weldable aluminum alloy with strength around 500 MPa coupled with high ductility and fracture toughness. It is lesser prone to weld cracking compared to AMg6. The weld strength achievable is 0.8 to 0.9 of the base metal strength.Sheets made out of 1970 alloy have natural superplasticity. High solid solution stability and wider temperature range of its subsistence which concur with the superplasticity temperature range, gives the sheets a considerable hardenability by cooling in air from temperature of superplastic shaping and then hardened by natural or artificial aging.This 1970 based new alloy was designed with low Scandium content called as 1975. Its application is in the form of pressed shapes and high load structures of bridge girders, transmission line poles and towers and in automobile and rail industries.

2.3 Weldability of Al-Zn-Mg alloys:

The ability of the material to be welded according to a particular process and procedure so as to obtain metallurgical and discontinuity defect free weldments which can perform satisfactorily in the intended service or function is termed as weldability. Fusion zone in welding is a cast structure with a non-equilibrium thermal history. Thus, metallurgical changes produced by welding become a significant deciding factor in order to designate the properties of the welded component or structure. By understanding, the metallurgy of welding alloys, properties required can be obtained or knowing the properties, design alterations can be made efficiently. As with other Al-alloys, there are a number of weldability issues associated with Al-Zn-Mg alloys, including susceptibility to defect formation during fabrication, alloys can be reviewed by discussing the porosity formation and prevention, weld cracking susceptibility and filler metal selection for various Al-Zn-Mg alloys.

2.3.1 Weld metal porosity:

It is the most common defect for all welding processes. Hence, control of porosity formation and the effect of porosity on weldment properties has been an area of great interest. Porosity could be gas related or solidification shrinkage related. In terms of size, shape and location, porosity can be described as interdendritic porosity and bulk porosity

[27,28,36]. Interdendritic porosity occurs when gas bubbles are formed or entrapped between dendritic arms in the solidifying weldment, whereas bulk pores are spherical pores that result from super saturation of the gases in weld pool. Therefore, the causes of porosity in weld metal are dependent upon the amount of dissolved gases and the welding process variables. Hydrogen is the principle cause of gas related porosity in weldment area of aluminum and its alloys. Hydrogen has relatively higher solubility in molten aluminum compared to solidifying aluminum [31-33].

The Fig. 1 shows the hydrogen solubility which is highest in molten aluminum. The difference in solubility acts as an instigation factor for porosity formation [34]. Gas bubble thus formed gets buoyed out naturally or by forced convection or high turbulence like in pulsing GMAW. When the pore's buoyancy velocity exceeds the

solidification fronts velocity, the gas pores may flee [35]. Hence, lower welding speeds i.e. lower solidification front velocity are favorable for attainment of low porosity weld.

Voids or porosity which in general are spherical in shape, are caused by the sharp decrease in solubility of hydrogen during solidification. The alloying elements significantly influence the hydrogen solubility in the matrix by affecting the solidification range and solidification mode.

The sources of hydrogen [36] includes

(1) H_2 from base metal

(2) H_2 from filler metal

(3) H_2 in shielding gas

The porosity problem though serious problem in Al-alloys can be easily rectified or at least minimized if we take certain precautions and maintain and employ a standard welding procedure.

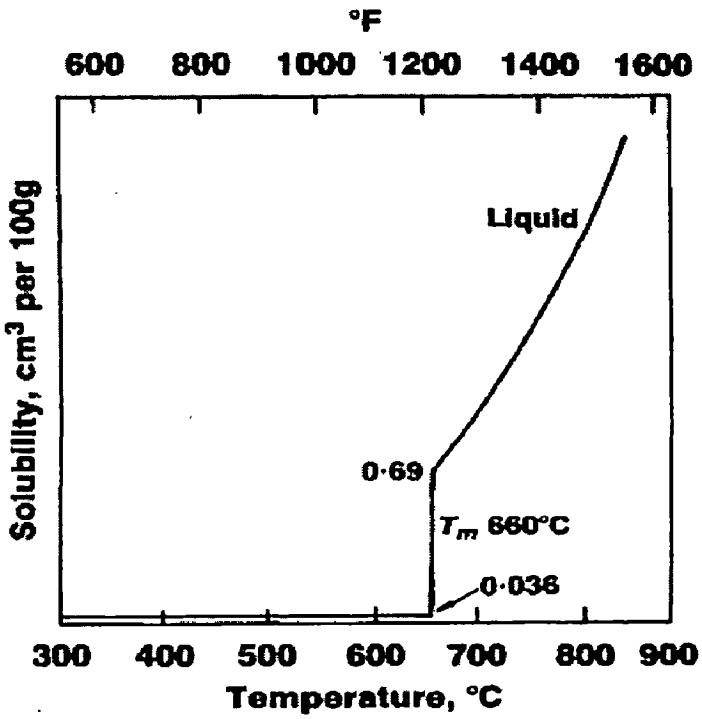

Figure 1: Hydrogen solubility in pure aluminum. [33]

2.3.2 Solidification Cracking:

Weld cracking in Al-alloys are mainly due to the aluminum's high thermal expansion which results into large change in volume upon solidification inside weldment and wide temperature gradient along the weldment. The 7xxx series Al-alloys are heat treatable alloys in which a small amount of copper is added to increase the strength but it hampers the weldability due to increased susceptibility to weld cracking. Hence, a copper free 7xxx alloy i.e. Al-Zn-Mg alloys will have appreciably lower propensity towards weld cracking compared to one with copper. Cracking can be minimized in presence of higher magnesium contents and zirconium. These alloys are multi-component system, hence, their nature of cracking tendency could be connected to the formation eutectic phases and the available liquid fraction at any particular instance. Alloys which have greater tendency to form eutectics and in which the eutectic liquid is able to wet the grain boundaries, can be expected to be more prone to cracking. Those compositions in which the content of alloying elements match with those of their binary counter parts of maximum cracking sensitivity are prone to cracking are kept in their minimum cracking limits, then cracking problems can be solved , such as in Weldalite -049 [37]. The plus point of these alloys is that these alloys show ability in the HAZ region to naturally age or become precipitation strengthened after the welding.[38-40]

2.3.3 HAZ degradation :

Heat Affected Zone is the region adjacent to the weld zone just next to fusion line with altogether different microstructure and degraded mechanical properties compared to the base metal microstructure and its mechanical properties as a result of the thermal cycles experienced by it during welding process. In case of heat treatable Al-alloys especially Al-Zn-Mg alloys in which the number of alloying elements are more, the HAZ gets a distinguishable structural modification by dissolution or growth of precipitates. HAZ width is mainly controlled by diffusion mechanism and thermal gradient experienced by it during the weld cycles [41]. The HAZ is normally measured in terms of change in hardness along the cross-section, starting from center of the weld and towards the base metal.

In case of Al-Zn-Mg alloys system, it exhibits a precipitation sequence of metastable precipitates, with principle strengthening phase occurring early in the sequence in the form of GP zones (Guinier-Preston zones). The transformation of these precipitates in terms of morphology at higher temperatures occurs in smooth and continuous manner which is controlled by diffusion rate and supersaturation thermal, finally resulting into non-strengthening phases

- **Effect of Heat input in the HAZ:** The transformation of base metal structure to HAZ is clearly dependent upon the thermal gradient along the cross-section which is indirectly dependent upon the welding process and its parameters, thereby controls the extent of HAZ degradation. High heat input and pre-heating greatly influences both the degree and width of the HAZ. Thus, the use of multi-pass welding procedure and controlled optimum heat input can minimize the HAZ width.
- **Post weld heat treatment:** It can greatly improve the strength of the HAZ for heat-treatable Al-Zn-Mg alloys. It may involve complete post weld solution heat treating and followed by aging or just post weld aging only. There are advantages of using the post weld aging treatment over the previous in the sense that the temperatures used are lower compared to the post weld solution heat treatment followed by agin, as it does not involve water quenching resulting into lesser residual stresses and distortion in the welded assembly. The heat-treatable Al-Zn-Mg alloys show property of natural aging at room temperature in HAZ region with only drawback being the amount of time required is more (normally upto 14 days).

2.4 Gas Metal Arc Welding (GMAW):

Gas metal arc welding is an electric arc welding process which produces coalescence of metals by heating them with an arc established between a continuously fed filler metal (consumable) electrode (in the form of wire) and the material to be joined at certain welding parameters like heat input, joint design, etc. Shielding of the arc and molten weld pool is obtained entirely from an externally supplied gas or gas mixtures as shown in Figure.3. The process is also referred to as MIG/MAG.

All position welding capability, semi-automatic mode, absence of fluxes, suitability for both ferrous and non-ferrous metals, cleanliness and ease of

mechanization are the surplus features of GMAW. In many ways, GMAW is a direct competitor of shielded metal arc welding (SMAW) process. It is faster in similar applications but the cost of the equipment and consumable is much higher. The quality of welds is comparable and selection is often based on relative costs. GMAW is perhaps, the most widely used process in terms of range of metals and applications if not in terms of filler metal deposition [42]

GMAW has the following advantages [42]:

1. It overcomes It has default advantage of limitless electrode length with shielded metal arc welding.
2. Welding can be performed in all positions which is a direct limitation of SMAW.
3. Absence of slag, continuous electrode feed and higher filler metal deposition rates ensures higher welding speeds in case of GMAW process as compared to SMAW process.
4. Deeper penetration can be achieved in GMAW process over SMAW process, which permits the use of smaller size fillet welds for equivalent strengths.

GMAW process is found to be useful in production of car bodies where freedom from frequent electrode changing and need for flux removal, ensures higher production rates. Even in case of welding thick plates, the higher filler metal deposition rate ensures minimization of production costs. GMAW process is extensively used in fabrication of structures, pressure vessels, tanks, pipes, domestic equipment, general and heavy electrical engineering and the aircraft engine manufacturing industries. It is also used successfully for the fabrication of railway coaches and in the automobile industry where long –high speed welds of fairly thick sections are used. The welding of lorry frames is an example of the application of dip transfer GMAW [42]. GMAW can be used satisfactorily in conjunction with robotic welding; hence its use in future is bound to increase. Although all metals whose filler electrode wires are available can be welded by this process yet its application is more significant in fabrication of aluminum alloys, carbon and low alloy steels and stainless steels [43].

2.4.1 Continuous Current GMAW process:

In Continuous Current GMAW process, a direct current is supplied by establishing a stable arc between continuously fed filler electrode wire and the work piece to be joined. This process is eminently used for welding Al and its alloys. The characteristic of the GMAW process is the use of high current density to facilitate metal transfer. The type of metal deposition across the weld arc is dependent upon the type of shielding gas atmosphere and its flow rate, welding current, power supply characteristics, electrode extension and electrode composition.

Primarily, there are three modes of metal transfer namely short circuit, globular and spray. Short circuit metal transfer occurs at relatively low welding current and the arc voltage is set low so that each drop grows until it gets transferred to the weld pool via short circuit. This type of metal transfer produces a small and quickly solidifying weld pool that are generally suited - for joining thin sections, for out of position welding and for filling large root opening. There is no transfer of metal across the arc gap. Metal is transferred from the electrode only when it is in contact with the weld pool. The electrode makes the contact with the molten weld metal at a steady rate in the range of 20 to 200 times per second.

Globular transfer occurs when welding is carried out by using argon or argon/ CO_2 mixture with are relatively low current and free arc (high arc voltage). It is characterized by drop that grows in to much larger diameter than that of the filler wire. The arc length must be long enough to assure detachment of the metal droplet from the electrode.[44,45]

2.4.1.1 Process variables:

A list of some of the variables that affect weld penetration and bead geometry and HAZ formation is given as below:

1. Welding amperage,
2. Arc voltage,
3. Travel Speed
4. Electrode extension,
5. Electrode inclination,
6. Electrode size
7. Weld joint penetration,

8. Shielding gas flow rate

Knowledge and control of these variables are essential if sound welds are to obtained. Shielding gas selection also influences weld penetration and bead geometry. The importance of one variable over another differs. However regardless of the particular application, the adjustment of variables is significantly influenced by [46] :

1) Composition , metallurgical structure and thickness of the metal
2) Electrode composition
3) Welding position
4) Quality requirements
5) The quality of completed weldments requirements

a) **Welding Current:** When all other variables are held constant, the welding current varies with the electrode speed or melting rate in a non-linear relation. As the electrode feed speed is varied, the welding amperage will be vary in alike manner with a constant feed speed is varied, the welding amperage will vary in a manner with a constant voltage power source. At the lower amperage range for each electrode size, the curve is nearly linear. However, at higher welding amperages, particularly with small diameters, the melting rate curve becomes non-linear progressively at a higher rate as welding amperage increases. This change can be attributed to resistance heating of the electrode extension beyond the contact tube. When the diameter of the electrode is increased at any electrode feed speed; higher welding current is obtained. Each type of wire (e.g. steel, aluminum) has different melting rate characteristics [44]. With all other variables held constant, an increase in welding current(electrode feed speed) will result in

1. Increasing the depth and width of the weld penetration
2. Increasing the deposition rate
3. Increasing the size of the weld bead

The welding current also affects the mode of metal transfer. The axial spray transfer mode is established at a minimum current level for any given electrode diameter (current density). This current level is generally termed

"the transition current". A well defined transition current exists only with a gas shield containing a minimum of 80 % argon, at the current level below the transition current- the metal drop size increases (larger than the diameter of the electrode). The arc characteristics are quite unstable in this operating range [47].

b) **Arc Voltage:** With a fat characteristics power source, the arc voltage is controlled mainly by setting the open circuit voltage. The change in the arc voltage leads to change in arc length and that affects the bead geometry directly. The change in arc voltage leads to change in arc length and that affects the bead geometry directly. The change in arc voltage not only affects the outer dimensions of the bead but also influences the microstructure and even the success and the failure of the operation by affecting the mode of metal transfer. When the arc voltage is too low the metal transfer occurs by either by short-circuit mode(at low wire feed rate) or by dip transfer(at higher feed rate).Such mode of metal transfer makes the process for use in position welding and normally takes place at lower metal temperature with lesser loss of alloying elements.[47]

No specific values of arc voltage are consistently appropriate for normal production welding [48], trial runs are necessary to adjust the arc voltage if it is to produce the most favorable filler metal transfer and weld bead appearance. These trails runs are essential because arc voltage is dependent upon a variety of factors including metal thickness, the type of joint, the position of welding, electrode size, shielding gas composition and the type of weld. From any specific value of arc voltage, a voltage increase tends to flatten the weld bead and increases in the fusion zone width. Reduction in voltage results in a narrower weld bead with a high crown and deeper penetration. Excessively high voltage may cause porosity, spatter and undercutting and low voltage may cause porosity and overlap at the weld edges. [51]

c) **Welding speed:** The linear rate at which the arc is moved along the weld joint is known as welding speed. With all other conditions held constant, weld penetration is a maximum at some travel speed. The penetration will decrease when the travel speed is changed and the weld will be either narrower or wider [45]. When the travel speed is decreased , the filler metal deposition per unit length increases & a large cum shallow weld pool is produced. The welding

arc impinges on this pool rather than the base metal as the arc advances. This limits penetration but produces a wide weld bead [45].

As the travel speed is increased the amount of thermal energy supplied by the arc decreases. Therefore, melting of the base metal is slowed down & it occurs nearer to the surface of the base metal, thus the penetration & bead width are decreased. As the travel speed is further increased, there is tendency towards undercutting along the edges of the weld bead because there is insufficient deposition of filler metal in order to fill the path melted by the arc. Travel speed should be coordinated with the filler metal wire feed speed. The proper welding speed must be maintained to control, the amount of root penetration into the joint. Moving too slowly may results into higher root penetration which in turn will cause melt through of thin metal section or in other words the weld pool will flow into the joint ahead of arc on thicker metal.

d) **Electrode size:** Each electrode wire has a workable limit within which it can be effectively used to give satisfactory weld quality. When welding current used is lower than the optimal range, it results in lack of fusion & higher current. Hence it causes increased spatter, porosity 7 poor bead appearance. Electrode size also affects the penetration & weld width in that for the same current, lower diameter wire gives deeper penetration while wider beads with shallow penetration are obtained with bigger diameter wires [45].

Overall, there is a tendency to use smaller wires because of the following reasons [49]:

1) Rapid arc length adjustment
2) Spray mode of metal transfer
3) Easy to spool
4) Higher deposition efficiency

e) **Shielding gas flow rate:** The gas flow rate is to be so maintained as to get defect free welds. If the gas flow is inadequate porous bead is formed while excessive gas flow rate may cause blowing out of metal from the weld pool. The gas flow rate is associated with the nozzle-to-work distance, hence longer this distance more the gas flow rate is required for proper protection of the molten metal. The flow rate of argon is often chosen based upon the welding current, electrode stick-out, nozzle to work distance, welding speed & the joint design. The proper amount of gas shielding usually results in a rapidly cracking or sizzling arc sound. Inadequate gas shielding will produce a

popping arc sound with resultant weld discoloration, porosity & spatter [50].

2.4.2 Pulsed current gas metal arc welding:

In pulse current process, the power source provides two current levels viz. a steady background current which is incapable of metal transfer as its value is too low and a peak current which is superimposed upon the background current at a regular interval as schematically shown in Fig. 4 which is actually responsible for metal transfer. The peak current is well above the transition during each pulse with suitable setting of pulse parameters. The combination of two currents produces a steady arc with axial spray transfer at an effective welding current which is below that required for conventional spray arc welding.

The characteristic pulse is defined by the frequency of the pulse which is defined as:

$$f = \frac{1}{t_p + t_b}$$

Where f = pulse frequency; t_p = pulse on time; t_b = pulse off time.

In a pulse, the current actually shuffles between the two levels. The lower current level- I_b also called as background or base current, is lower than the transition current & is only responsible for maintaining the arc stability. The upper current level- I_p also known as the peak current which lies in the region which is above the transition current, influences the nature of the metal transfer. The total pulse time, t, is divided into pulse on time "t_p" and pulse off time "t_p", which can be set for different values of pulse current. The droplets detached are accelerated by the higher electromagnetic forces associated with the peak current level I_p which is above the transition current. The low average mean current, I_m, obtained in pulsed GMAW welding makes it possible to weld in almost all positions like say vertical or overhead positions, which is otherwise extremely difficult. This is solely due to higher current that makes the weld pool too fluid & molten metal runs downwards even through the high plasma stream in the welding arc [54,55]. The square wave current time diagram during pulsed current welding is as shown in Fig. 4. For the production of the quality weld, the choice of correct pulse current parameters (I_p, I_b, t_p, f) is of primary concern. The criteria for choosing these values depend upon the following consideration [56]:

a) The mean current, I_m, is determined by all the parameters which must give a burn-off rate matching the wire feed speed, so that a constant & stable arc length is maintained. Mean current or average current is obtained as follows [57]:

$$I_m = \frac{[(I_p . t_p) + (I_b . t_b)]}{t}$$

Where I_p = peak current; I_b= background current ; ; t_p = pulse on time; t_b = pulse off time; t = total pulse time.

b) For a given wire speed, the peak current and pulse duratipn must be adjusted that it gives at least one drop detached with each pulse.
c) Spray transfer must be produced.
d) The background current must exceed the minimum limit of current necessary to produce stable arc, otherwise the arc would extinguish.

The variables I_p, I_b, t_p, *f interact* very strongly and criteria may be obtained with a number of combinations of power supply settings.

2.4.2.1 Influence of pulse parameters on behavior of metal transfer:

i. **Peak current:** The peak current is of primary importance since it must exceed the transition current level for a legitimate period so as to form and detach a drop. There are findings which indicate that the peak current should slightly exceed the transition current to ensure spray transfer. The pulses of the peak current generate a large pressure fluctuations within the arc and in area of marginal shielding air may be aspirated into the inert jacket. Excessive peak current may also produce porosity in case of wielding of aluminum and its alloys. If current reaches excessively higher levels, the principle of one drop per pulse (ODPP) is violated due to arc forces which cause excessive melting of filler wire there by accelerating the multiple molten droplets to strike the molten pool and create excessive spatter [58]. The peak current influences the metal transfer but it does not act as a principle parameter in welding

operations.

ii. **Background current:** The background current is probably the least critical pulse parameter though it does have several key functions other than maintaining the stable welding arc between the pulses. Control over weld bead shape can be greatly enhanced by maintaining the appropriate background current. In order to minimize the heat input to the weld pool & thereby controlling the HAZ width & residual thermal stresses, this current is kept to lowest possible value[58].

iii. **Pulse frequency:** The pulse frequency affects the I_b value as well as the minimum filler wire melting rate to a lot of extend. At higher frequency and high peak current for a given base current, there is a high probability that t_b value make prove insufficient for the semi-solidification process associated with the detached droplet resulting into continues melting of the wire even during the pulse-off time. Thus, in this casethe weld pool receives more molten filler metal causing wider HAZ region and residual stresses [59].

iv. **Pulse duration or pulse-on time:** Pulse duration has been found to act as a variable which can be altered in order to achieve the ultimate reduction in the heat input through the weld arc to the weld pool while sustaining the spray transfer. Changes in the arc shape have been found to be associated with t_p which actually affects the heat transfer to the weld pool through arc. A square wave is more effective over the sine wave or triangular wave. In order to ensure material transfer with each pulse, the pulse must have a minimum duration. This threshold level decrease slightly as the peak current level increases [60].

2.4.2.2 Weld thermal cycle under pulse GMAW:

The difference in weld thermal cycle of the pulsed & continuous welding processes is result from the following reasons:

1) During pulsed current GMAW, initially the rate of heating grows relatively slower compared to that observed with continuous GMAW process followed by a rapid temperature rise.

2) In case of pulsed current GMAW, intermittent cooling of the detached molten drop during each t_b period, thus results into some amount of cooling of the weld pool during that period which is assisted by the high thermal conductivity of the material to conduct the heat away from the weld zone. Also, the freezing metal releases the latent heat causing rise of heat inside the weld pool which significantly reduces the amount of heat required to complete the welding operation satisfactorily.

Comparison of different HAZ thermal cycles obtained from the welds made at different modes of metal transfer therefore shows relatively lower peak temperatures for the pulsed arc welds. In the pulsed arc weld, the thermal curves are generally much wider, having relatively slower heating and cooling rate.

The growth rate of heating is slower in pulsed GMAW compared to the continuous GMAW because the temperature of the molten pool decreases with the increase in frequency due to reduction in temperature of droplets reaching the pool. The decrease in the droplet temperature with the increase in frequency may have been resulted due to decrease in time spent by the droplet in the arc gap with increase in the pulse frequency. The overheating of the droplet is also reduced because the droplets are forcibly removed from the electrode tip at higher pulse frequency. The interruption in heat input during the pulsed current GMAW, delays the cooling cycle of HAZ and thus widens the curves of thermal cycle as compared to that observed in case of continuous current GMAW. [61]

2.4.2.3 Mechanism of solidification:

Solidification of molten metal pool significantly affects the quality of weld joint [62]. As the rate of solidification increases, segregation process on a macroscopic scale in the weld metal are suppressed, but an intermittent process of solidification may cause laminar heterogeneity in the fusion zone. Thus, combining the rate and nature of solidification, the shape of the molten pool & the structure of its boundaries depend upon the type of weld metal, the welding method and the heat source in use.

It is observed [62] that the solidification mechanism in pulsed GMAW is somewhat different from that of continuous GMAW in which solidification inside

the molten pool occurs around the whole outline of the molten pool. Investigation carried out on the solidification of the molten pool during pulsed current GMAW revealed that the crystal growth in the front part of the pool surpasses the movement of the solidification from the back part, because of the high temperature gradients across the molten pool. In pulsed GMAW, the heat balance depends upon the process parameters such as the pulse-off time (t_b) and the pulse-on time (t_p)

During the pulsing, the pattern of solidification approximates to that in continuous current GMAW. During the pulse-off period, solidification continues in the front part of the molten metal pool is remelted while the next pulse is applied and the back part continues to solidify. Thus, the solidification time inside the molten pool can be divided into two ranges i.e. solidification in off time and solidification in initial period of development of a weld pool when the next pulse is applied. The peculiar form of the heat balance is found to be affecting the nature of the cast structure of the weld pool. If the cycle time is long enough for the spot to start solidifying in the pulse off time, the directional development of the grains towards the centre of each separate weld spot.[62]

Also, the solidifying pool releases latent heat which further super heats the weld pool thus reducing the amount of heat input to the pool and maintain semi-solid conditions inside the pool avoiding dedritic growth. In the continuous GMAW, solidification is delayed as continuous supply of heat coming from the direction of heat source keeps the weld pool in front to superheated condition but as weld cools, the latent heat is slowly released resulting into dendritic growth within the weld pool. If the cycle time and the pitch are reduced, the arrangement of the crystals appears rather similar to the microstructure of a weld made under continuous GMAW. In that case, often there is a axial growth of grains extending along the whole weld. The extent of the axial growth depends upon the degree of periodic interruptions in the heat flow & continuously changing shape of the molten pool.[62]

2.4.2.4 Influence of pulsed current welding on microstructure of weld and HAZ:

- **Microstructure of weld deposit:**

In most of the cases, the microstructure of the weldment obtained using the pulsed GMAW on aluminum shows relatively finer grained structure over that obtained in continuous GMAW process. The welds show soundness & contain lesser oxide inclusion than that observed in case of weldment obtained using the continuous GMAW. The joints obtained by the pulsed GMAW are superior to joints obtained using continuous GMAW in the following aspects: soundness of welds, higher corrosion resistance, smaller HAZ * smaller grain size in the microstructure. In case of Al-alloys, a specific set of pulse parameters has been found to refine the weldment microstructure. In this connection, the mean current and frequency are found to be most important factors. The use of mean current beyond the transition current & suitable combination of pulse off time, super heating and size of the droplet has been found very much effective in microstructure refinement. During the solidification of the weld pool, the deposition of the new droplet during pulse on time over the previous solidified droplet may result in localized remelting of the upper region of earlier bead and thereby imparts a thermal shock in the subsequent lower region adjacent to it. The extent of the heat affected zone(HAZ) mainly depends upon the size of the droplet and the heat input i.e. degree of superheating of the droplet. The local melting may cause necking and pinching-off of dendrite arms and the crystals are removed from the liquid solid interface. They get disturbed in the liquid region of the weld metal by a convection current of the liquid metal caused by the agitation resulting from the thermal gradient. Many of these crystallites reach the higher temperature region of the liquid which exists at the upper part of the weld bead eventually remelts, nut others retained in relatively low temperature liquid part of the weld pool grow into new randomly oriented crystals resulting into a finer grain cast structure inside the weld pool by grain multiplication process. The upper part of the weld ment tends to solidify with coaxial growth of dendrites till it receives the droplet from the next pulsation and the process continues for other droplets.

During welding, for a given wire feed rate, the size of the droplets decreases with the increase in frequency. The reduction in the droplet time & the pulse off time obtained by increasing the pulse frequency significantly affects the cooling characteristics of the droplet. Under the given condition of heat input, lowering of the droplet size enhances the extent of the solidifying dendritic axial growth where as the decrease in the pulse off time minimizes

the same. [60-65]

- **Heat affected zone:**

  In case aluminum alloys, the heat affected zone resulted during pulsed current GMAW has been found to be of lesser width of recrystallised region adjacent to fusion line than that observed in case of HAZ obtained using continuous GMAW. This may be caused due to reduction in peak temperature obtained in the HAZ region resulted from the intermittent heat input from pulsed current GMAW technique which is not the case with continuous current GMAW process. The recrystallisation of HAZ region primarily depends upon the amount of heat input to the molten weld pool as well as the heat build-up in the weld pool. In case of continuous current GMAW process, the increase in heat input is mainly due to the increased degree of super heating, propelled by the release of latent heat of solidification by the solidifying weld pool which in turn causes heat build-up. But in case of pulse current GMAW process, the heat build-up is significantly controlled by the pulse parameters such as mean current, frequency and pulse-off time. Also, the thermal conductivity of Aluminum and its alloys is significant (just next to copper), hence more the heat input, more is the heat conduction to the HAZ region resulting into increase in its width. Thus, weakening of the HAZ region significantly depends upon the type of alloy, its micro-alloying content and the welding parameters. [60-65]

Table 1: Chemical composition of various 7xxx series aluminum alloys [66]:

Aluminum Association	Composition, weight %								
	Si	Fe	Cu	Mg	Cr	Zn	Ti	Al, minimum	Other alloys
7001	0.35	0.4	1.6-2.6	2.6-3.4	0.18-0.35	6.8-8.0	0.2	Rem	
7010	0.12	0.15	1.5-2.0	2.1-2.6	0.05	5.7-6.7		Rem	0.1-0.16 Zr
7014	0.5	0.5	0.3-0.7	2.2-3.2		5.2-6.2		Rem	0.2(Ti + Zr)
7046	0.2	0.4	0.25	1.0-1.6	0.2	6.6-7.6	0.06	Rem	0.1-0.18 Zr
7146	0.2	0.4		1.0-1.6		6.6-7.6		Rem	0.1-0.18 Zr
7149	0.15	0.2	1.2-1.9	2.0-2.9	0.1-0.22	7.2-8.2	0.1	Rem	
X7064	0.12	0.15	1.8-2.4	1.9-2.9	0.06-0.25	6.8-8.0		Rem	0.1-0.5 Zr
7178	0.4	0.5	1.6-2.4	2.4-3.1	0.18-0.28	6.3-7.3	0.2	Rem	
7278	0.15	0.2	1.6-2.2	2.5-3.2	0.17-0.25	6.6-7.4	0.03	Rem	
7091	0.12	0.15	1.1-1.8	2.0-3.0		5.8-7.1		Rem	0.2-0.6 Co
7090	0.12	0.15	1.1-1.8	2.0-3.0		7.3-8.7		Rem	1.0-1.9 Co

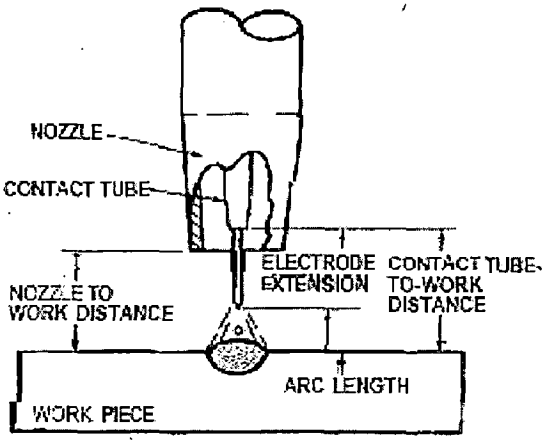

Figure 2: Gas Metal Arc Welding Terminology [67]

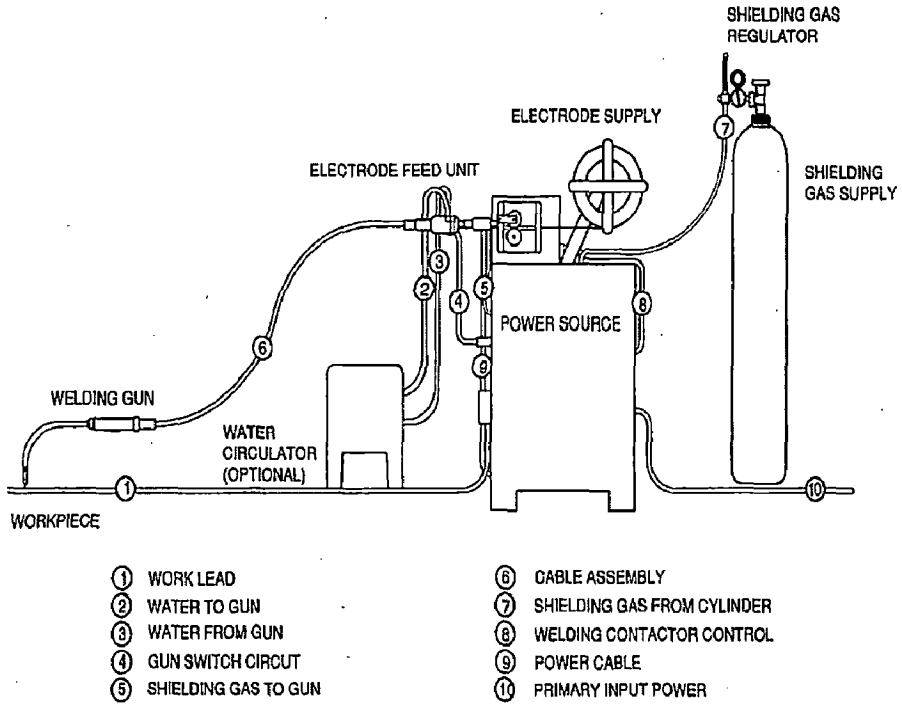

Figure 3: Basic arrangement of the GMAW system [68]

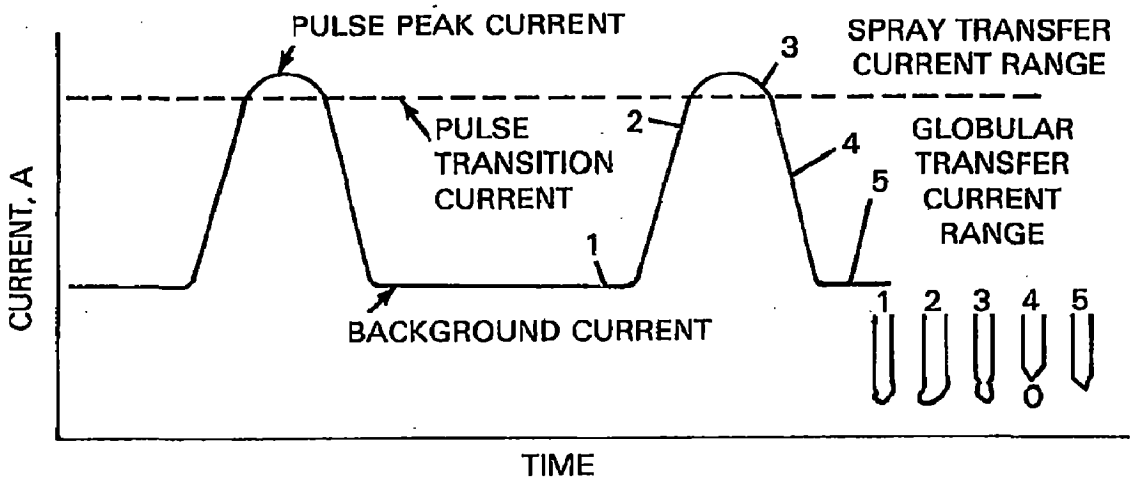

Figure 4: Characteristics of the Pulse-spray welding arc current [69]

Chapter 3: Problem Formulation:

Al-Zn-Mg alloys which come under the high performance heat treatable 7xxx series of wrought Aluminum alloys are intended for the use in aircraft and aerospace industry. Most high strength Al-alloys used in aircraft structures are mechanically fastened, which are the reasons behind the slow assembling process and limits the joining possibilities of thin sections. Welding is a good alternative for fabrication of structures in order to rectify these short comings, provided the technology developed should be of certain minimum standard which is acceptable globally to get desirable weld quality and impart as well as maintain the strength of the structure. Many investigators have worked on various welding processes for joining of light weight high strength Al-Zn-Mg alloys. But there are certain fundamental problems that are associated with almost all Al-alloys viz. i) the formation of tenacious Al_2O_3 film which not only protects it from corrosion but also impairs welding if not minimized, ii) high thermal conductivity of Al alloys demand for more heat input in order to get desired weld quality there by creating a wider HAZ region , iii) the molten weld pool of aluminum has a greater solubility for hydrogen and very low solubility after solidification. This hydrogen gets entrapped in the freezing pool resulting into considerable porosity, iv) heat treatable Al-alloys are susceptible to weld cracking

High strength in 7xxx alloys is achieved by adding alloying elements viz. zinc, magnesium and often copper combined with controlled thermal and mechanical processing. Copper provides the strength to the alloy but increases the weld cracking susceptibility. An important characteristic of the 7xxx series alloys is the ability of HAZ to age naturally after welding for as long as 30 days. The study of these alloys by employing general welding processes like GTAW and GMAW helps in weldability characterization of these alloys. Significant amount of work has been reported on GTAW as well as GMAW welding of with & without scandium inoculated Al-Zn-Mg alloys rolled sheets but less amount of work has been done on pulsed GMAW of open-die forged Sc inoculated A-l-Zn-Mg alloy plates & subsequently strengthening of the of HAZ which is the primary objective as the most failures occur in this region.

In present study, four ingots of experimental Al-Zn-Mg alloys with scandium inoculation were cast using a metal mold which were further homogenized, open die-forged with almost 30 % reduction in 12-15 strokes to get thickness of 8 mm and annealed. Further, standard solution heat treatment(W Temper) followed by precipitation heat treatment T73 were employed. This processed material was further welded at different pulse GMAW parameters using continuous and pulse currents by keeping a constant travel speed. In order to characterize the weldability of these experimental alloys, effect of heat input as well as pulse parameters and scandium inoculation(wt %) were studied in terms of metallurgical and mechanical properties. Also the weld geometry, dilution, porosity content and microstructure were studied. Effects of heat input and Sc inoculation on HAZ strengthening were investigated. Also, effect of post weld aging on HAZ strength was investigated through study of microstructure and hardness.

4.2 Materials & their processing:

4.2.1 Sample Calculation regarding amounts of each element to be added in alloy making:

Total wt. of casting = 1200 gm

For 100 gm specimen, considering average values of std. composition,

Wt. of Zn = Desired Zn % in Casting + Loss due to high temp. oxidation (15% by wt.)

= 5.6 x 1.15 = 6.44 gm

Wt. of Mg = Desired Zn % in Casting + Loss due to high temp. oxidation (20% by wt.)

= 2.5 x 1.2= 3 gm.

To add Sc, we will be adding Al 2% Sc Master Alloy with 50% loss consideration – i.e. if 100 gm Master alloy contains 2 gm Sc then, for 0.6 gm(with 50% loss consideration in final casting) Sc desired in final alloy cast is 30 gm of master alloy is required to be added.

Hence, 100 gm sample = pure Al 70 gm + 30 gm Master alloy

Thus, in 1200 gm casting = [1200/100] x (70 + 30)

= [840 gm pure Al] + [460 gm Al2%Sc Master alloy]

Amount of Zinc = [1200/100] x 6.44 = 77.28 gm

Amount of Mg = [1200/100] x 3 = 36 gm

Initially, a dummy casting was tried out on the mold for checking the leakages. The casting was done successfully without any leakages.

In order to save material & optimize its use (especially Master alloy Al 2% Sc due to its relatively high cost), pure Aluminum of 99.97% purity was used in making castings.

4.2.2 Steps observed in order to get casting compositions [Al-Zn-Mg alloy with Sc inoculation]:

1) First step is to make small pieces of the lumps (components like Mg, Al, Al2%Sc) as far as possible since this will increase the surface area required for melting & thus saving up the heat input. This was done using power saw & shear machine.

Chapter 4: Experimental work

4.1 Mold Design and Fabrication:

First the dimensions of the casting were decided based upon which a mold 3D model was created using a software Pro-E version 2.0. A mold of mild steel was fabricated to obtain a desired casting of size [150mm X 90mm X 24mm]. The mold was made up of two halves joined by using nut and bolt arrangement.

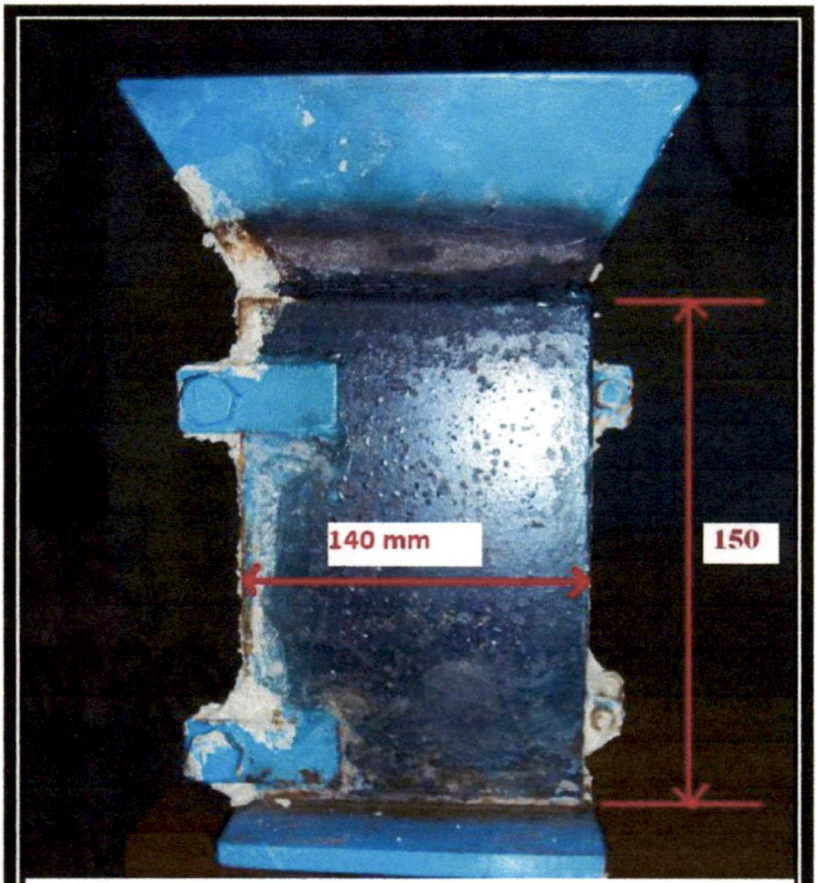

Figure 5: Photograph of Mold used for casting

Continued on next page.....

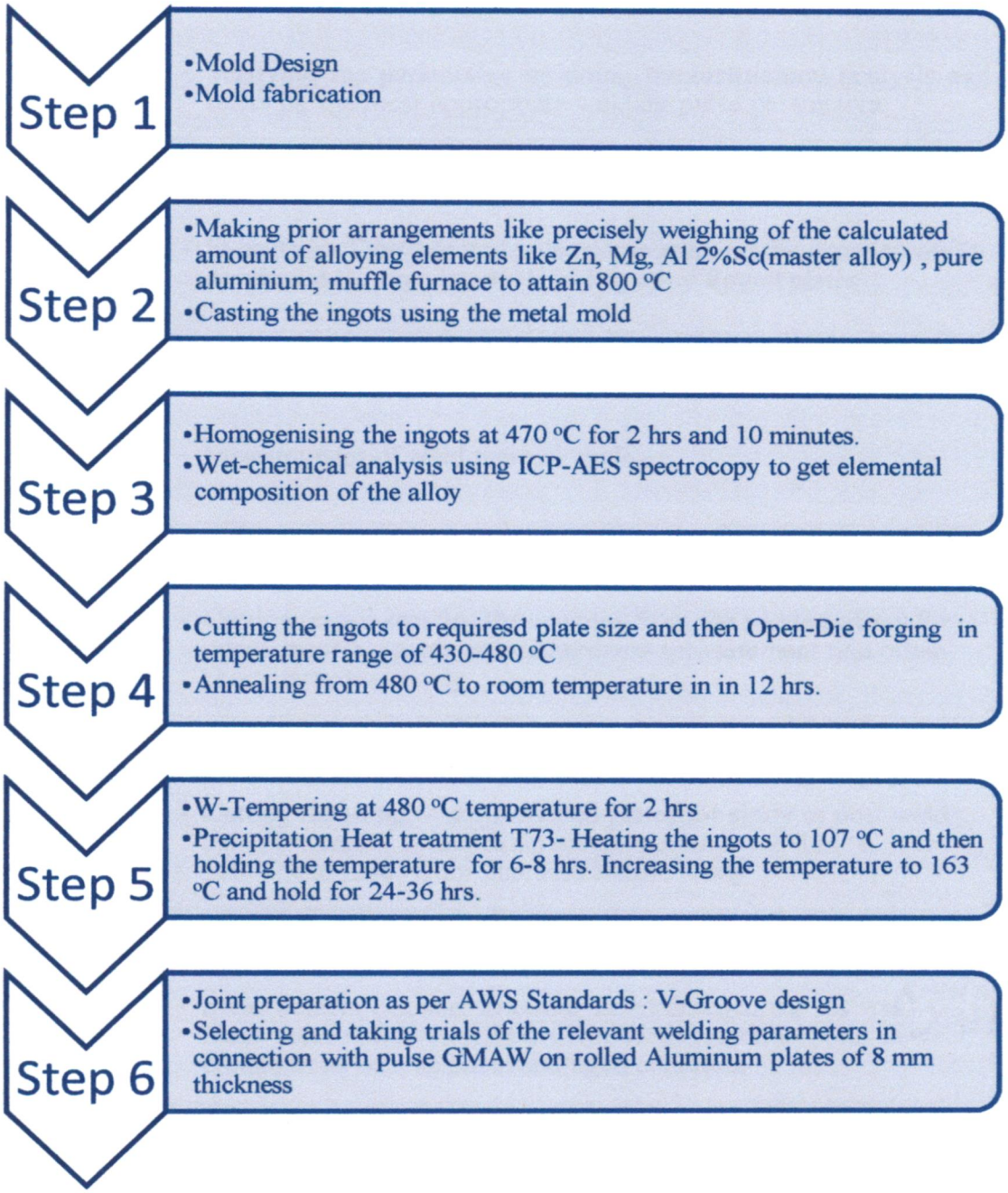

Figure 6: Process Flow Chart indicating the priorities involved in execution of the experimental work (continued on next page)

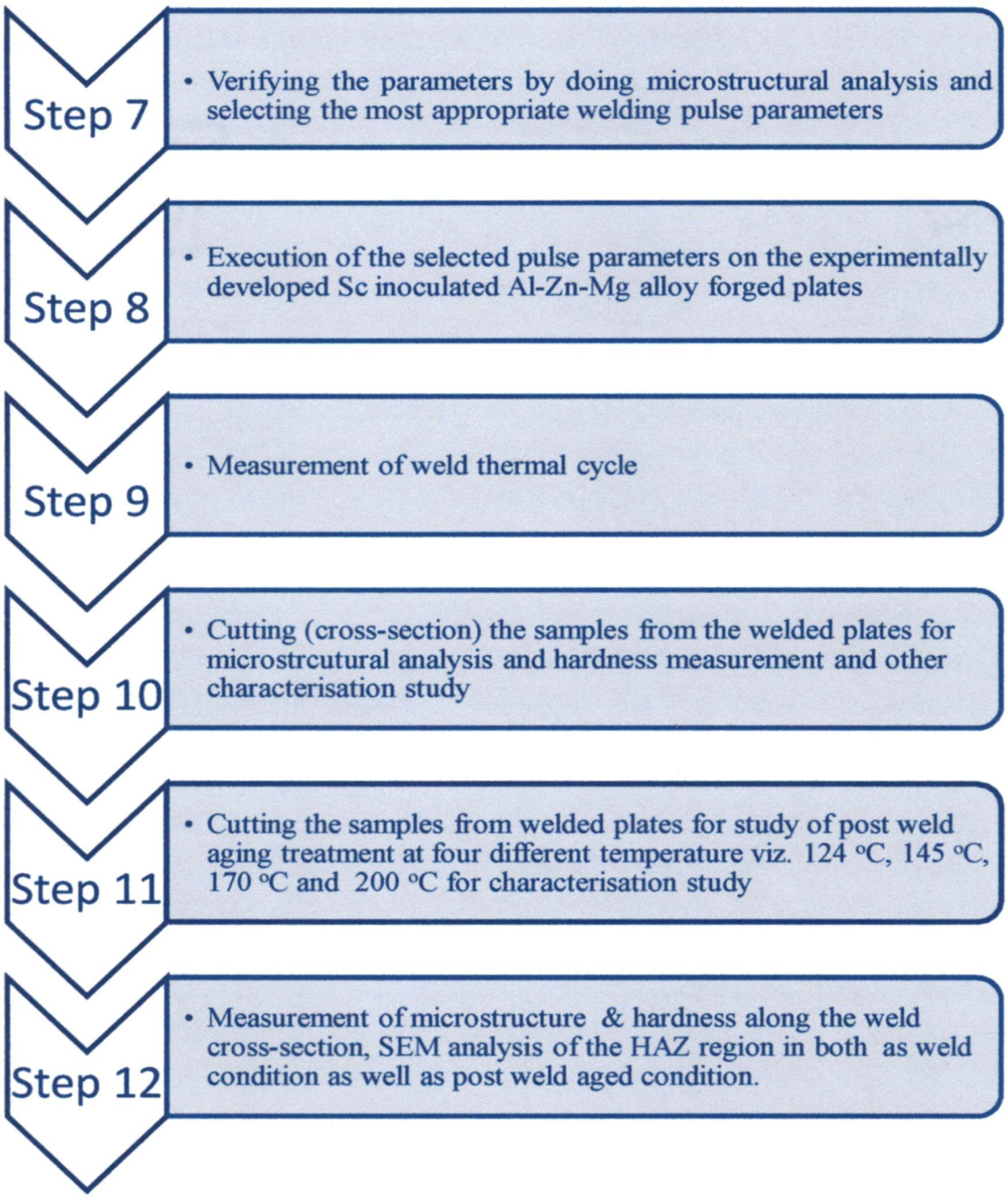

Figure 6: Process Flow Chart indicating the priorities involved in execution of the experimental work

2) Second step is to calculate the theoretical weights of the each component and then using sensitive balance ensuring the accuracy upto 4 decimals weigh the components to be added to the castings.
3) Preparation of the Mold:

   (i) Thorough cleaning of the mold & sealing the mold with clay to avoid leakage.

   (ii) Preheating of the mold to 100 °C to get the water vapor out of the sealing clay.
4) Placing the crucible (with Al lumps inside it) inside the electric furnace & heating it to the 850°C.
5) After reaching the furnace temperature at 850 °C, addition of the calculated amount of Al 2%Sc master alloy pieces to the molten metal is done. There will be sudden drop in temp. by 50 to 60 °C as heat energy is utilized in melting the master alloy pieces. Then waiting for rise in temperature. Up to 850°C till all the master alloy is completely melted into it.
6) After removing the crucible from furnace, addition of the calculated amount of zinc pieces folded in to Aluminum foil is ensured until it gets dissolved completely into the hot melt. Further addition of the calculated amount of Mg pieces folded in Aluminum foil is done until Mg gets completely dissolved. Since Mg burns easily at flame temperature, it is necessary on our part to be careful while adding Mg to melt otherwise the yield will be poor.
7) Finally, quenching the mold into the water & then releasing the mold to get the casting.

Thus, for each respective composition of casting with varying amounts of Sc the above steps need to be followed.

4.2.2 Wet Chemical analysis:

This test was to be performed in order to identify the exact composition of the ingots obtained after casting through wet chemical analysis using a machine called ICP – Mass Spectrometer or ICP-AES at Institute Instrumentation Centre facility. This test identified the percentages of Zn, Mg, Fe, Si and Sc. accurately in the given samples of each casting. The composition of the alloy is as shown in the Table 2.

Table 2: Chemical composition of the cast ingots given by wet chemical analysis:

Type of material*	%Zn	%Mg	%Fe	%Si	%Al	%Sc
BM-2	6.8	3.41	0.083	0.097	Bal	0.65
BM-3	7.86	3.92	0.068	0.088	Bal	0.28
BM-4	6.1	3.22	0.064	0.069	Bal	0.43
BM-5	6.32	3.14	0.079	0.1	Bal	0.11

Note: *the values are verified by ICP-AES analysis

** BM=Base material

Table 3: The composition of filler wire provided by manufacturer is given below:

Type of material	Zn	Mg	Mn	Fe	Si	Cu	Cr	Ti	Al
Filler Wirel (ER5183) A5.10	-	5	1	-	-	-	0.2	0.2	Balance

4.2.3 Homogenizing of the cast Sc inoculated Al-Zn-Mg alloy ingots:

The cast ingots were given a homogenization heat treatment in order to dissolve all the precipitates and get a homogenous structure throughout the material. The cast ingots were homogenized in a pre-heated muffle furnace at temperature 470 °C for a period of 2 hours and 15 minutes. Here, 15 minutes soaking time is provided for material to get stabilized thermally at 470 °C by absorbing the heat energy after sudden change in ingot temperatures from room temperature to furnace temperature.

4.2.4 Open-Die forging of the cast Sc inoculated Al-Zn-Mg alloy ingots:

The castings were cut suitably with the help of power saw, in such a way that 4 parts of equal size were obtained. Screw forging presses, also called energy restricted machine, of 100 tons was employed for forging of the cast ingots. The open-die forging press is as shown as in Fig.7. In cases of forging, the main control-parameters are as follows:

- Temperature of the part to be forged (around 430-480 °C for Al-Zn-Mg alloy)
- Temperature of the die (around 150 °C)
- Forging tonnage (around 60-100 tons)

- Thickness reduced per hit
- Number of hits required to get the desired thickness

The temperature of the die was taken care of by considering a 30 °C increase in casting's temperature (at around 510 °C). The castings were heated in a pre-heated muffle furnace to a temperature of 510 °C. The initial soaking time employed was around 20 minutes. During the transportation of the casting from furnace to forging die & till completion of forging action, a temperature drop of around 50-60 °C was assumed. After every single forging action, the casting was immediately transferred to the furnace & allowed to soak the lost heat & regain the temperature of 510 °C with a average soaking time of around 8 minutes. The process was repeated for almost 12-15 times on every cast cum cut pieces (pieces of around 12 mm thickness) until the thickness of about 8 mm was finally achieved.

Figure 7: Screw-Forging Press

4.2.5 Heat Treatment of the forged Sc inoculated Al-Zn-Mg alloy plates:

1) Annealing: After holding the forged parts at 480 °C for 2 hrs, parts were annealed from 480 °C to room temperature in a time period of 13 hrs.
2) W Temper (Solution Heat Treatment): For forgings, heat to 466 °C, hold temperature for two hours, and then quench in water.
3) T73 (Precipitation Heat Treatment)—Heat to 107 °C and hold temperature for six to eight hours. Then, heat to 162 °C and hold for 24 to 30 hours for sheet and plate. Followed by water quenching.
4) The post weld aging was performed by first cutting the sample of say 8 mm thickness from the welded plates and then the aging was done in a muffle furnace at different aging temperatures viz. 124°C, 145°C, 170 °C and 200 °C for a period of 15 hrs.

4.3 Filler wire:

Aluminum-magnesium filler wire (E 5183) of 1.6 mm diameter is used as the filler for the welds. The chemical composition is as shown in the Table [ ] as per the manufacturer.

4.4 Shielding gas:

Commercial Argon (99.97%) gas is used as a shielding gas for the welding of the processed material. A gas flow rate of 16-18 l/min is maintained during the welding. A gas flow-meter is used to determine the gas flow rate.

4.5 Welding:

4.5.1 Welding Equipment:

The welding of the processed Sc inoculated Al-Zn-Mg alloy forged plates of different compositions was carried out using Gas Metal Arc Welding (GMAW) process with direct current electrode positive (DCEP). The welding machine used is ESAB ARISTO-2000 LUD 450W, supplied by ESAB India Ltd. The wire feed system was

of the push type which consisted of two sets of drive rollers. The drive rollers were adjustable for

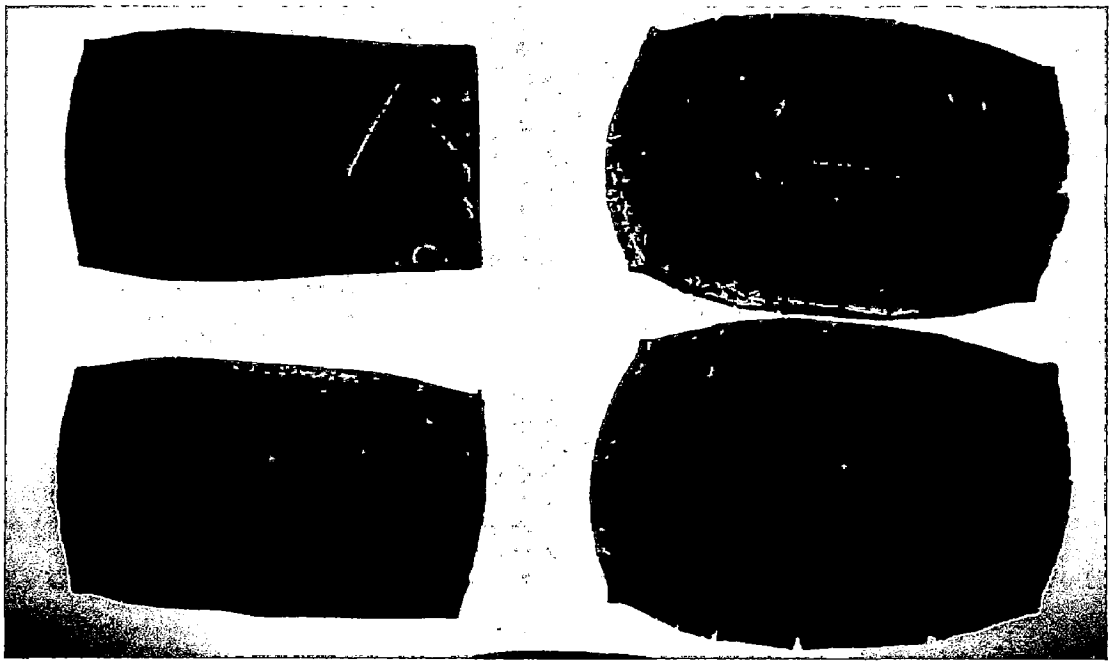

Figure 8: Photograph showing forged plates (Top View)

Figure 9: Photograph showing forged plates (Side View)

providing the required pressure. The water cooled welding torch was mounted on an independently driven variable, speed carriage, supplied by Gullco, Canada. The torch was mounted using a clamping device already mounted on the carriage, which enables

providing the required pressure. The water cooled welding torch was mounted on an independently driven variable, speed carriage, supplied by Gullco, Canada. The torch was mounted using a clamping device already mounted on the carriage, which enables use of different angles of welding torch. A stand-off distance of 15 mm was maintained between the electrode nozzle holder and the work piece during welding.

4.5.2 Joint Design & Preparation:

The processed Sc inoculated Al-Zn-Mg alloy forged plates of different compositions of approximately size (150X45X8) were cut from the centre longitudinally with the help of power saw. As per AWS WHB-2 90 (0784265 0010924), the joint specification for the given plate thickness was chosen as shown in the Fig. 10. Using the shaper machine, the dimensions of the V-groove design were achieved within the prescribed tolerance limits. Pre-welding cleansing operation on the plates was performed mechanically with wire brush and chemically with acetone, so as to remove the dirt or any other foreign matter clinging to the plate. The plates were mechanically fastened/clamped. A root gap of 1.6 mm was maintained by keeping steel spacers at the ends. Run-on and run-off plates are kept so as to increase the weld output and decrease the unwanted start position and end portion of the weld.

4.5.3 Welding parameters:

Both the conventional and pulsed current welds of processed Sc inoculated Al-Zn-Mg alloy forged plates of different compositions was conducted by considering different heat inputs by adjusting different welding parameters where travel speed was kept constant. The welding currents were chosen based upon the transition current (I_t). The conventional GMAW process was done in Synergic mode. The parameters used and the respective heat inputs are tabulated. Refer to Table 4. In case of pulse GMAW, the pulse parameters set manually fed in the semi-automatic machine which controlled the desired wire feed rate for given current value. The voltage is maintained constant during both the processes in the range of ±1 volt. The total heat input is calculated using the formula:

$$H_T = \frac{(V \times I)}{S}$$

Where, H_T = Total heat Input, kJ/cm; V = Arc Voltage, volts; I = welding current, Amperes; S= Welding Speed, cm/min

The parameters were chosen by doing a hit and trial method on the rolled commercial aluminum plates of size 150X60X8 mm. The bead on plate was checked as well as the dummy Aluminum plates were joined to verify the parameters. The tip to work piece distance was kept constant at 15 mm and the shielding gas used is commercial argon(99.97% pure) gas at a flow rate of 18 L/min.

4.6 Specimen collection:

The plates after welding were cleaned mechanically with a wire brush and cleansed by acetone to remove any unwanted matter from a welded plates. The run-on and run-off plates were carefully removed so as to avoid any physical damage to the weld bead. The weld is cut transversely for the purpose of microstructural and hardness analysis. The specimen collection is shown schematically in Fig. 12.

4.7 Analysis of weld geometry:

Weld geometry of the welds are measured with in terms of the bead width, root bead width, dilution and amount of filler metal deposited. The measurements are carried out graphically using transparent graph paper. The data is tabulated and effect of heat input in continuous and pulsed GMAW on dilution, amount of filler metal deposited and bead geometry is studied.

4.8 Dilution measurement:

The dilution of the weld bead was calculated using transparent graph paper with a least count of 1 mm^2. The percentage of dilution in the weld deposit is estimated as below:

$$\%Dilution = \frac{Area\ of\ fused\ base\ metal}{area\ of\ weld\ bead} \text{ X } 100$$

The schematic representation of the measurement procedure is as shown in fig.13. The data is tabulated in Table [ ]and the graph is plotted to show the effect of heat input on dilution in both pulse current and conventional current GMAW processes.

obtained as discussed previously. The specimens were first belt polished. Then the specimens were polished with various grades of emery paper viz. 180, 400, 600, 800, 1000, 1200, 2000 from coarse to fine grades respectively. The final polishing was achieved by using cloth disc polishing machine using alumina as abrasive. Two grades-600 mesh and 800 mesh, of alumina powder were used for final polishing, so as to make the sample scratch free. The polished specimens were then cleansed using the flowing stream of water to remove the unwanted matter. The specimens were then etched using the Kellers's reagent (15 ml HCl + 25 ml HNO_3 + 10 ml HF + 50 ml distilled water) through a cotton swab for 10-15 seconds. The specimens were immediately washed under the flowing water to avoid over etching and then dried using forced hot air.

4.10 Optical Metallography:

The etched samples were then studied using the Leica software and microscope. The study of the weld microstructure and HAZ width was perceived by taking the photographs using the Leica system at different magnifications viz.10X, 20X, 50X. The effect of heat input on the microstructure has been studied.

4.11 HAZ width measurement:

HAZ width measurement is carried out along with the microstructural studies. In normal cases the grain coarse region adjacent to the fusion line is considered as the HAZ of the welded plates. The width of the grain coarsened region is measured under optical microscope using the Leica system (software + microscope). The HAZ width was measured and different regions on both sides of the weld, then the average of the values is taken as HAZ width of a particular heat input. The values obtained were then tabulated (Refer Table 6) and the effect of heat input on HAZ width was studied for weld of the both conventional current and pulsed GMAW.

4.12 Porosity measurement:

The porosity content of the weld deposit was estimated by metallographic technique using the standard point counting method. The volume fraction of porosity was estimated by random measurement of area fraction of porosity, which appears as

a black round spot in a matrix of unetched polished specimen. The area fraction is taken as the volume fraction in this case because the volume fraction is a linear function of area fraction. A reticule having 100 grid points (10X10) is taken and used at a magnification of 50X, which is found to be adequate to carry out the work. At this size, the spot size of porosity is found small enough to avoid touching of the two given points at a time and appropriate weigthage has been given to the larger points to their size. At least 15 readings were taken randomly inside the weld area to calculate the porosity and the values have been tabulated.

4.13 Hardness measurement:

Hardness measurement on the welded specimens was performed using Vicker's Hardness tester. The hardness measurement was carried out at a load application of 10 kg. The hardness is measured along the weld section, starting from the weld bead centre and moving outwards towards the base metal with a distance of 3 mm in between the two consecutive readings or indentation. This minimum distance is required to avoid any strain hardening. The schematic representation of the hardness of the hardness measurement is as shown in Fig. 14. The diagonal made by the square based diamond pyramidal indenter were measured and then the average is taken. Then using the hardness conversion tables provided along with the machine are noted down. The hardness values are then tabulated and studied. The same procedure is used for hardness measurement of the post weld aged sample.

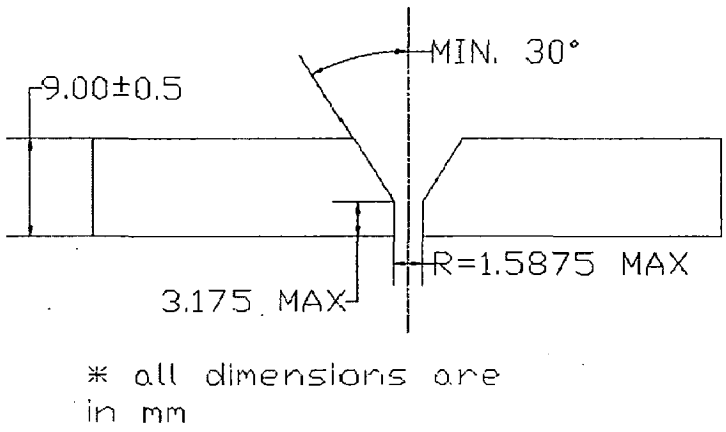

Figure 10: Joint Design generated using Auto-Cad 2007

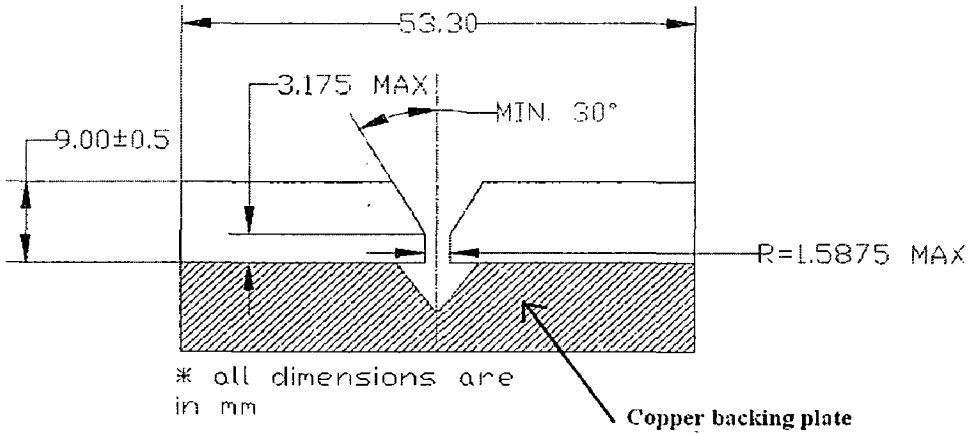

Figure 11: Line diagram shows the welding setup of plates with copper backing plate

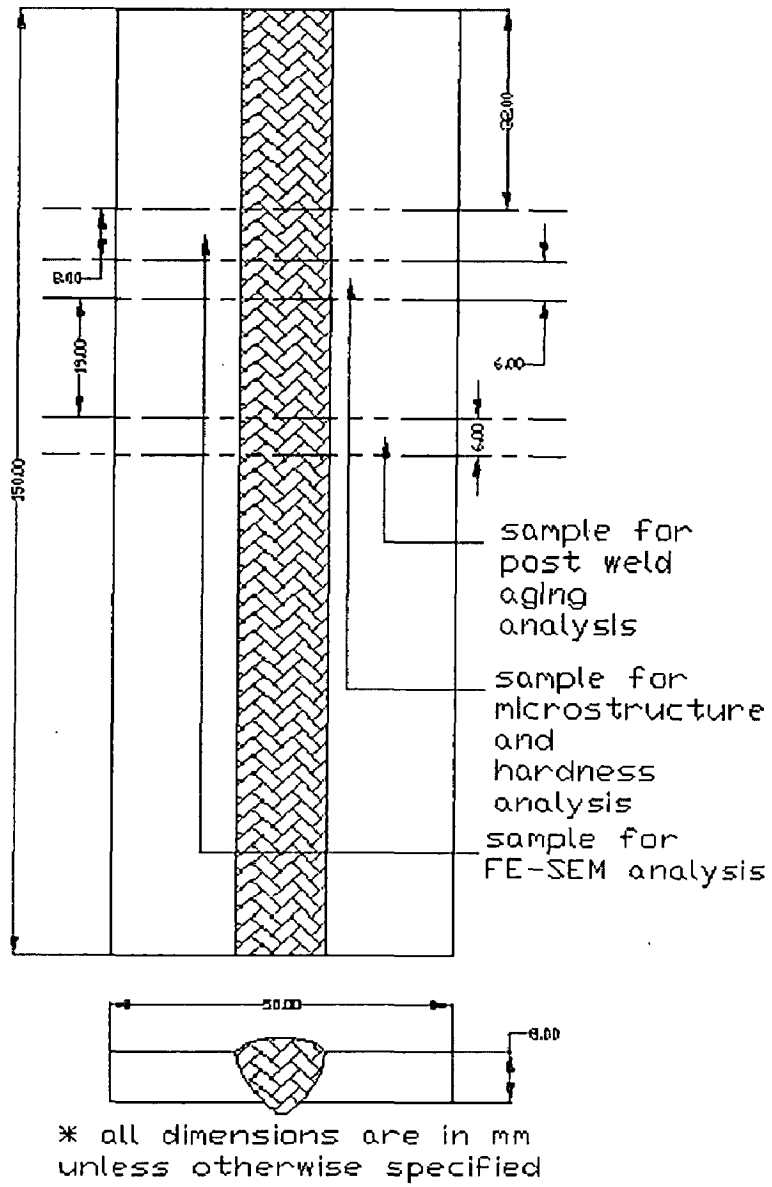

Figure 12: Schematic view of the sample collection from the welded plates

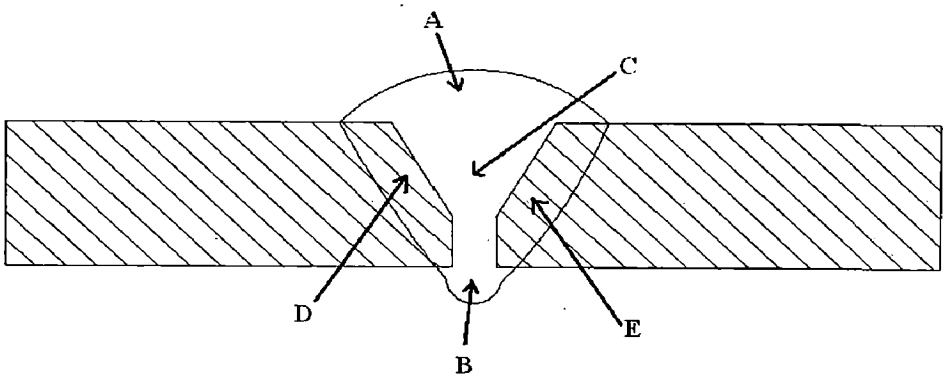

Figure 13: Schematic representation of dilution calculation graphically

$$\% \text{ Dilution} = \frac{D+E}{A+B+C+D+E} X\ 100$$

D+E = Area of base material in the weld area, mm^2

A+B+C+D+E = Total Weld Area, mm^2

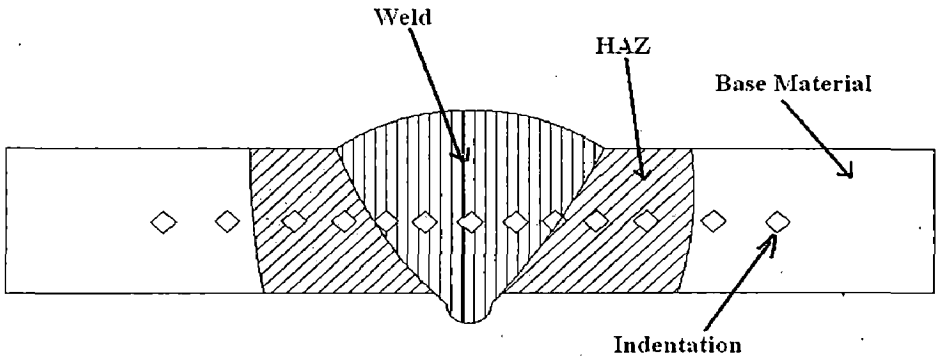

Figure 14: Schematic representation of the microhardness measurement

Chapter 5: Results and Discussion

5.1 Base material:

The four ingots of experimental Al-Zn-Mg alloys with scandium inoculation were cast using a metal mold to get the ingots of dimension 150 X 90 X 24 mm which were further homogenized at 470 °C for 2 hrs and 15 minutes. To understand the hardening nature of the material, the samples of as-cast material were given suitable aging cycle at two different temperatures viz. 125 °C, 150 °C and the hardness was measured at different periods starting after 18 hrs extended up to 32 hrs. The graph of hardness versus time was plotted as shown in Fig.15-18. The homogenized ingots were further cut into equal parts and then the cut plates were heated upto 510 °C and were given 20 minutes soaking time. After which the cut plates were open die-forged under a 100 ton screw hammer forging press with an average soaking time of 5 minutes per hit. The cut plates thickness was given almost 30 % reduction in thickness in 12-15 strokes to get thickness of 8 mm, after which the forged parts were annealed to room temperature from 480 °C over a span of 13 hrs. Further, standard solution heat treatment (W Temper) followed by precipitation heat treatment T73 were employed on the annealed forged plates. These forged and heat treated alloy plates were further used for their weldability characterization using the pulse GMAW process. This experimental alloy plates were tested only in terms of weld geometry, hardness and its microstructure. The microstructures of the all four base materials are shown in (d) part of the Fig. 34-37, Fig. 38-41, Fig. 42-45, Fig, 46-49 respectively.

5.2 Welding:

The welding parameters used and the corresponding heat inputs is shown in the Table 4. The data shows the different heat inputs applied during the continuous current and pulsed current GMAW. Table 4 also indicates the values of ϕ calculated for various pulse parameters used in welding the experimentally developed forged cum heat treated Sc inoculated Al-Zn-Mg alloys. Figures 19-22 show different

weld beads (for each experimental alloy) formed in continuous current GMAW as well as pulse current GMAW.

5.3 Weld geometry:

5.3.1 Weld size:

The macrographs of the weld beads of both continuous current GMAW as well as pulse current GMAW on the experimentally developed forged cum heat treated Sc inoculated Al-Zn-Mg alloys are as represented in Fig.23-24 . The figure shows the macrographs of the weld section at different heat inputs.

From the macrographs and Fig. 23-24, it's clearly visible that amount of heat input to the weld governs the size of the weld bead in a proportion which is in accordance with the previous reported work [70,71]. Hence, as the heat input increases, the amount of filler metal deposited is more i.e. a bigger weld bead is formed proportionately. Full penetration is observed in all the cases of welded parts of experimental alloys. This full penetration can be adjudged by observing the root bead dimensions in each and every case. The Fig.23-24 shows the effect of variation in weld geometry with change in pulsing frequency of the pulse current used in GMAW which is accordance with the previous reported work[71,72]. Here, it's worth noting that the effect of frequency on the weld geometry is nearly independent of the base material composition variations which can be justified from the graph. The data of the amount of filler metal deposited for various welding parameters and the heat inputs is tabulated in the Table 7. The graph showing the effect of heat input on the amount of filler metal deposited is plotted. Refer to Figure 64. From the data and the graph, it's clear that the amount of filler metal deposited primarily depends upon the weld parameters which govern the heat input as well as on the filler wire material characteristics.

5.3.2 Dilution:

The data collection done using the graphical method for calculating the dilution in the weld bead is tabulated in Table 5 & 6 for continuous current GMAW and pulsed current GMAW respectively. Using the data calculated, the effect of heat input on dilution for both continuous current and pulsed current GMAW was shown

on a graph. Refer Fig.26 From the graph, it's a clear indication that the amount heat input governs the dilution in weld bead i.e. as the heat input increases, the weld dilution increases remarkably for both the process routes. With the increasing heat input, the amount of base material melting increases in same proportion i.e. weld dilution is a direct measure for estimating the weld fill-up characteristics. The weld-macrographs shown in Fig.23-24 justify the above statement. Weld dilution is also an indirect indication of dependency of amount of filler metal added to the weld pool. The welding parameters in the pulse GMAW significantly control the filler metal melting characteristics and the arc nature and its stability. At the same time, the shielding gas controls the heat delivery along the arc to the base material. Hence, the characteristics of the shielding gas indirectly control the dilution rate. Hence, the weld dilution rate is a function of many welding parameters including the nature of base material and filler material.

5.4 Porosity Content:

Here, the porosity content is measured using the metallographic technique. The microstructural analysis of the weld zone revealed the black pores in white unetched polished background. Using the software " Dewinter Material Plus 4.1" , the area of the pores was measured with respect to the area under consideration. The porosity in terms of area percentage was calculated by the software. Fifteen such readings were taken and then the average of it was taken as a porosity value and is tabulated in Table 5 and Table 6. The porosity is a direct function of cleanliness of the welding setup as well as thorough pre-welding cleaning procedures being followed on the base material as per standards. It also depends upon the shielding gas quality. Here, porosity was found to be distributed throughout the weld zone in both the cases of continuous current GMAW as well as the pulse current GMAW. In some cases, porosity was relatively higher near weld bead top while in some cases it was found along the weld fusion line. The porosity was not found near the root which may be due to the thorough welding achieved by higher heat input. The continuous current GMAW yielded more porosity compared to the pulsed current GMAW because the amount of heat added in continuous current GMAW is more compared to the pulse GMAW. Due to excess heat added to the weld pool, it cools at a slower rate in case

of continuous current GMAW compared to pulse GMAW. As a result, the hydrogen absorption capacity of the liquid is highest in case of welds with continuous current GMAW over the pulse GMAW. During the pulse current GMAW, thepusing nature of the current may result in fluctuations inside the inert jacket of shielding gas which may allow for air aspiration into the arc environment resulting into increment into level of porosity [70,73]. Finer and low porosity was observed in case of low heat input weld which contributes to higher weld joint strength as compared to the high heat input weld. Using the data obtained, a graph showing the effect of heat input and the frequency on the % porosity was plotted.(Refer Fig.27-28)

5.5 HAZ width:

The widths of the HAZ measured for the welds, obtained from both the processes viz. continuous current GMAW and pulse GMAW on different compositions are tabulated in Table 6. Using the data obtained, graph was plotted between the heat input and the HAZ width to study the effect of heat input on the width of HAZ. Refer Fig. 29

The graph clearly indicates that the increase in heat input drastically increases the HAZ width, this is because of high thermal conductivity associated with aluminum and its alloys. A HAZ width obtained in case of welds with pulse current GMAW is more than the continuous current GMAW welds. When the heat content is more, the droplets are smaller in size and the heat content of the molten droplets is more compared to low heat input case.

5.6 Microstructure and Hardness Analysis:

- Fig.23-24 shows the microstructures of the weld transverse sections of the Al-Zn-Mg-Sc alloys viz. BM-2, BM-3, BM-4, BM-5; welded with both the pulse current GMAW and continuous current GMAW at different heat inputs and welding parameters shown in Table 4. The microstructures show a) weld bead center, b) fusion line, c) HAZ region and d) Base Material.
- The microstructure of the weld fusion zone shows (Refer part (b) of Fig.34-49), a non-dendritic structure is observed which can be attributed to the pulsing nature of the heat input or current. During the pulse-off period, as the

molten filler metal from the previous pulse-on period, the molten metal starts to freeze wherein arc heat input and new molten filler metal droplets arrives in from the next pulse-on period resulting into disruption in the dendritic growth of the molten filler metal. Since, the molten metal hits the bare metal at the root of the joint, the freezing of molten pool first begins at close to the fusion line at the root. Thus, coarse columnar grains tend to grow from weld fusion line towards the weld bead center. The microstructure of the weld zone as reported in the previous work[74] says that normally in case of 7xxx series alloys, the weld zone contains coarse columnar structures grains, due to the existence of the thermally instigated weld metal solidification behavior. This degrades the mechanical properties and instigates its tendency of hot cracking. Numerous methods of refining the weld fusion zone have been under experimentation e.g. inoculation with heterogeneous nucleants, microcooler addition, surface nucleation induced by gas impingement and introduction of physical commotion through controlled processes like pulse-GMAW[75,76]. Thus, the combined effect of pulse GMAW process and its parameters on the Scandium inoculated Al-Zn-Mg alloys resulted into a refined fusion zone with absence of columnar grain structures as justified by the microstructures in part (b) of Fig. 34-49. Hence, the weld zone formed is more of approximately fine spherical grains without any dendrites, thereby giving homogeneity to the weld bead zone structure which is completely in accordance with the observed microstructures.(Refer part (a) of Fig.34-49).

- Also, previous work reports [77] indicate that there are structural changes associated with the HAZ of the Al-Zn-Mg alloys viz. increased growth rate of precipitates, degeneration of some precipitates, transformation of precipitates to equilibrium forms, the direct nucleation of more equilibrated precipitates. These changes depend upon the factors like base metal composition and thermal history which in turn is affected by the welding process & its parameters as well as joint type.
- The previous investigations [77] reveal that the high temperatures experienced by the region adjoining to the fusion line prevails for sufficient time resulting into precipitate dissolution within in the grains. The η' and η precipitates

quickly dissolve(in < 10 secs) in the temperature range of 300-350 °C. The η precipitates at grain boundaries and sub-grain boundaries completely dissolve at temperatures above 400 °C and below 350 °C they remain in equilibrated cum coarsened condition. Thus, during the cooling phase, supersaturation state is reached which may result into hardening precipitates to form and strengthen the HAZ. This is in accordance with the observed peak hardness achieved in HAZ region (Refer Fig.30-33) with additional help from Scandium inoculation. Al_3Sc particles formed provide good confrontation to the recrystallization phenomenon as well as provide age harden ability which helps in retaining or increased strength, ductility, corrosion resistance etc. of the material in HAZ region [78]. This precipitation is reliant upon the quench sensitivity of the region. The grain boundary segregation after the dissolution reactions may alter the quench sensitivity of grain boundaries resulting into increased precipitation of η precipitates at grain boundaries. In outer regions, the time-temperature conditions are ideal for growth or transformation of precipitates into stable structures where as others dissolve. In temperature range 200-300 °C, η precipitates coarsen while η' precipitaes dissolve within 10-30 secs. In remaining HAZ, the temperatue which is below 200 °C, variety of precipitation and/or dissolution reactions may occur. Under the low heat input/slow heating rates, some of these reactions which are sluggish in nature, may result into formation of equilibrated precipitates which further transforms into G.P. zones + η' + η. If the G.P.zones are heated rapidly, they may dissolve to increase the supersaturation in the region. The cooling of these will obliviously give rise to new G.P.zones which helps in natural aging of the HAZ region. The whole of the above discussion seems to be in accordance with the data obtained. (Refer microstructures in Fig.33-48 and hardness profile curves in Fig.30-33)

- The welding problems associated with the Al-Zn-Mg alloy as reported in the previous work [79], indicates that in practice the failure occurs in the liquated region of the HAZ. The high heating rates associated with the welding processes tends to change the base metal's microstructure in the adjoining region to the weld fusion zone. This is due to the non-equilibrium melting

which needs due consideration [79]. In that case, the segregation of the grain boundary along with the η-precipitates getting heated at a rate which makes the diffusion time insufficient for homogenization of the structure. This may lead to inception of melting i.e. liquation of the grain boundaries. Microcracks may appear in the liquation zone in presence of hydrogen and/or instigative strain values. Also due to the change in composition in the regions may reduce the toughness after aging [80].

The control of liquation and liquation cracking in Al-Zn-Mg alloys could be achieved by attempting to control the grain size, amount of homogenization, insoluble impurities and alloying contents. Since, copper instigates the liquation cracking and in order to increase the weldability, its best to keep the copper content in the Al-Zn-Mg alloy to lowest possible value preferably below 0.2 %. The deterioration of the aging response may be due to the growth of η-precipitates at the expense of G.P. zones was indicated in the previous work [81].

In an attempt to minimize the above said drawbacks, the mechanically strengthening of the Scandium inoculated Al-Zn-Mg alloy was achieved by hot open-die forging of the material with approximately 34 % reduction in thickness followed by solution heat treatment and T73 heat treatment. The T73 which is reported to result into overaging in 7xxx series alloys, thereby reduce the mechanical strength in order to gain some resistance to stress-corrosion cracking. This mechanical processing combined with Scandium inoculation resulted into strengthening of the HAZ region indicated by peak hardness in the HAZ region shown in hardness profile graphs (refer Fig.30-33)as compared to that obtained in simple as cast aged structure(refer Fig.15-18). Also, due to scandium inoculation which shows anti-recrystallization property in Al-alloys, no significant grain coarsening occurred in the HAZ region as evident from the grain size measurement(Refer Table 6) and the microstructures reported in part (b) of Fig.34-49.

The hardness obtained in the weld bead center was lower compared to the HAZ region (Refer part (a) of Fig.34-49) which may be attributed to the presence of porosity inside the weld bead and work hardenable filler alloy

system.

5.8 Effects of post weld aging on the microstructure and hardness:

Significant, degradation of the microstructure was observed. There was grain coarsening(Refer Table 6) of the HAZ region and base metal with segregation of the Scandium at the grain boundaries as verified by the EDAX-SEM analysis and elemental mapping technique of the post weld aged HAZ. The drop in the hardness of both the HAZ region and the base metal was notable. These effects were pronounced as the post weld aging temperature increased.

5.9 Comparison of pulse current with continuous current GMAW:

In the present work, with the help of results obtained the effects of pulse current and continuous current in GMAW process on the weld zone of Sc inoculated Al-Zn-Mg alloys clearly are analyzed.

i. The arc stability, as observed during the experimentation indicated that pulse current arc was bit difficult to stabilize over the particular joint design due to the frequent interruptions in current. Since, the nature of the arc vastly depends upon the shielding gas nature, joint design, pulse parameters and wire feed rate, number of iterations/alterations are required to attain a stable arc in case of pulse current to get the desired weld quality. However, for higher heat inputs in pulse current GMAW, the mean current is high enough to give stability to the arc and vice versa. While in case of continuous current GMAW, the arc stability is achieved easily if the required heat input for the desired weld quality is known. With synergic mode of control, the welding arc could be stabilized even more quickly.

ii. The weld beads obtained in pulse GMAW are larger as compared to that obtained in continuous GMAW as shown in Fig.

iii. The dilution of the weld zone depends upon the amount of heat input and filler metal deposition. As the amount of heat added in pulse current GMAW is

relatively lower with high rate of filler deposition, the dilution rate is less compared as to that of continuous current GMAW.

iv. Porosity is a direct function of cleanliness procedures and the amount of heat input applied to the weld joint. With proper control of joint cleanliness by using mechanical and chemical procedures, the amount of porosity obtained could be minimized. As the amount of heat input increases, the fluidity of the molten weld zone remains for sufficient time to drive out the hydrogen gas bubbles(responsible for porosity) by buoyancy effect. But increased heat input has its own disadvantages as discussed previously. Hence, the pulsing effect of the arc should be sufficiently high enough to generate turbulence inside the molten weld zone to drive out the hydrogen bubbles. This depends directly upon the pulse frequency of the current used. Also, the shielding gas (free of moisture) flow rate should be high enough to avoid entrapment of the gas into the freezing molten weld zone. It's hard to optimize all the parameters as it requires number of iterations to arrive at optimum value. Best possible solution could be control of the heat input and the pulse parameters say Ø or use of multi-pass welding with reinforcement. In case of pulse current, the level of porosity achieved was lower in most cases where the heat input was high. The continuous current has higher heat input but the absence turbulence achieved by pulsing effect of the pulse current, makes it vulnerable for hydrogen absorption during freezing at the top of the weld bead which is in accordance with the observations. (Refer Fig.22-23)

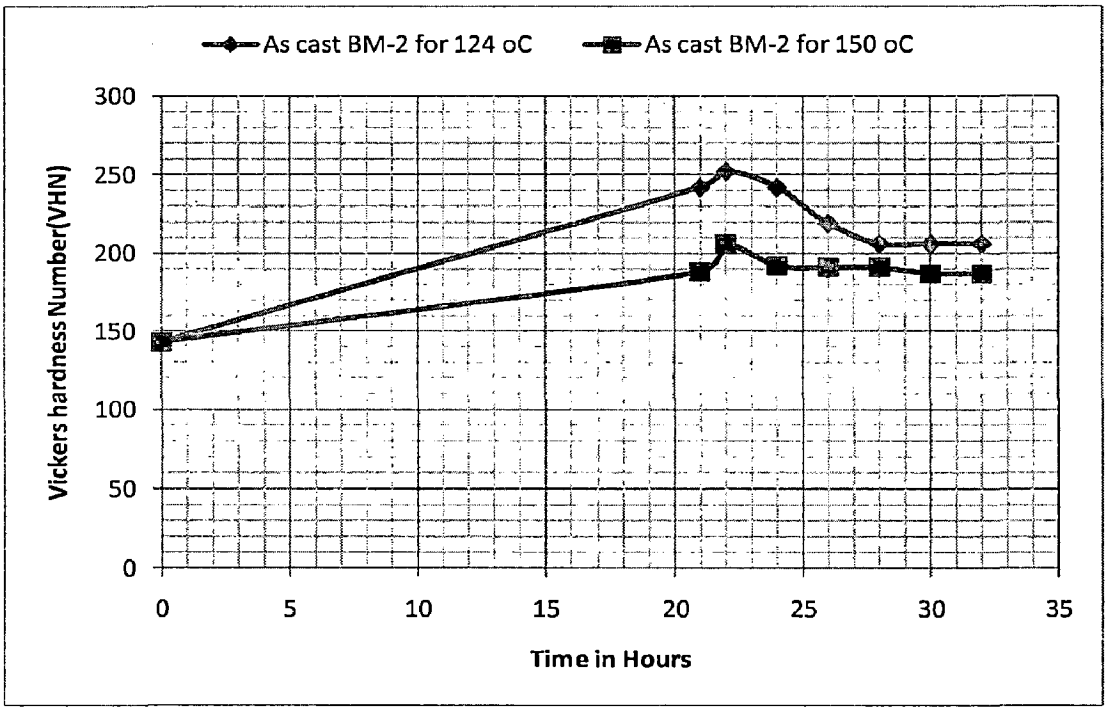

Figure 15: Aging curve for BM-2 at 124 °C and 150°C respectively.

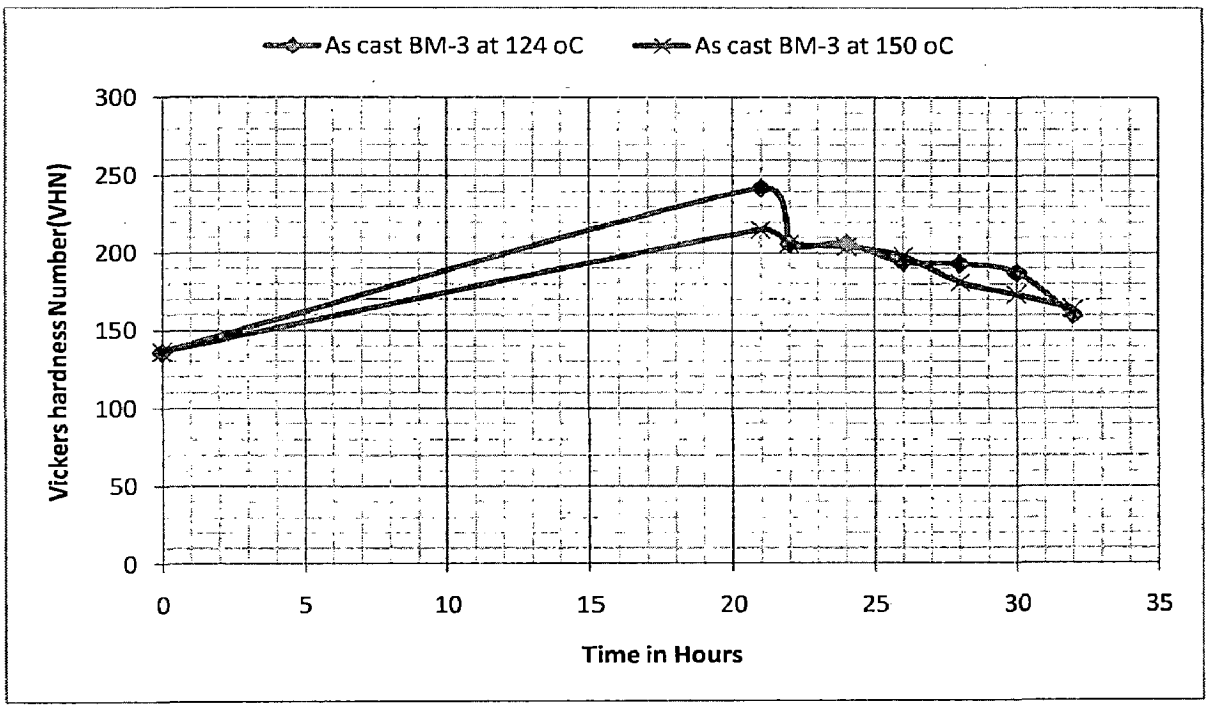

Figure 16: Aging curve for BM-3 at 124 °C and 150°Crespectively

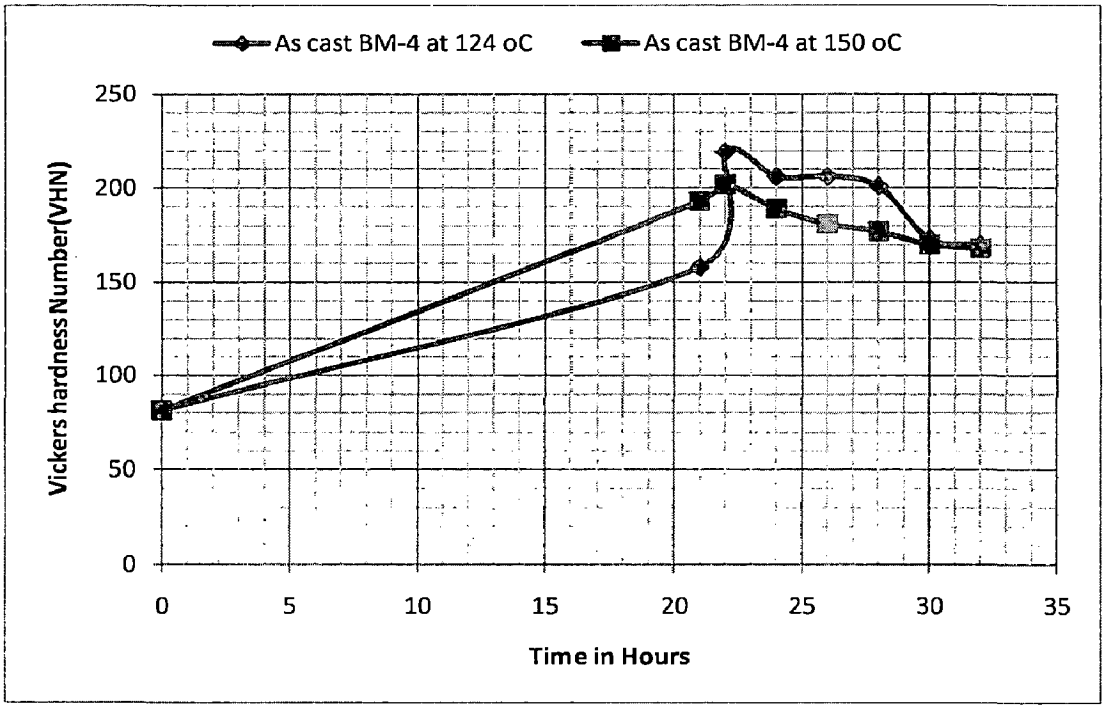

Figure 17: Aging curve for BM-4 at 124 °C and 150°Crespectively.

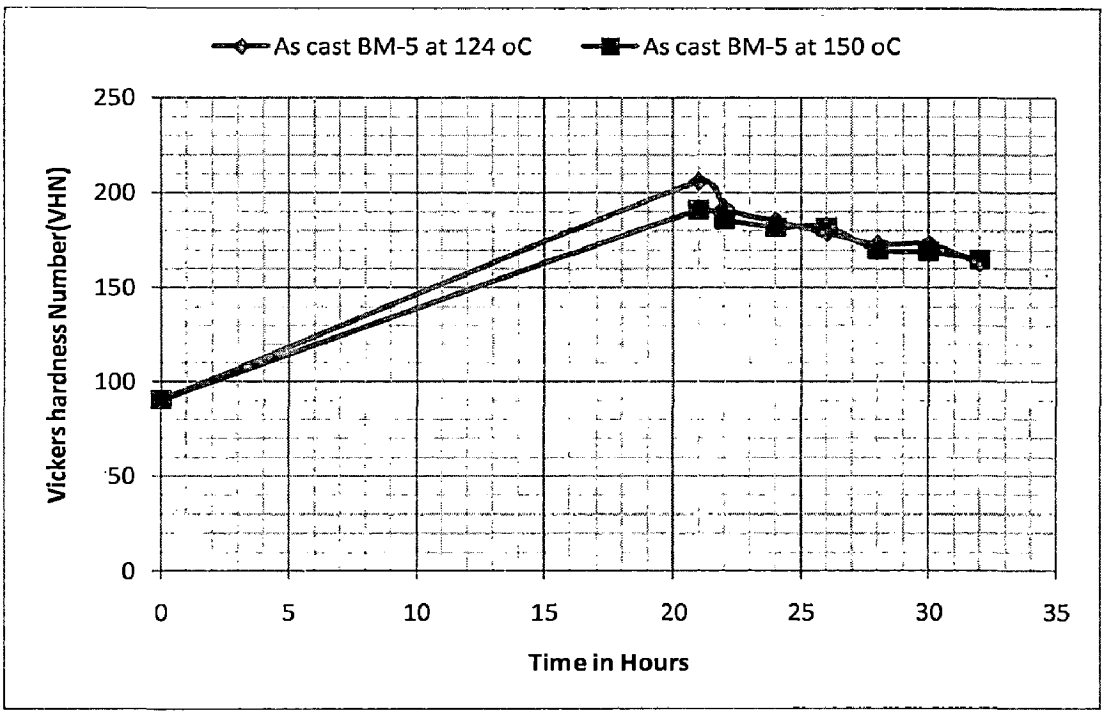

Figure 18: Aging curve for BM-5 at 124 °C and 150°Crespectively.

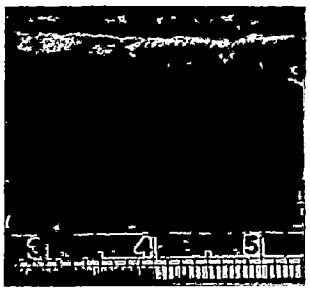

a) Material Designation: BM-2(1)							
V (volts)	I_p (Amp.)	I_b (Amp.)	f (Hz.)	t_p (ms)	t_b (ms)	V_w (m/min.)	V_t (cm/min.)
24	308	116	74	4.1	9.4	5	34.9

Ø	0.262
Heat i/p (kJ/cm)	7.1917

(a)

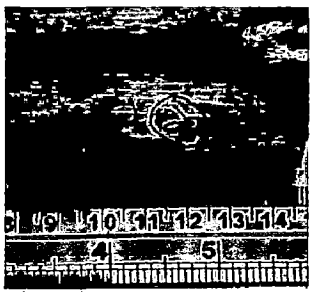

b) Material Designation: BM-2(2)							
V (volts)	I_p (Amp.)	I_b (Amp.)	f (Hz.)	t_p (ms)	t_b (ms)	V_w (m/min.)	V_t (cm/min.)
24	400	152	58	3.2	14	7.5	34.9

Ø	0.31
Heat i/p (kJ/cm)	8.173

(b)

c) Material Designation: BM-2(3)							
V (volts)	I_p (Amp.)	I_b (Amp.)	f (Hz.)	t_p (ms)	t_b (ms)	V_w (m/min.)	V_t (cm/min.)
26	392	58	40	7.6	17.4	6.6	34.9

Ø	0.2
Heat i/p (kJ/cm)	8.939

(c)

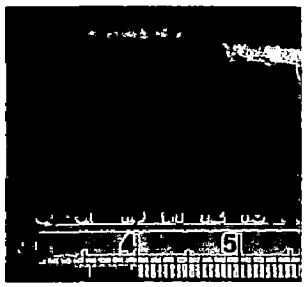

d) Material Designation: BM-2(4)							
V (volts)	I_p (Amp.)	I_b (Amp.)	f (Hz.)	t_p (ms)	t_b (ms)	V_w (m/min.)	V_t (cm/min.)
25	265	-	-	-	-	5	34.9

Ø	1
Heat i/p (kJ/cm)	11.389

(d)

Figure 19: Different weld beads produced (a),(b),(c) by pulse GMAW and (d) by continuous GMAW for BM-2.

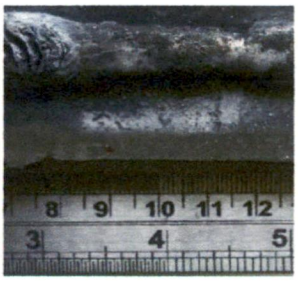

a) Material Designation: BM-3(1)							
V (volts)	I_p (Amp.)	I_b (Amp.)	f (Hz.)	t_p (ms)	t_b (ms)	V_w (m/min.)	V_t (cm/min.)
24	372	92	66	8.9	6.3	9.5	34.9

Ø	0.1
Heat i/p (kJ/cm)	10.562

(a)

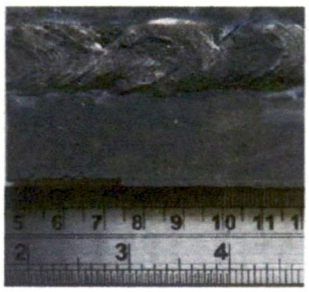

b) Material Designation: BM-3(2)							
V (volts)	I_p (Amp.)	I_b (Amp.)	f (Hz.)	t_p (ms)	t_b (ms)	V_w (m/min.)	V_t (cm/min.)
24	424	136	72	5.4	8.5	9.8	34.9

Ø	0.2
Heat i/p (kJ/cm)	10.273

(b)

c) Material Designation: BM-3(3)							
V (volts)	I_p (Amp.)	I_b (Amp.)	f (Hz.)	t_p (ms)	t_b (ms)	V_w (m/min.)	V_t (cm/min.)
24	452	212	88	1.9	9.5	10	34.9

Ø	0.39
Heat i/p (kJ/cm)	10.397

(c)

d) Material Designation: BM-3(4)							
V (volts)	I_p (Amp.)	I_b (Amp.)	f (Hz.)	t_p (ms)	t_b (ms)	V_w (m/min.)	V_t (cm/min.)
28	389	-	-	-	-	10.2	34.9

Ø	1
Heat i/p (kJ/cm)	18.725

(d)

Figure 20: Different weld beads produced (a),(b),(c) by pulse GMAW and (d) by continuous GMAW for BM-3.

a) Material Designation: BM-4(1)							
V (volts)	I_p (Amp.)	I_b (Amp.)	f (Hz.)	t_p (ms)	t_b (ms)	V_w (m/min.)	V_t (cm/min.)
25	388	100	64	8.8	6.6	9	34.9

Ø	0.1451
Heat i/p (kJ/cm)	11.372

(a)

b) Material Designation: BM-4(2)							
V (volts)	I_p (Amp.)	I_b (Amp.)	f (Hz.)	t_p (ms)	t_b (ms)	V_w (m/min.)	V_t (cm/min.)
23	444	140	74	5.7	7.6	9	34.9

Ø	0.1773
Heat i/p (kJ/cm)	10.684

(b)

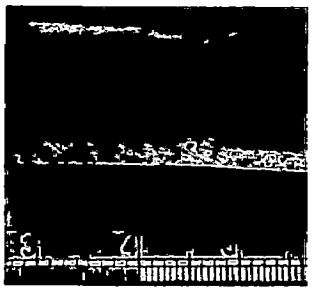

c) Material Designation: BM-4(3)							
V (volts)	I_p (Amp.)	I_b (Amp.)	f (Hz.)	t_p (ms)	t_b (ms)	V_w (m/min.)	V_t (cm/min.)
26	456	160	78	4.1	8.2	9	34.9

Ø	0.2244
Heat i/p (kJ/cm)	11.559

(c)

d) Material Designation: BM-4(1)							
V (volts)	I_m (Amp.)	I_b (Amp.)	f (Hz.)	t_p (ms)	t_b (ms)	V_w (m/min.)	V_t (cm/min.)
24	250	-	-	-	-	8.4	34.9

Ø	1
Heat i/p (kJ/cm)	11.372

(d)

Figure 21: Different weld beads produced (a),(b),(c) by pulse GMAW and (d) by continuous GMAW for BM-4.

a) Material Designation: BM-5(1)							
V (volts)	I_p (Amp.)	I_b (Amp.)	f (Hz.)	t_p (ms)	t_b (ms)	V_w (m/min.)	V_t (cm/min.)
26	416	144	54	4.6	14.1	9	34.9

Ø	0.2635
Heat i/p (kJ/cm)	9.431

(a)

b) Material Designation: BM-5(2)							
V (volts)	I_p (Amp.)	I_b (Amp.)	f (Hz.)	t_p (ms)	t_b (ms)	V_w (m/min.)	V_t (cm/min.)
24	472	220	88	1.8	9.6	9	34.9

Ø	0.3937
Heat i/p (kJ/cm)	10.48

(b)

c) Material Designation: BM-5(3)							
V (volts)	I_p (Amp.)	I_b (Amp.)	f (Hz.)	t_p (ms)	t_b (ms)	V_w (m/min.)	V_t (cm/min.)
24	412	212	62	2.4	13.7	9	34.9

Ø	0.437
Heat i/p (kJ/cm)	10.934

(c)

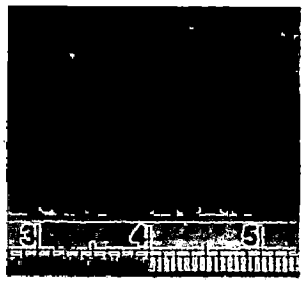

d) Material Designation: BM-5(2)							
V (volts)	I_p (Amp.)	I_b (Amp.)	f (Hz.)	t_p (ms)	t_b (ms)	V_w (m/min.)	V_t (cm/min.)
24.5	250	-	-	-	-	8.4	34.9

Ø	1
Heat i/p (kJ/cm)	10.53

(d)

Figure 22: Different weld beads produced (a),(b),(c) by pulse GMAW and (d) by continuous GMAW for BM-5.

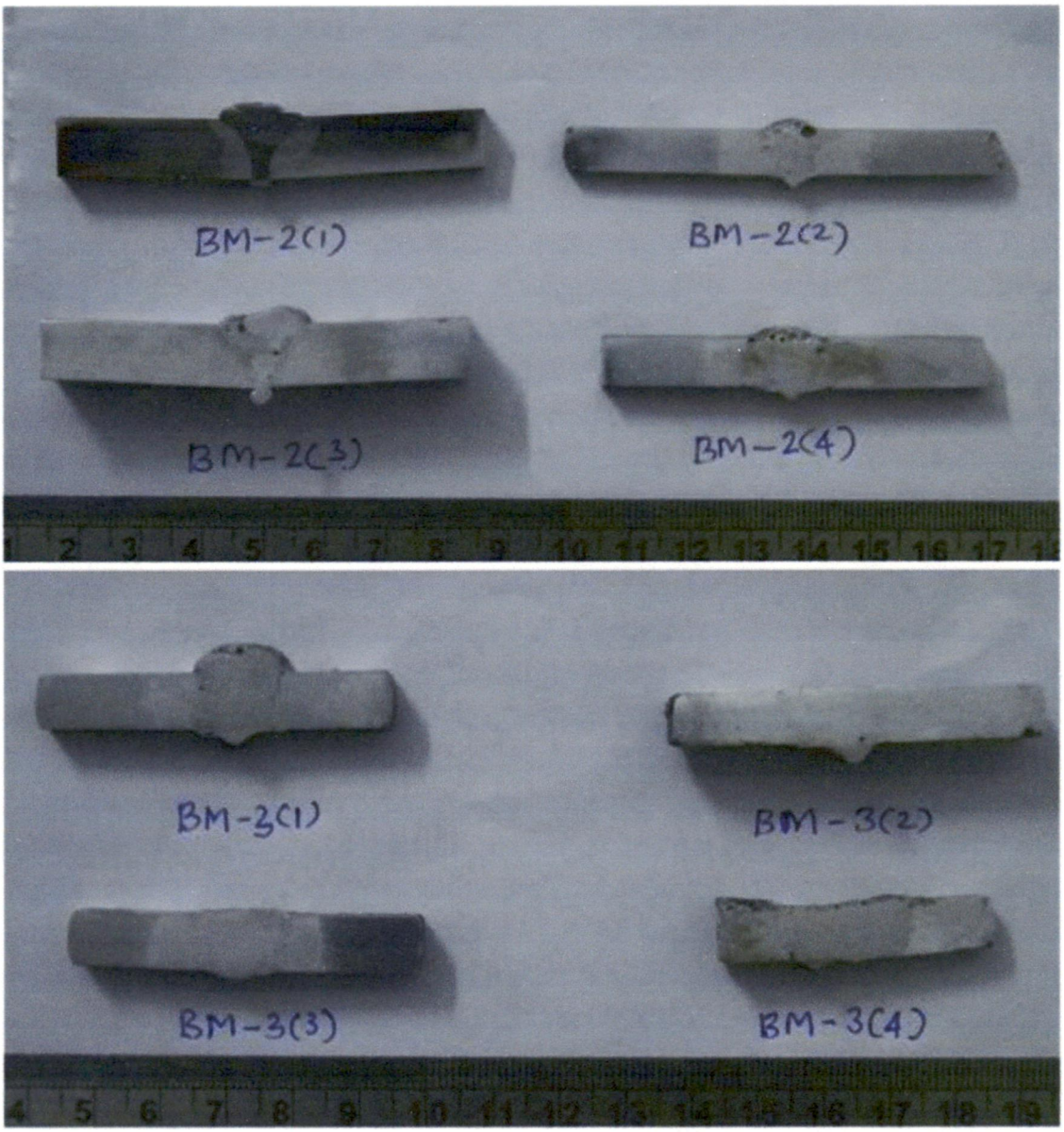

Figure 23: Weld Transverse sections of the GMA welded plates of BM-2 and BM-3 material at different welding parameters

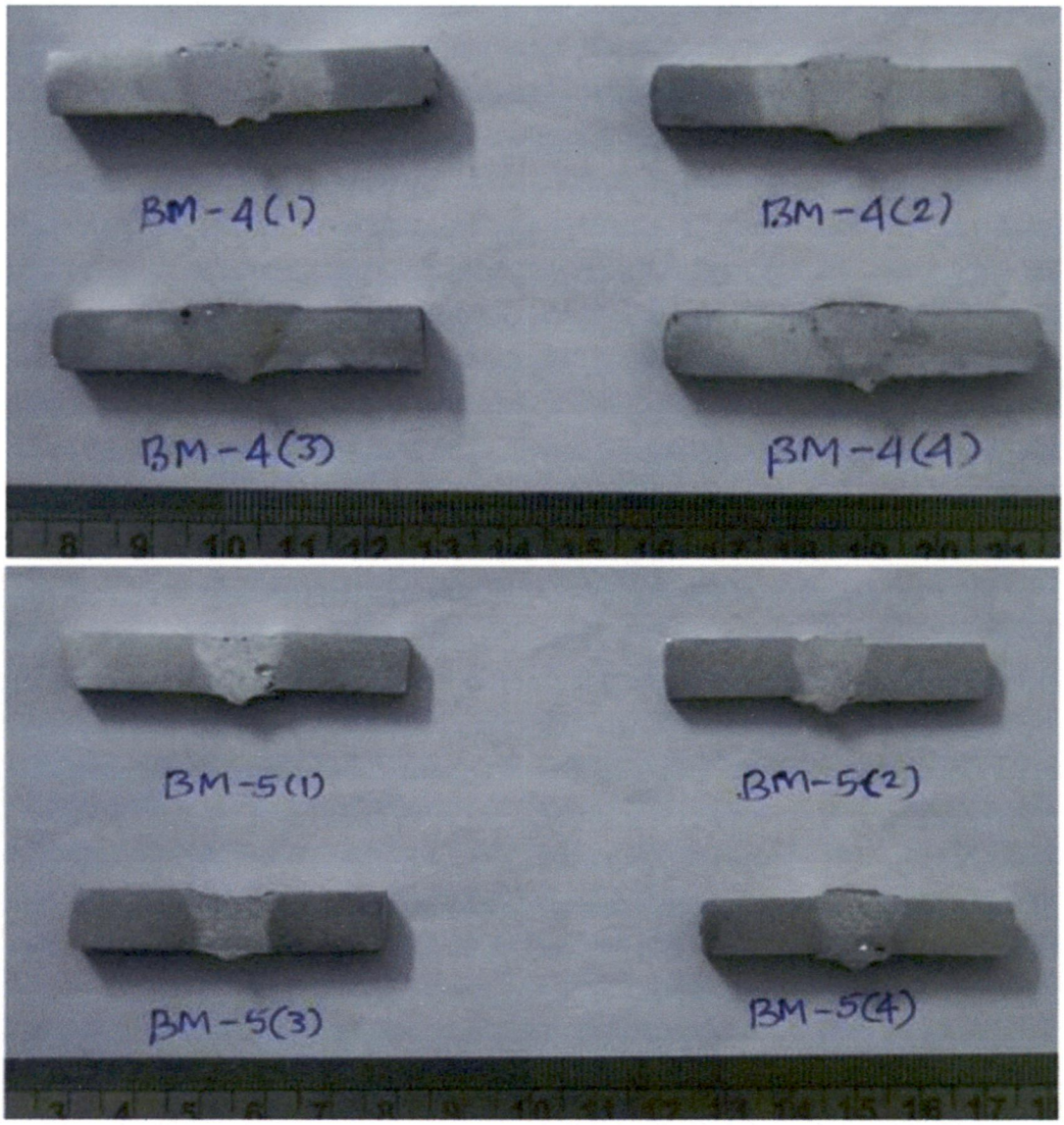

Figure 24: Weld Transverse sections of the GMA welded plates of BM-4 and BM-5 material at different welding parameters

Table 4: Various Welding Parameters and heat inputs used in pulse as well as continuous current GMAW:

Material Designation	V_w (m/min)	Arc voltage (V)	I_m (A)	V (cm/min)	Heat Input (kJ/cm)	I_p (A)	I_b (A)	f (Hz)	t_p (ms)	t_b (ms)	Ø
BM-2(1)	5	24	174.3	34.9	7.1917	308	116	74	4.1	9.4	0.262
BM-2(2)	7.5	24	198.1	34.9	8.173	400	152	58	3.2	14	0.31
BM-2(3)	6.6	26	200	34.9	8.939	392	58	40	7.6	17.4	0.2
BM-2(4)	8.4	25	265	34.9	11.389	-	-	-	-	-	1
BM-3(1)	9.5	24	256	34.9	10.562	372	92	66	8.9	6.3	0.1
BM-3(2)	9.8	24	249	34.9	10.273	424	136	72	5.4	8.5	0.2
BM-3(3)	10	24	252	34.9	10.397	452	212	88	1.9	9.5	0.39
BM-3(4)	10.2	28	389	34.9	18.725	-	-	-	-	-	1
BM-4(1)	9	25	264.6	34.9	11.372	388	100	64	8.8	6.6	0.1451
BM-4(2)	9	23	270.2	34.9	10.684	444	140	74	5.7	7.6	0.1773
BM-4(3)	9	26	258.6	34.9	11.559	456	160	78	4.1	8.2	0.2244
BM-4(4)	8.4	24	250	34.9	10.315	-	-	-	-	-	1
BM-5(1)	9	26	211	34.9	9.431	416	144	54	4.6	14.1	0.2635
BM-5(2)	9	24	254	34.9	10.48	472	220	88	1.8	9.6	0.3937
BM-5(3)	9	24	265	34.9	10.934	412	212	62	2.4	13.7	0.437
BM-5(4)	8.4	24.5	250	34.9	10.53	-	-	-	-	-	1

Table 5: Comparison of Weld Geometry, % Dilution and % Porosity for given Ø and heat inputs.

Material Designation	Bead top A(mm)	Bead root B(mm)	Geometric Parameter, Ratio r =B/A	Heat Input (kJ/cm)	Ø	% Dilution	% Porosity
BM-2(1)	12.5	2.6	4.807	7.1917	0.262	38.99	1.51
BM-2 (2)	9.8	6.5	1.507	8.173	0.31	28.23	5.12
BM-2(3)	13.5	6.2	2.177	8.939	0.206	38.67	4.9
BM-2 (4)	12.6	7.5	1.68	11.389	1	42.309	5.47
BM-3(1)	14.5	11.5	1.26	10.562	0.1	33.795	6.84
BM-3 (2)	17.1	12.5	1.368	10.273	0.2	37.19	1.79
BM-3 (3)	14.5	10.5	1.38	10.397	0.39	49.86	1.11
BM-3 (4)	18	16.5	1.09	18.725	1	70.54	2.4
BM-4 (1)	15.5	9	1.723	11.372	0.145	39.87	2.33
BM-4 (2)	14.5	8.5	1.705	10.684	0.177	41.67	1.44
BM-4 (3)	17.1	13	1.315	11.559	0.224	34	1.94
BM-4 (4)	16.5	7.5	2.2	10.315	1	54.03	1.82
BM-5 (1)	13	8.5	1.529	9.431	0.264	50.4	5.3
BM-5 (2)	11.5	7.5	1.54	10.48	0.394	60.85	2.9
BM-5 (3)	14.5	11.5	1.26	10.934	0.437	56.76	0.89
BM-5 (4)	13.5	10.8	1.25	10.53	1	58.73	3.2

Table 6: Comparison of HAZ width, % dilution, % porosity, average grain size in HAZ[2, 6] and Base material[3, 7], Peak Hardness in HAZ[1, 5] for given Ø and heat inputs

Material designation	Ø	Heat Input (kJ/cm)	HAZ width (mm)	HAZ hardness[1]	% Dilution	% Porosity	HAZ Grain size[2], µm	Base metal Grain size[3], µm	PWAT[4]	HAZ hardness[5],VHN	HAZ Grain size[6], µm	Base metal Grain size[7], µm
BM-2(1)	0.262	7.1917	3.75	190	38.99	1.51	20.12	19.35	124 °C	126	38.55	35.23
BM-2 (2)	0.31	8.173	8.25	148	28.23	5.12	22.67	20.87	145 °C	193	42.45	28.08
BM-2(3)	0.206	8.939	9.5	182	38.67	4.9	20.52	18.57	170 °C	152	22.15	20.56
BM-2 (4)	1	11.389	8	168	42.309	5.47	26.45	24.41	200 °C	132	48.25	42.66
BM-3(1)	0.1	10.562	7.25	169	33.795	6.84	19.12	18.18	124 °C	136	20.81	19.45
BM-3 (2)	0.2	10.273	11.5	191	37.19	1.79	19.45	18.58	145 °C	198	21.13	20.55
BM-3 (3)	0.39	10.397	6.9	180	49.86	1.11	19.12	18.39	170 °C	129	22.37	21.88
BM-3 (4)	1	18.725	27	158	70.54	2.4	19.44	18.89	200 °C	135	32.11	24.44
BM-4 (1)	0.145	11.372	9	192	39.87	2.33	21.37	20.12	124 °C	132	24.85	21.12
BM-4 (2)	0.177	10.684	12	176	41.67	1.44	20.75	18.91	145 °C	179	24.11	21.28
BM-4 (3)	0.224	11.559	11.75	188	34	1.94	20.19	18.34	170 °C	162	21.79	19.38
BM-4 (4)	1	10.315	12.75	191	54.03	1.82	20.95	20.14	200 °C	136	27.96	21.83
BM-5 (1)	0.264	9.431	9.5	158	50.4	5.3	51.24	44.51	124 °C	128	54.22	47.54
BM-5 (2)	0.394	10.48	10.5	155	60.85	2.9	54.55	46.42	145 °C	169	64.23	56.83
BM-5 (3)	0.437	10.934	6.5	148	56.76	0.89	52.78	45.83	170 °C	158	64.72	56.83
BM-5 (4)	1	10.53	7	155	58.73	3.2	53.67	47.33	200 °C	120	64.83	52.33

[1, 2, 3]: Applicable for as weld samples; [4]: Post Weld Aging Temperature; [5, 6, 7]: Applicable for post weld aged samples

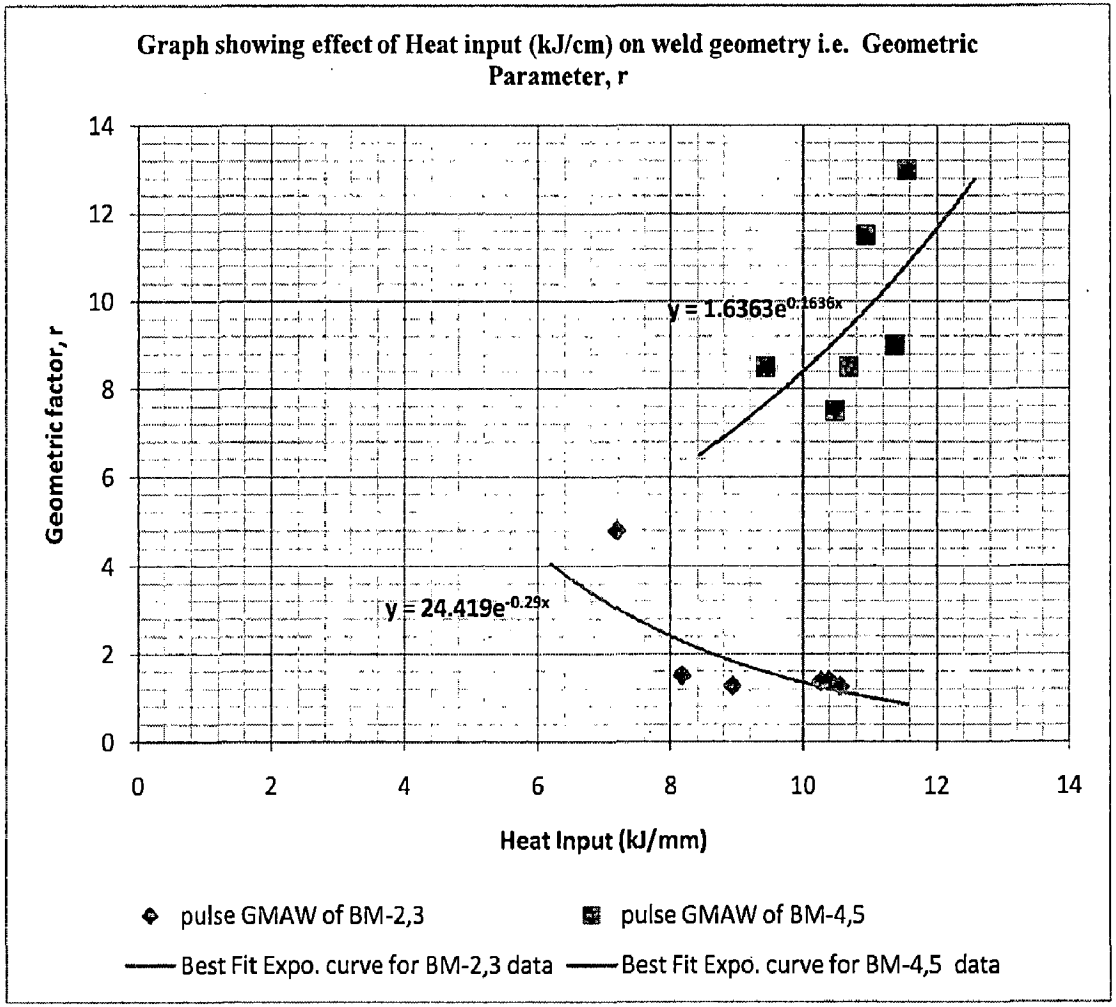

Figure 25: Graph shows effect of heat input on Geometric Parameter, r

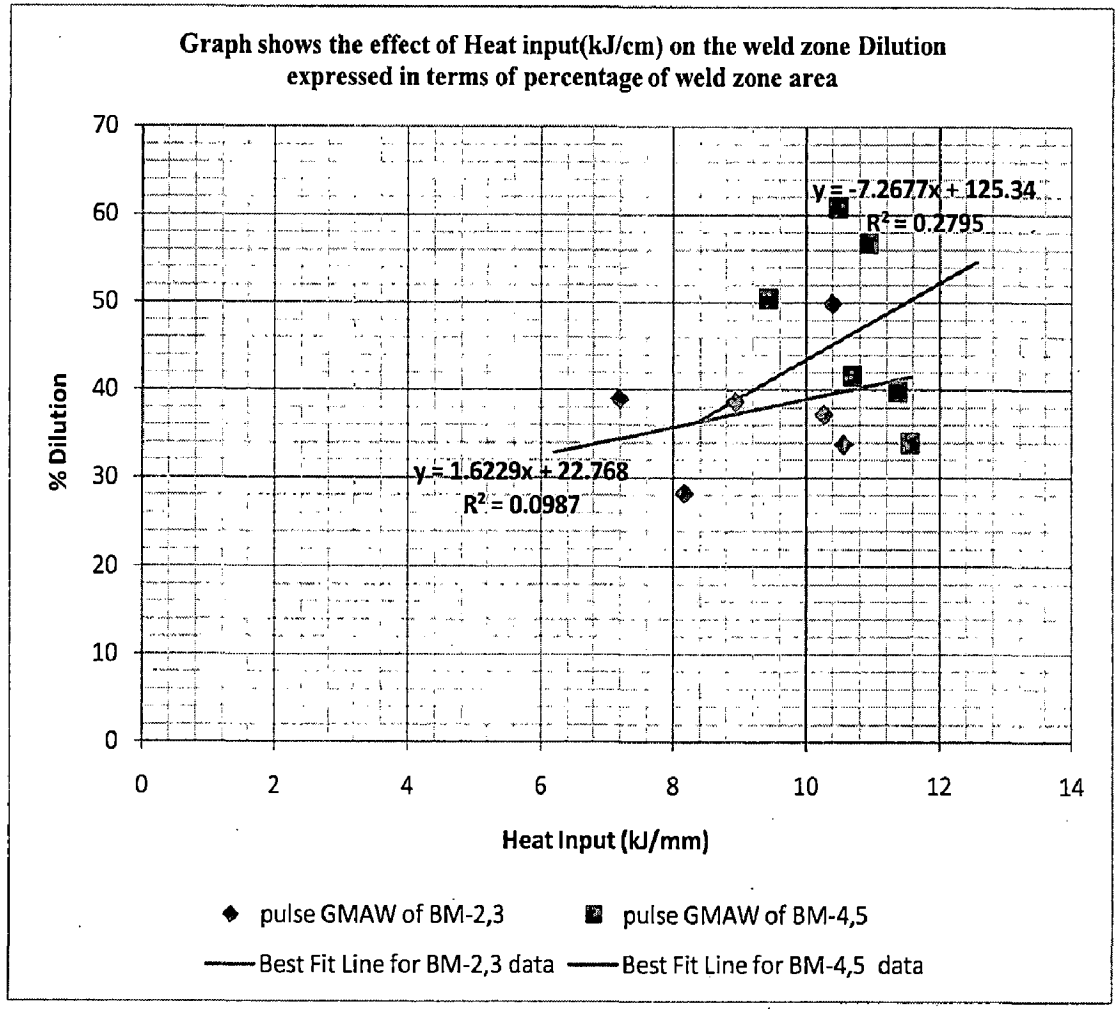

Figure 26: Graph shows the effect of heat input on the weld zone dilution

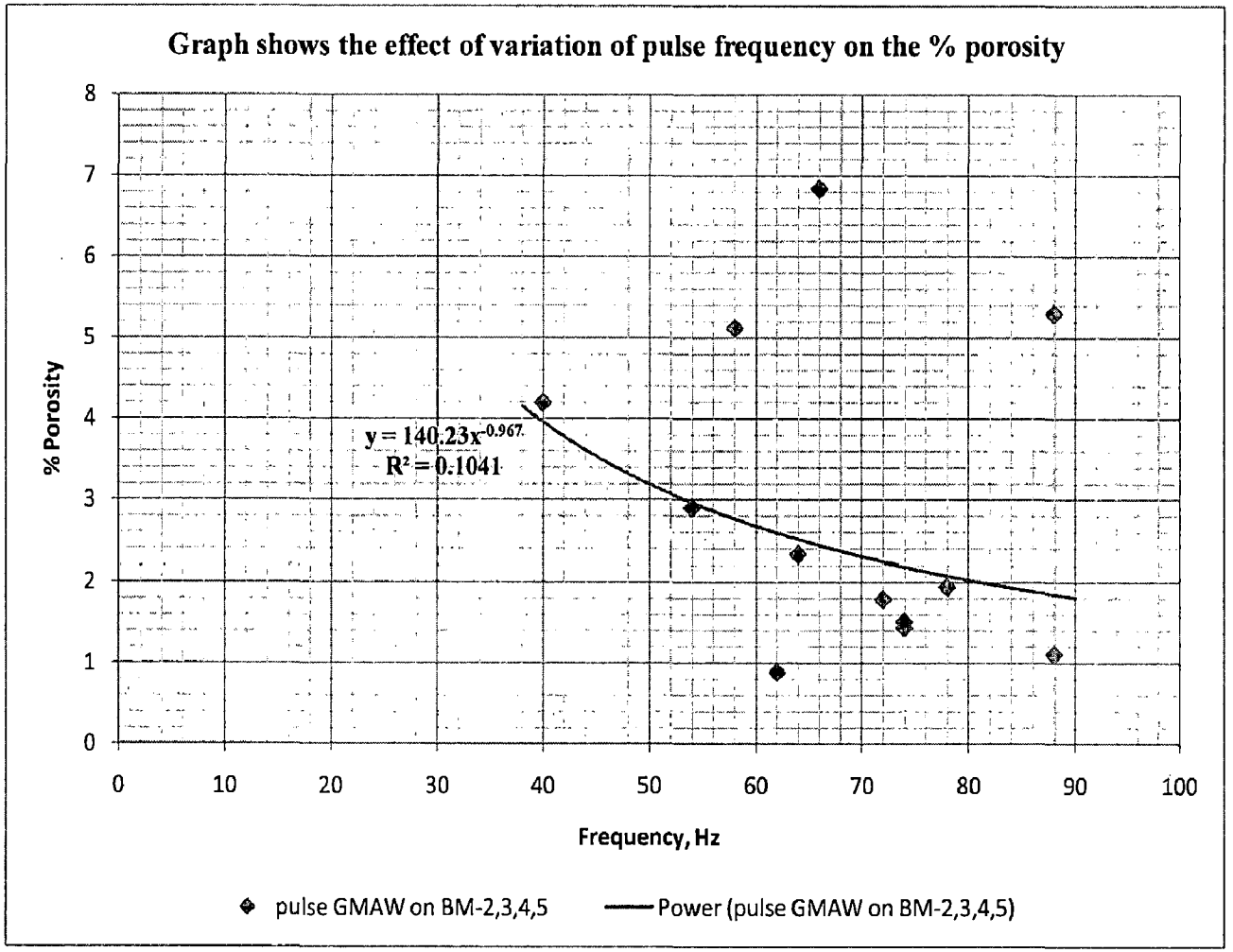

Figure 27: Graph shows the effect of pulse frequency on the %porosity in pulse GMAW of BM-2,3,4,5

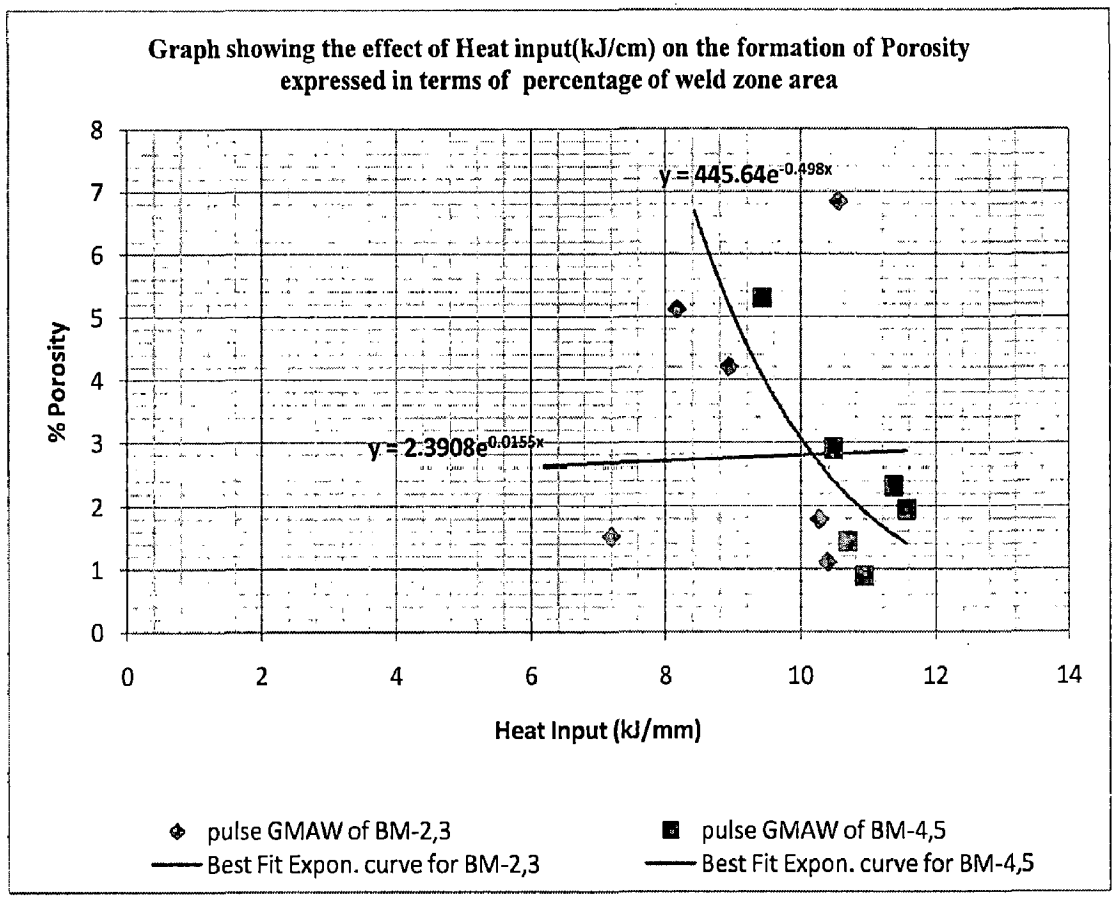

Figure 28: Graph shows the effect of the heat input on the percentage porosity

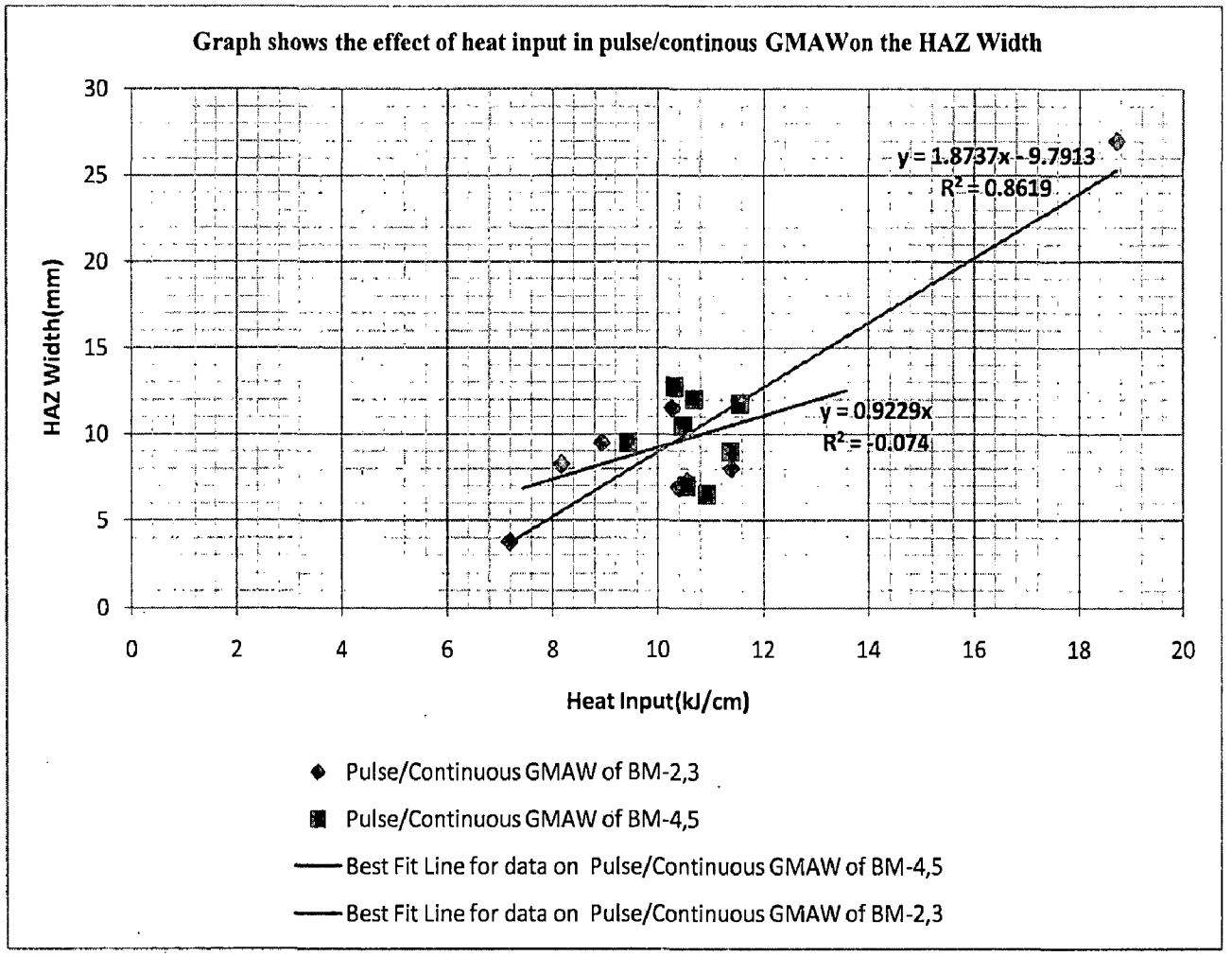

Figure 29: Graph shows the effect of heat input on the HAZ width under pulse/continuous GMAW process

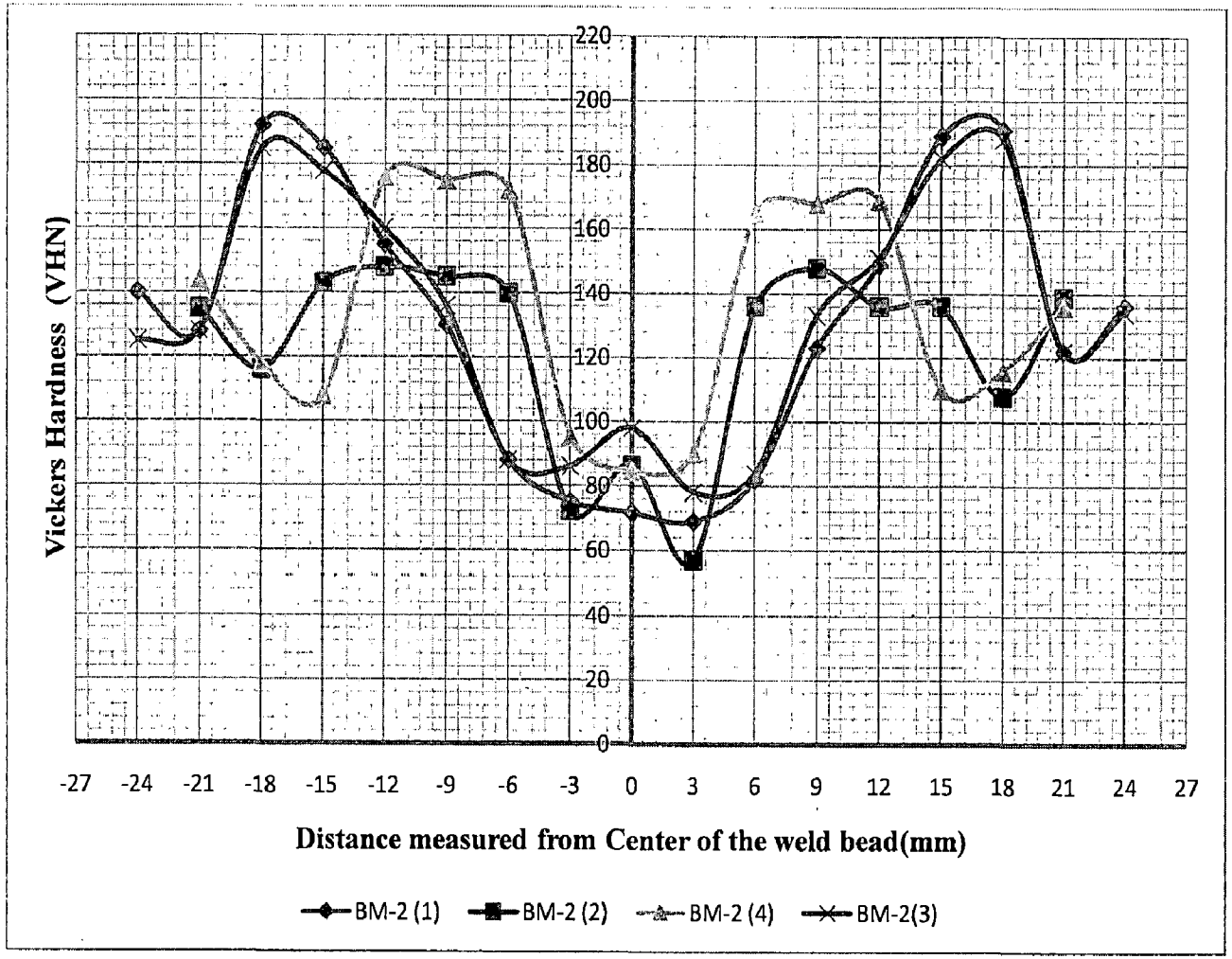

Figure 30: Graph shows the hardness variation along the weld section versus the distance measured from the weld bead center for BM-2.

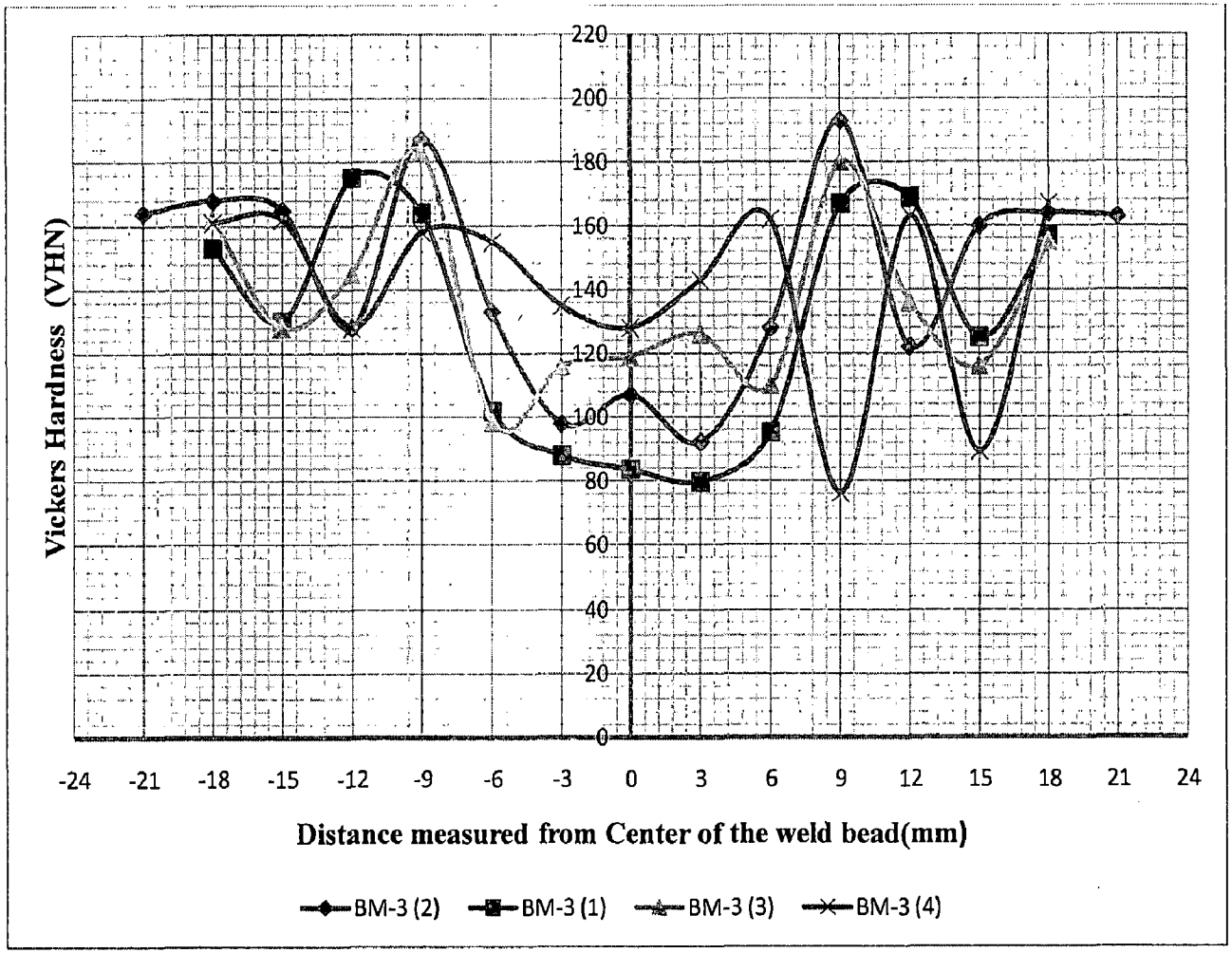

Figure 31: Graph shows the hardness variation along the weld section versus the distance measured from the weld bead center for BM-3.

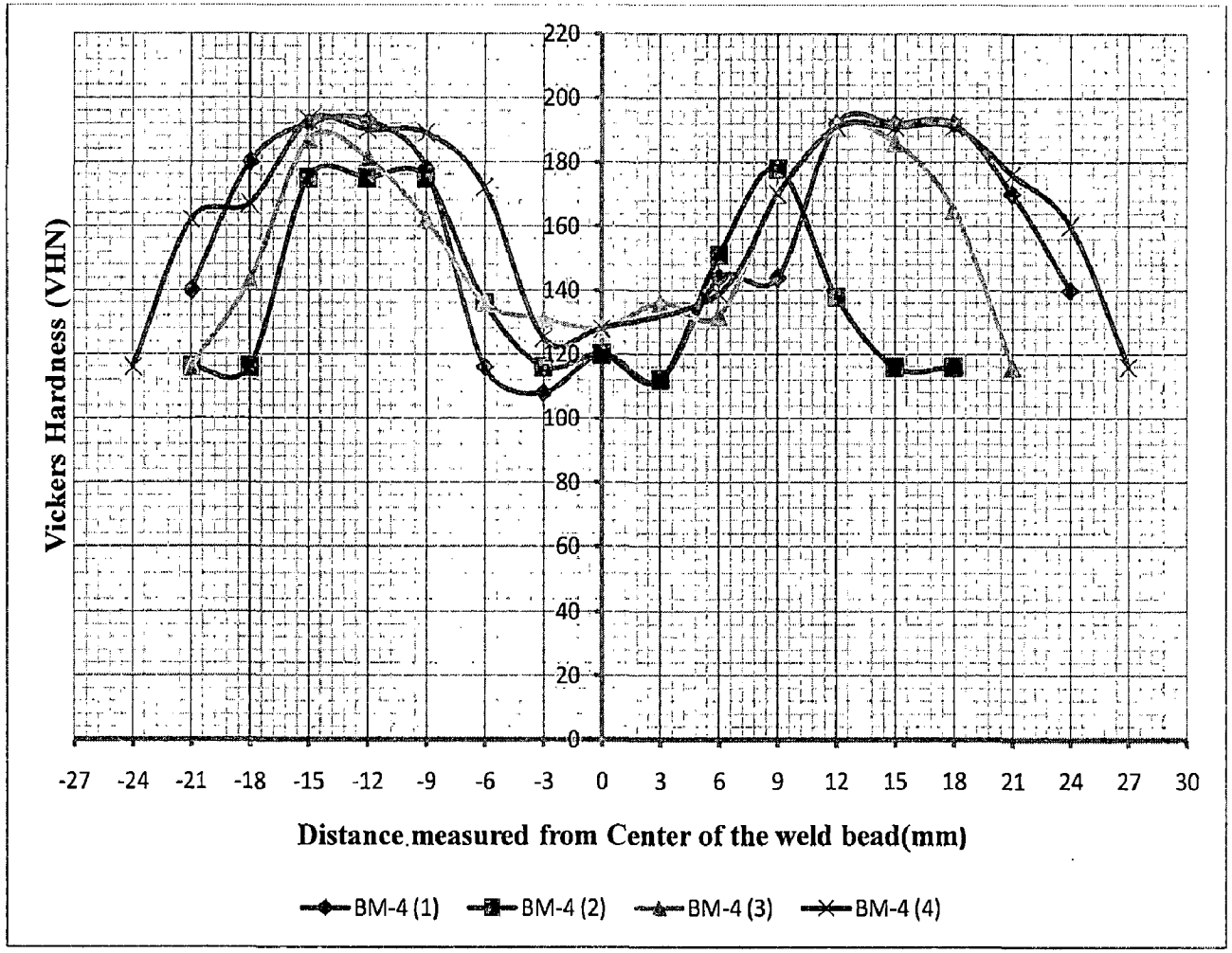

Figure 32: Graph shows the hardness variation along the weld section versus the distance measured from the weld bead center for BM-4.

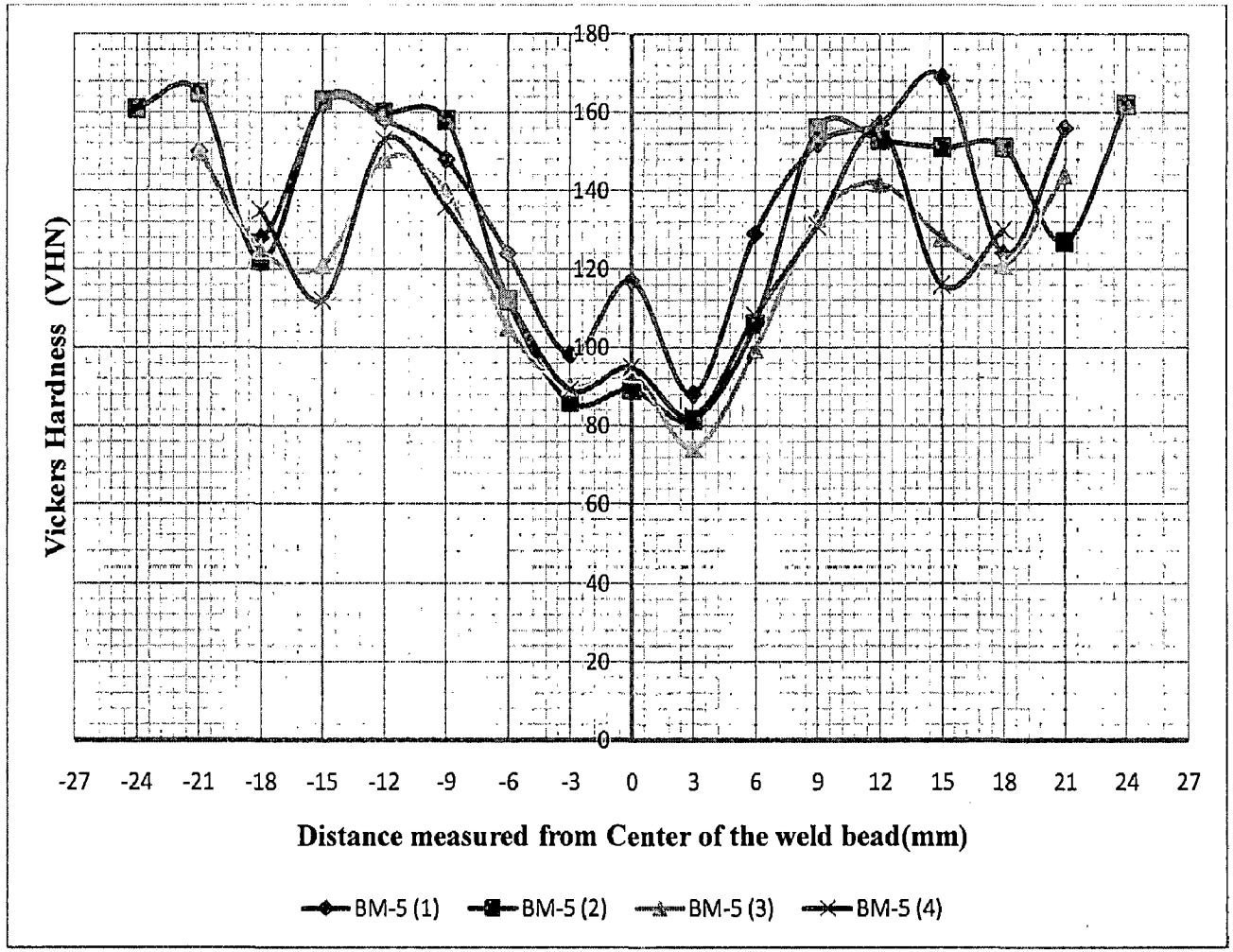

Figure 33: Graph shows the hardness variation along the weld section versus the distance measured from the weld bead center for BM-5.

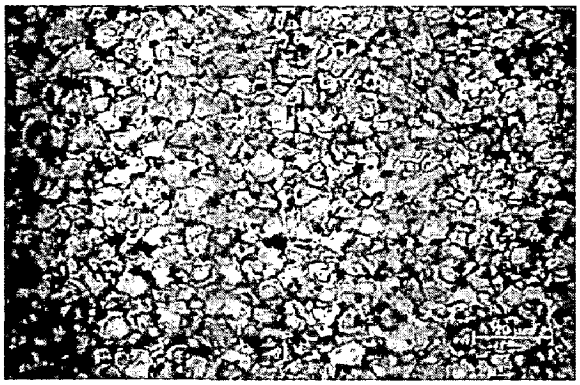

(a) Center of the weld zone

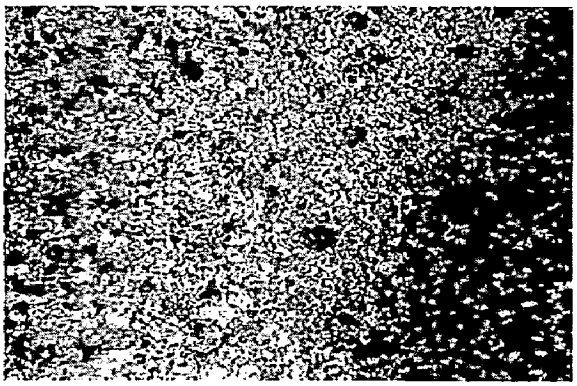

(b) Weld fusion zone

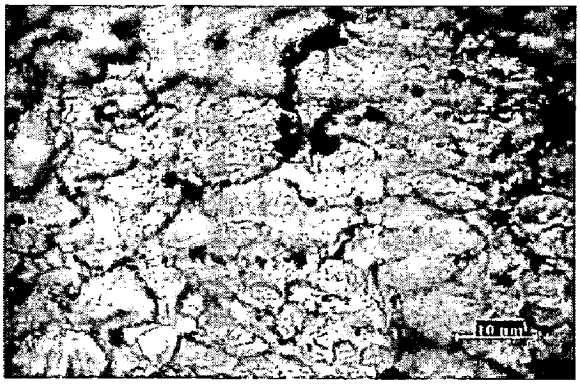

(c) HAZ region

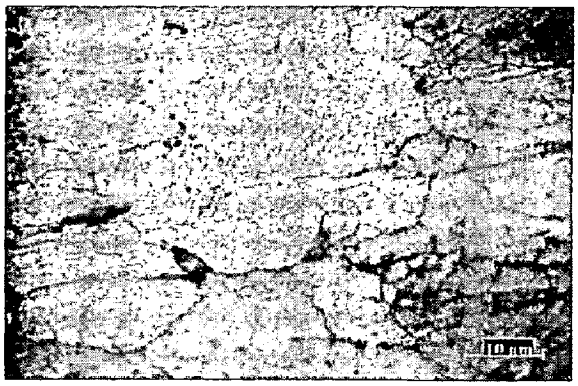

(d) Base metal region

Figure 34: Microstructures of the welded sections of BM-2(1) specimen using pulse current GMAW, 7.1917 kJ/cm

(a) Center of the weld zone

(b) Weld fusion zone

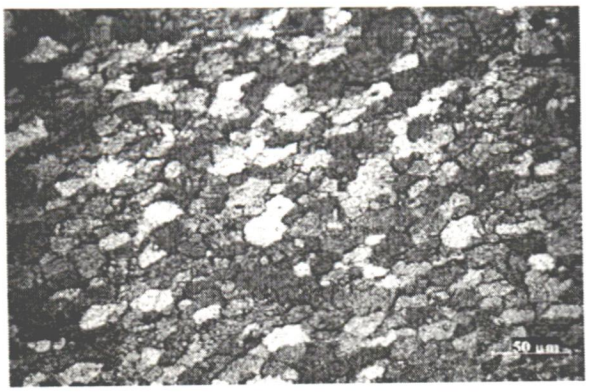

(c) HAZ region

(d) Base metal region

Figure 35: Microstructures of the welded sections of BM-2(2) specimen using pulse current GMAW, 8.173 kJ/cm

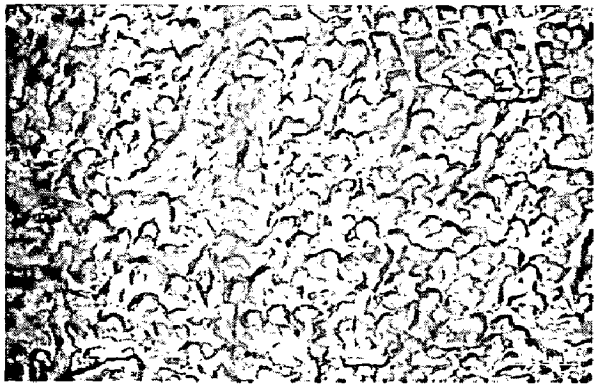

(a) Center of the weld zone

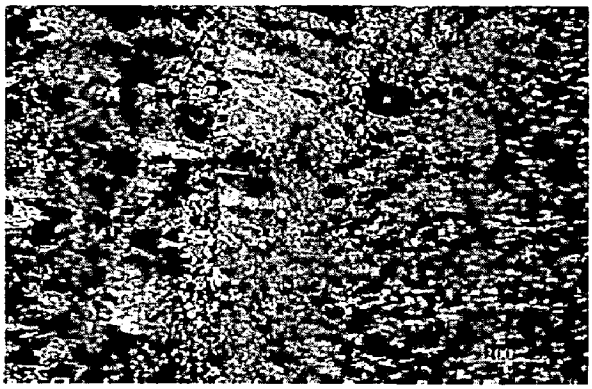

(b) Weld fusion zone

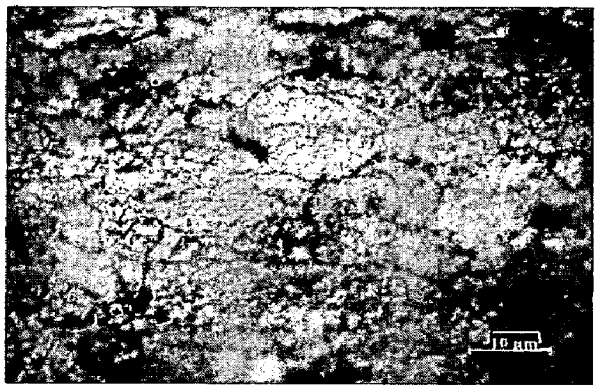

(c) HAZ region

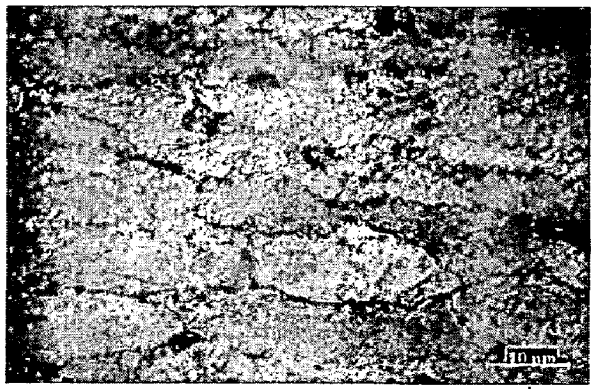

(d) Base metal region

Figure 36: Microstructures of the welded sections of BM-2(3) specimen using pulse current GMAW, 8.939 kJ/cm

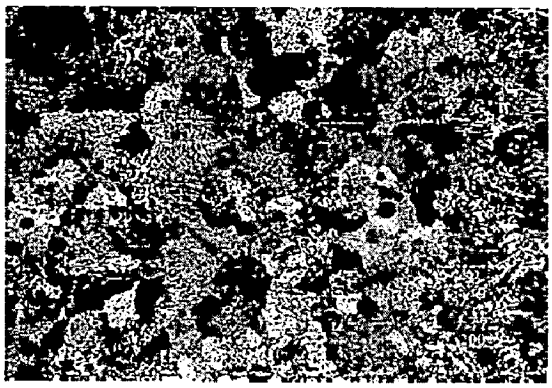

(a) Center of the weld zone

(b) Weld fusion zone

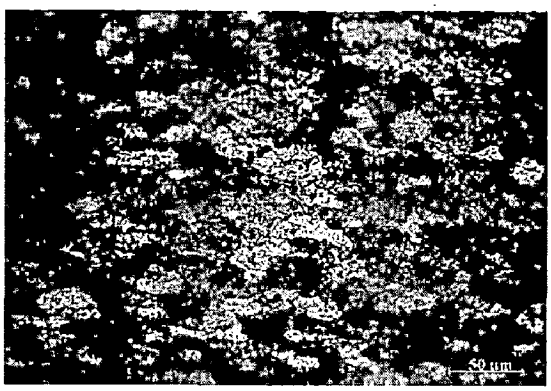

(c) HAZ region

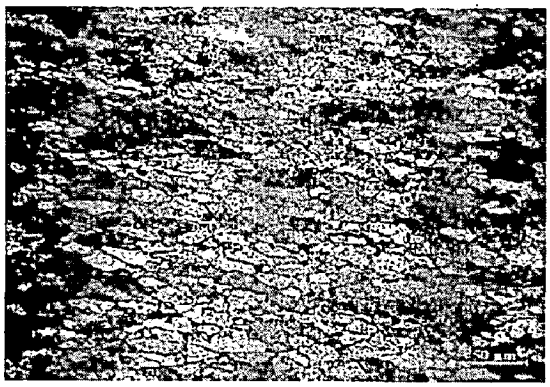

(d) Base metal region

Figure 37: Microstructures of the welded sections of BM-2(4) specimen using continuous current GMAW, 8.939 kJ/cm

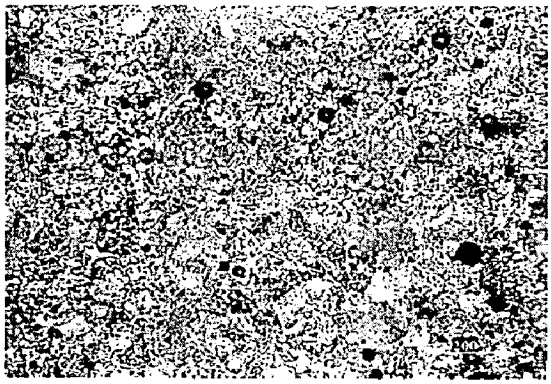

(a) Center of the weld zone

(b) Weld fusion zone

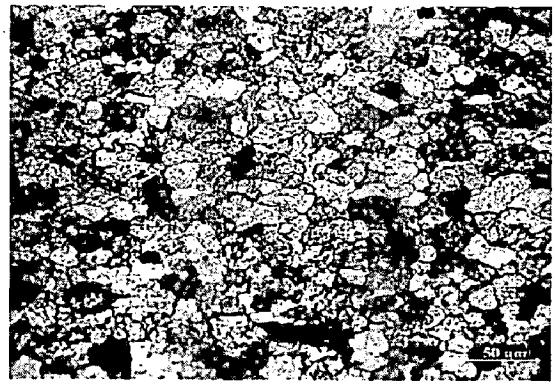

(c) HAZ region

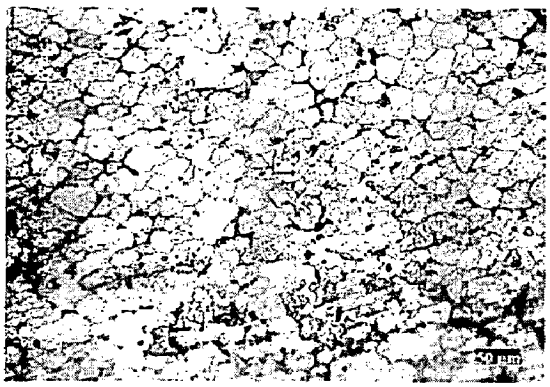

(d) Base metal region

Figure 38: Microstructures of the welded sections of BM-3(1) specimen using pulse current GMAW, 10.562 kJ/cm

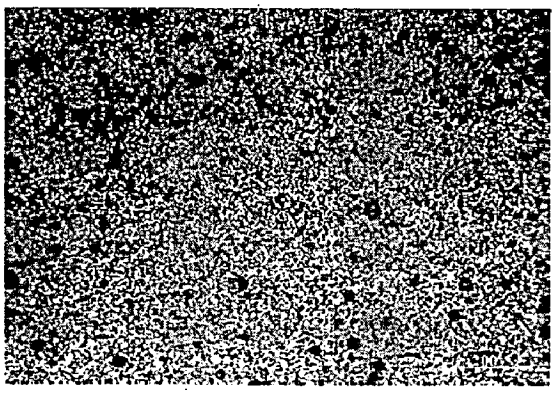

(a) Center of the weld zone

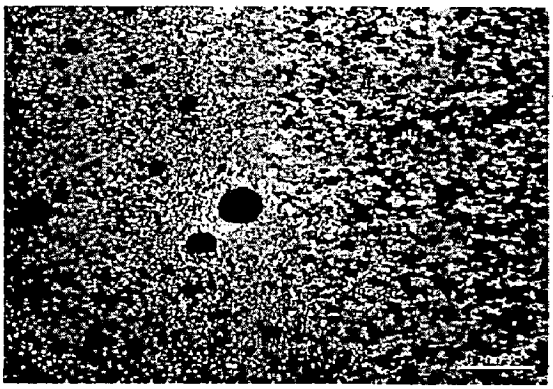

(b) Weld fusion zone

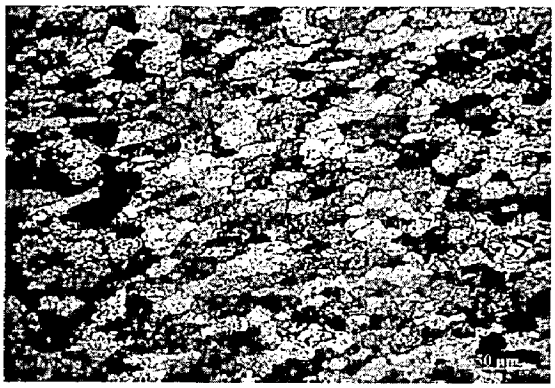

(c) HAZ region

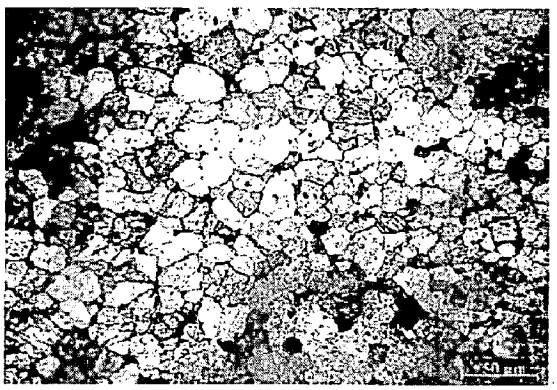

(d) Base metal region

Figure 39: Microstructures of the welded sections of BM-3(2) specimen using pulse current GMAW, 10.273 kJ/cm

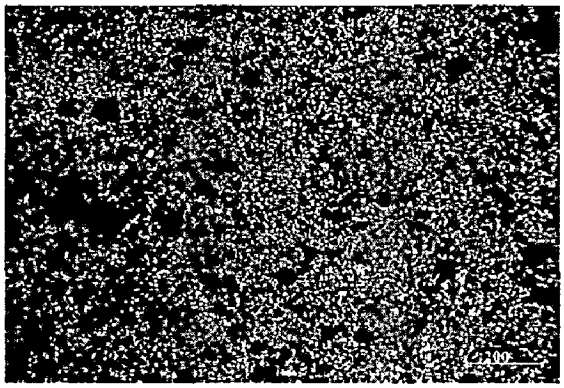

(a) Center of the weld zone

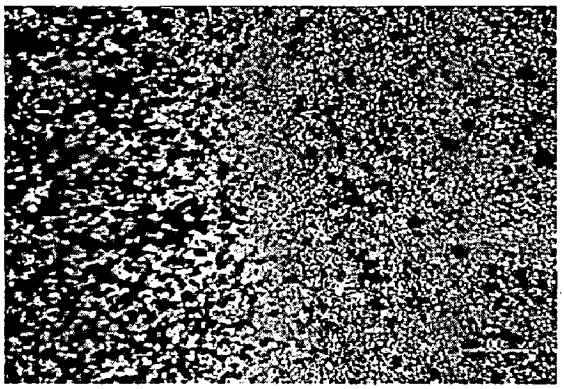

(b) Weld fusion zone

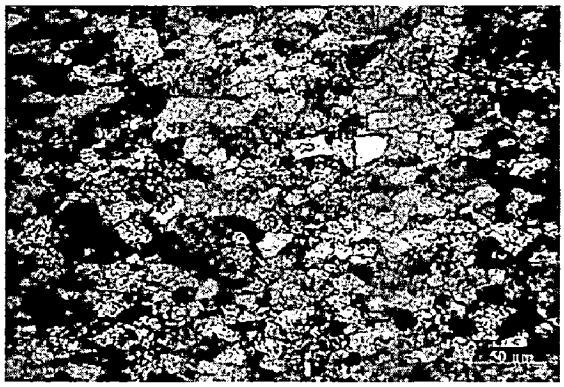

(c) HAZ region

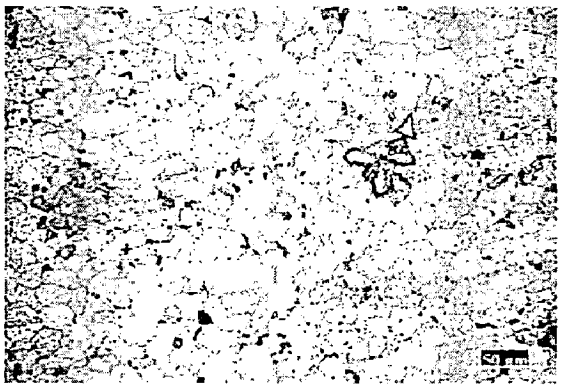

(d) Base metal region

Figure 40: Microstructures of the welded sections of BM-3(3) specimen using pulse current GMAW, 10.397 kJ/cm

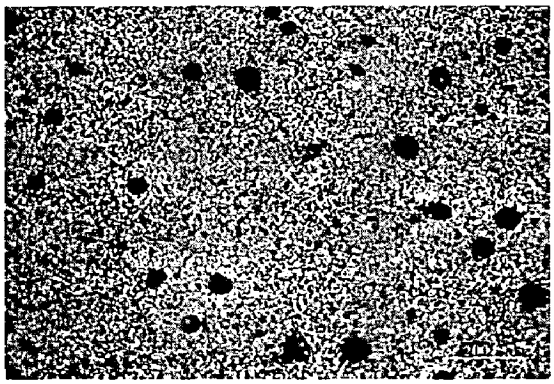

(a) Center of the weld zone

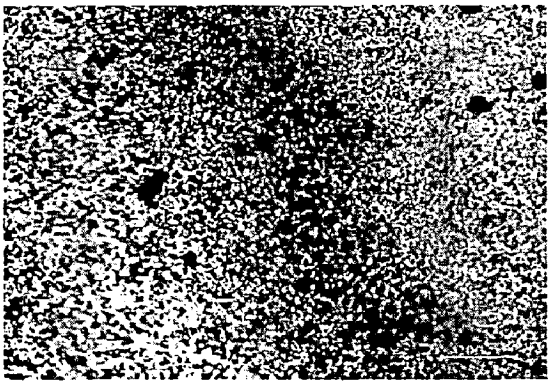

(b) Weld fusion zone

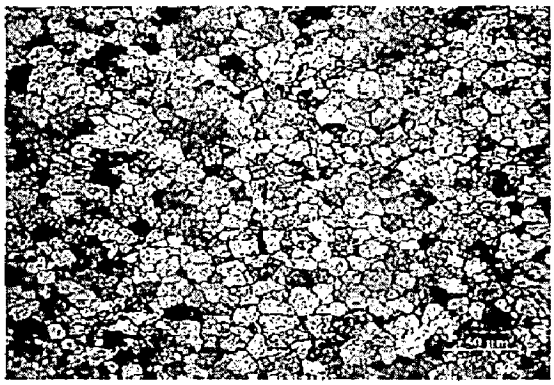

(c) HAZ region

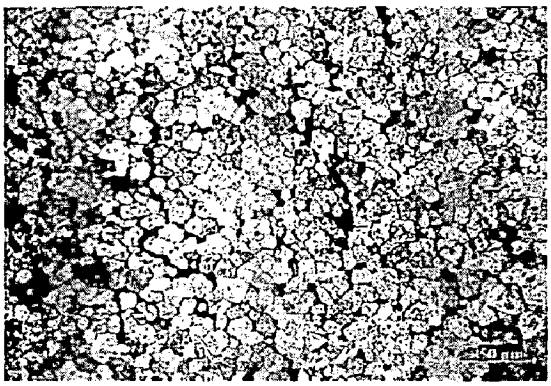

(d) Base metal region

Figure 41: Microstructures of the welded sections of BM-3(4) specimen using continuous current GMAW, 18.725 kJ/cm

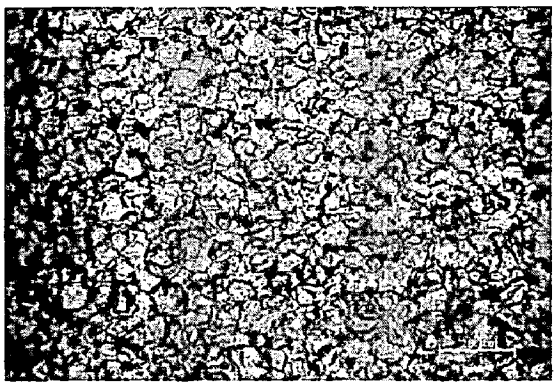

(a) Center of the weld zone

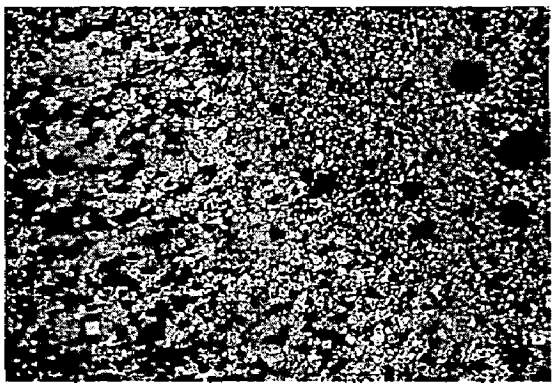

(b) Weld fusion zone

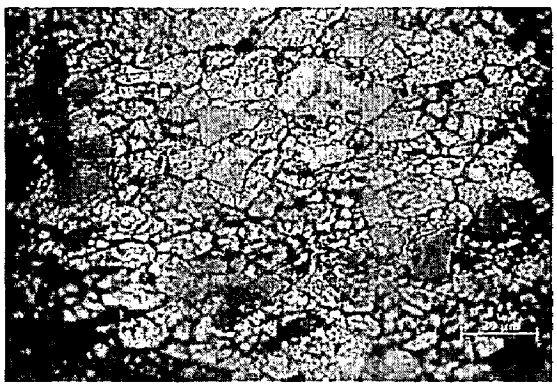

(c) HAZ region

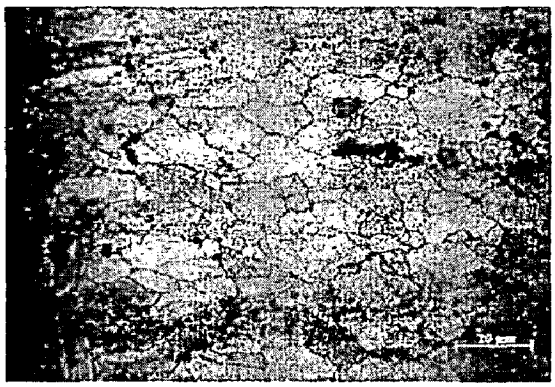

(d) Base metal region

Figure 42: Microstructures of the welded sections of BM-4(1) specimen using pulse current GMAW, 11.372 kJ/cm

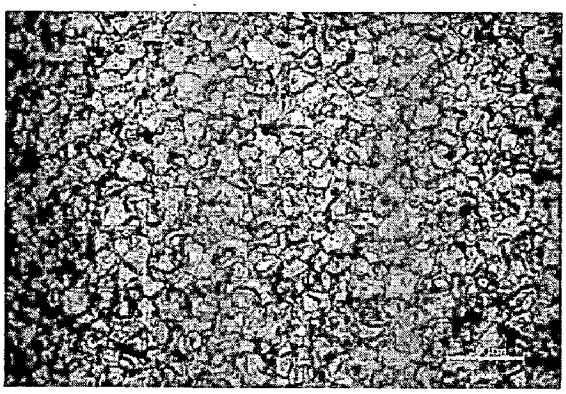

(a) Center of the weld zone

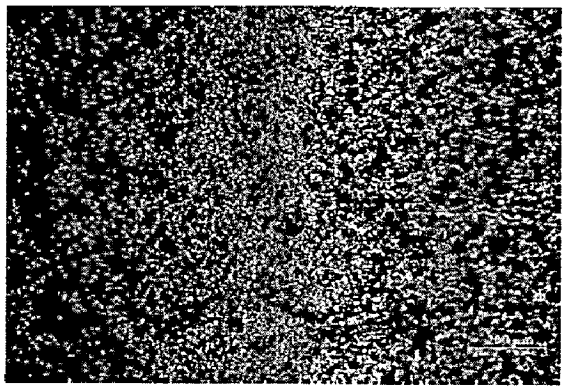

(b) Weld fusion zone

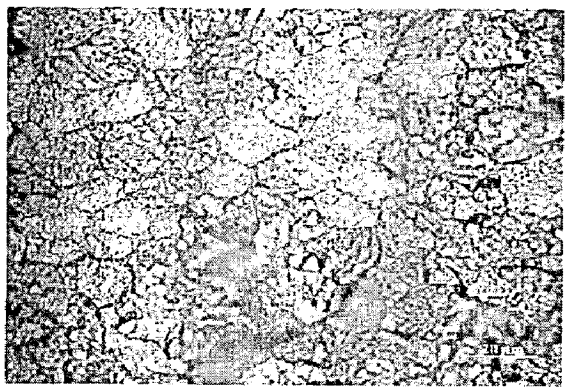

(c) HAZ region

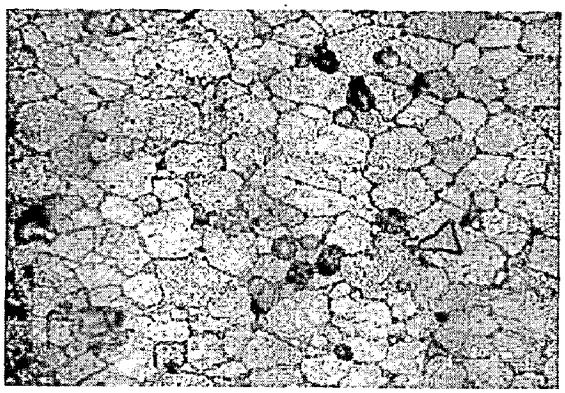

(d) Base metal region

Figure 43: Microstructures of the welded sections of BM-4(2) specimen using pulse current GMAW, 10.684 kJ/cm

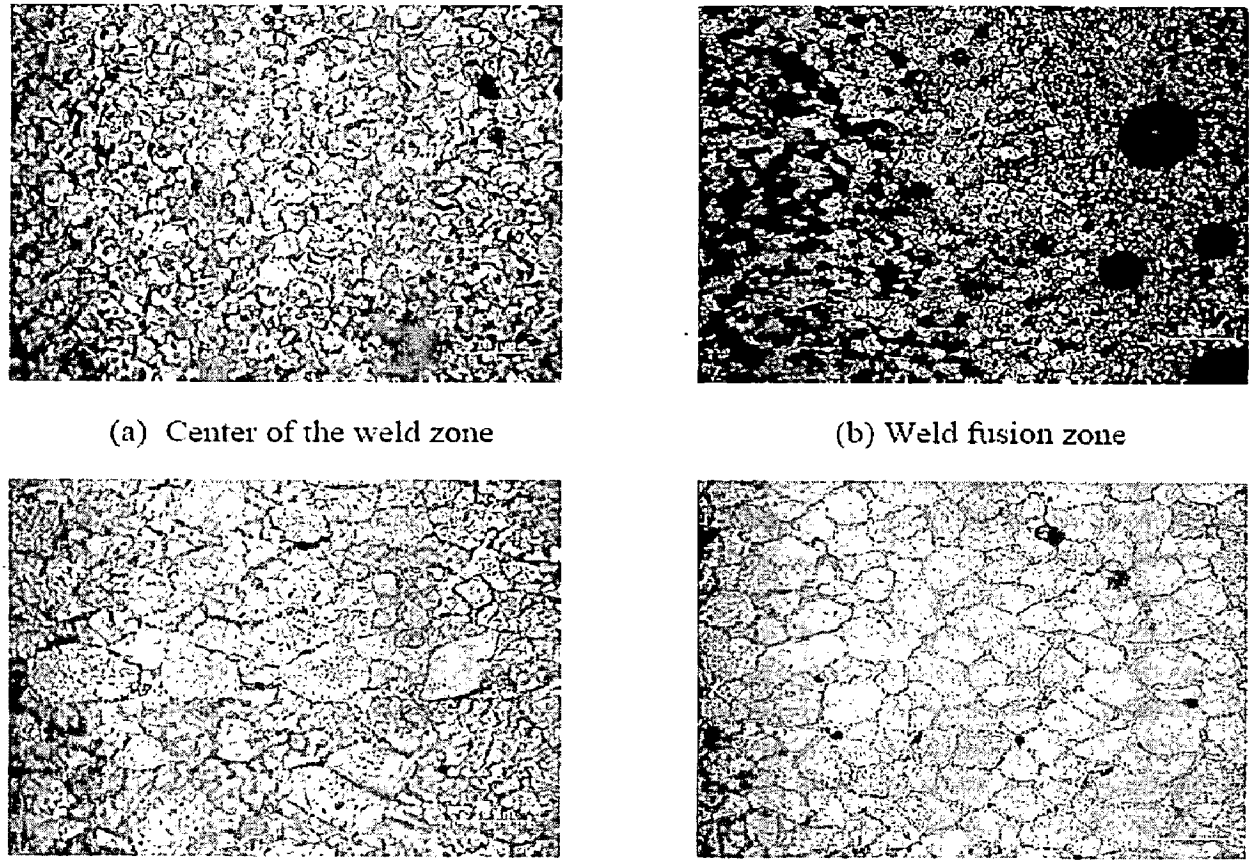

(a) Center of the weld zone

(b) Weld fusion zone

(c) HAZ region

(d) Base metal region

Figure 44: Microstructures of the welded sections of BM-4(3) specimen using pulse current GMAW, 11.559 kJ/cm

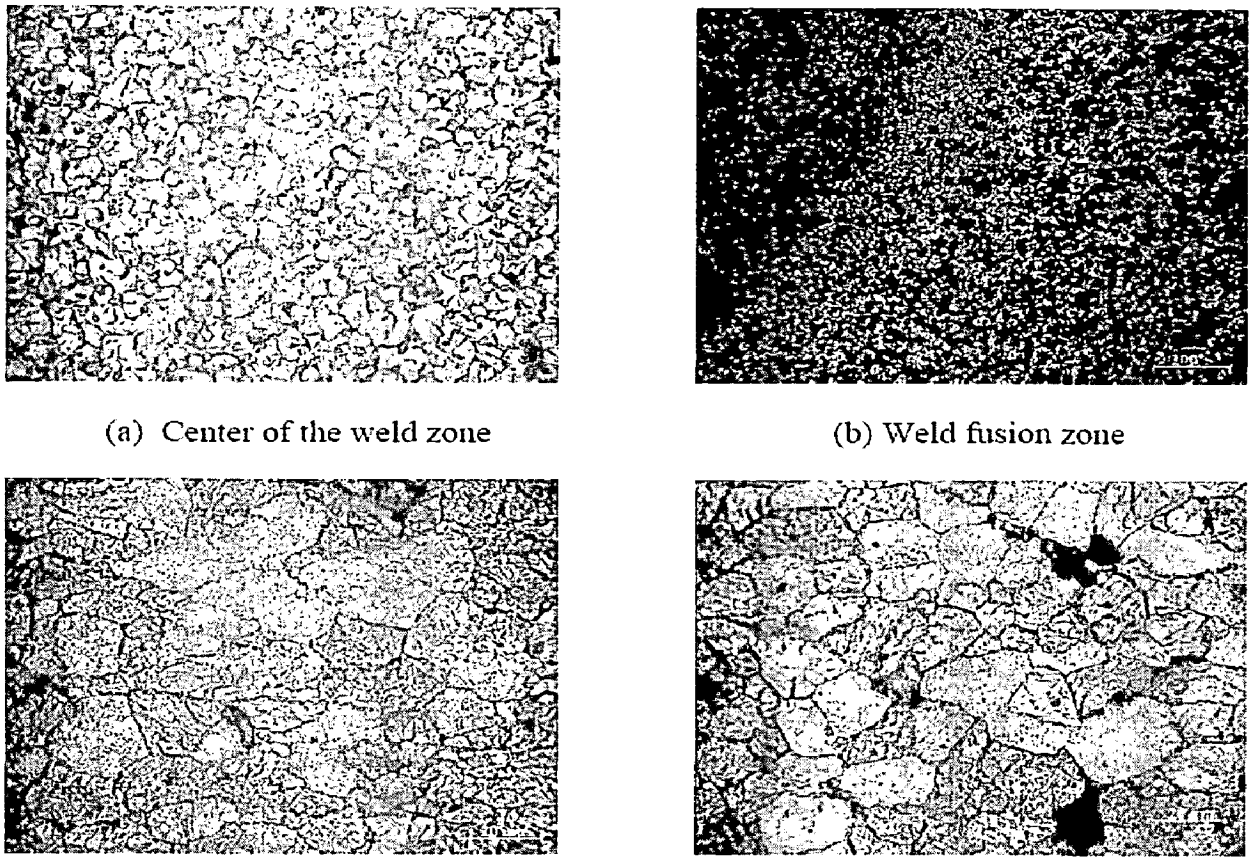

(a) Center of the weld zone

(b) Weld fusion zone

(c) HAZ region

(d) Base metal region

Figure 45: Microstructures of the welded sections of BM-4(4) specimen using continuous current GMAW, 10.315 kJ/cm

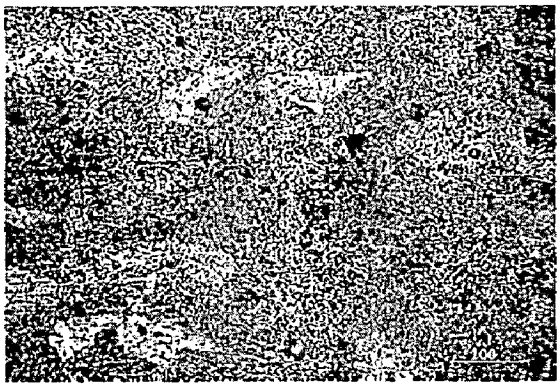

(a) Center of the weld zone

(b) Weld fusion zone

(c) HAZ region

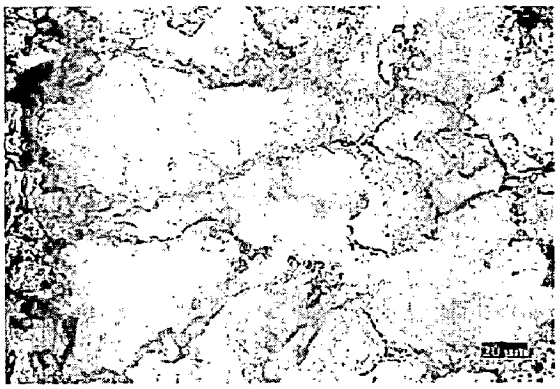

(d) Base metal region

Figure 46: Microstructures of the welded sections of BM-5(1) specimen using pulse current GMAW, 9.431 kJ/cm

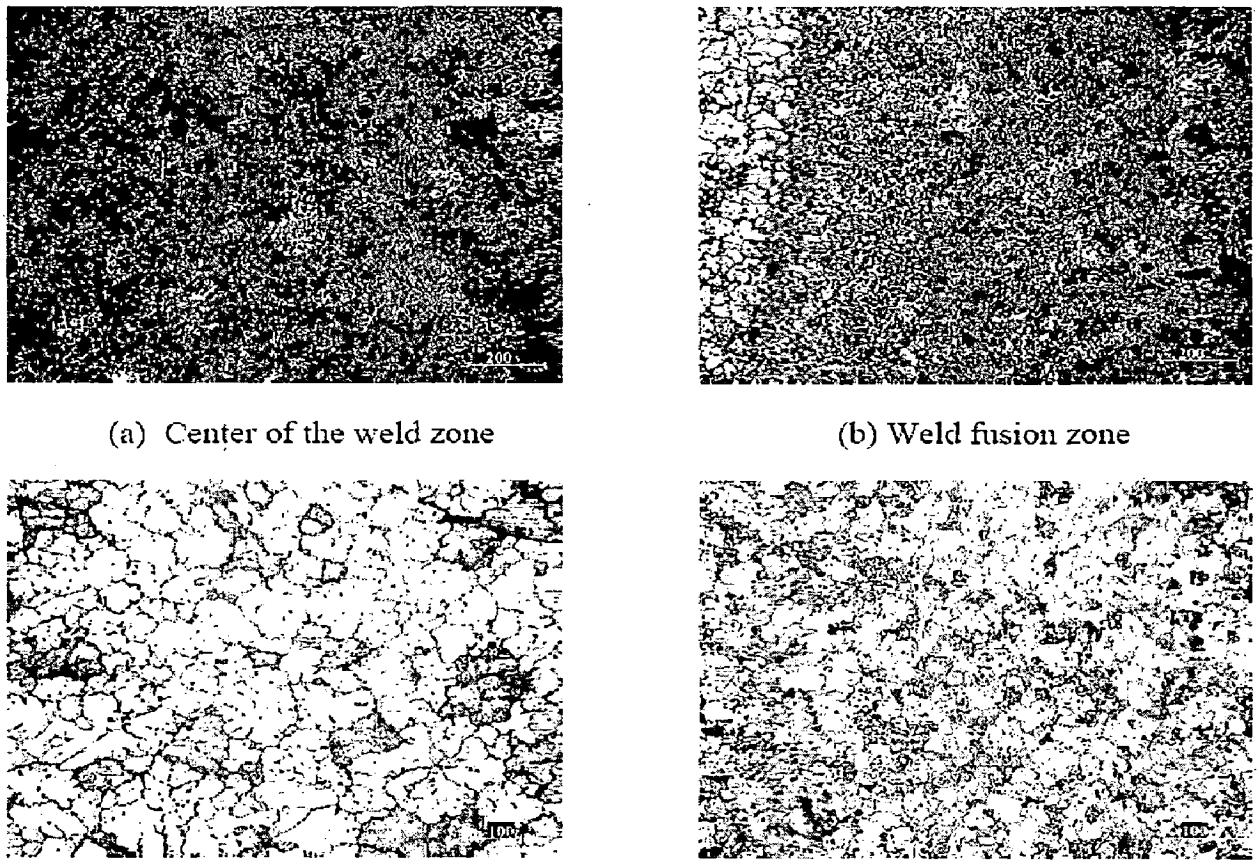

(a) Center of the weld zone

(b) Weld fusion zone

(c) HAZ region

(d) Base metal region

Figure 47: Microstructures of the welded sections of BM-5(2) specimen using pulse current GMAW, 10.480 kJ/cm

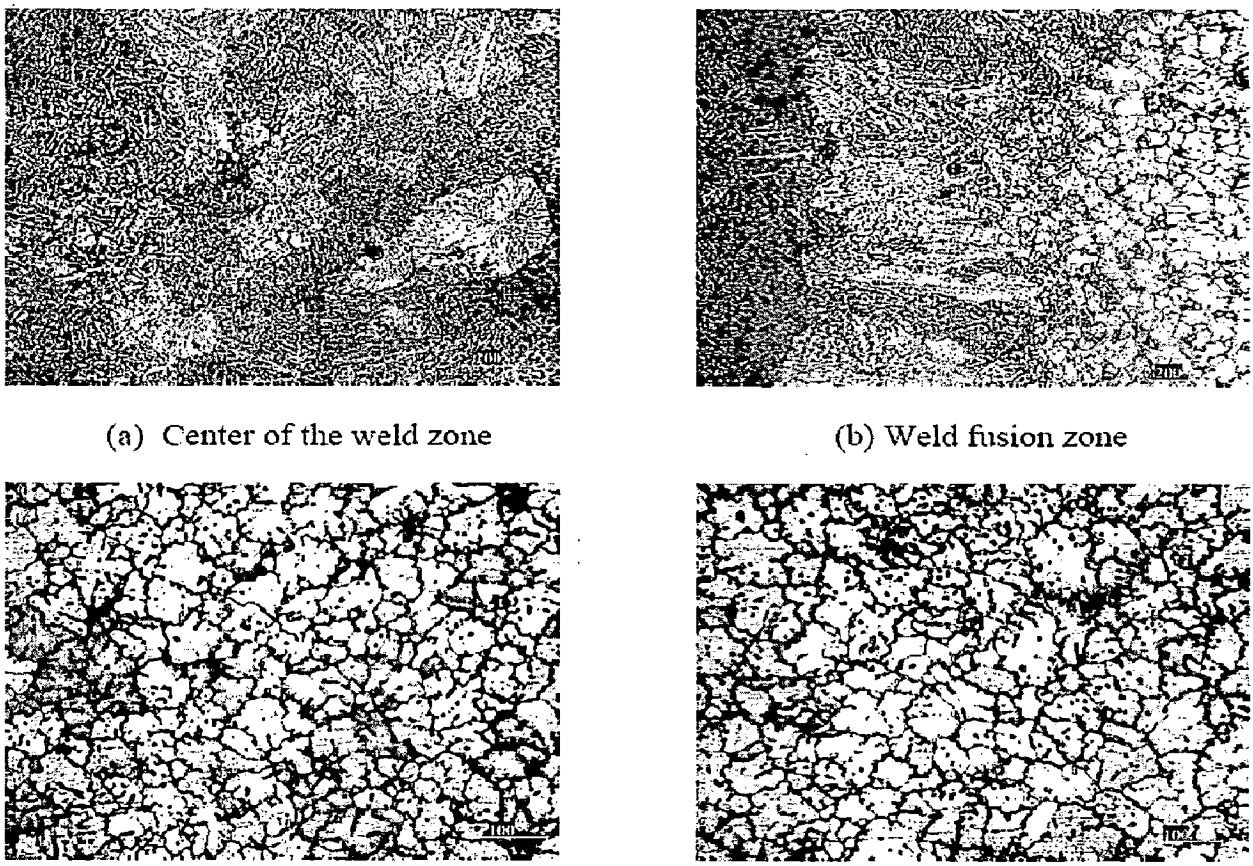

(a) Center of the weld zone

(b) Weld fusion zone

(c) HAZ region

(d) Base metal region

Figure 48: Microstructures of the welded sections of BM-5(3) specimen using pulse current GMAW, 10.934 kJ/cm

(a) Center of the weld zone

(b) Weld fusion zone

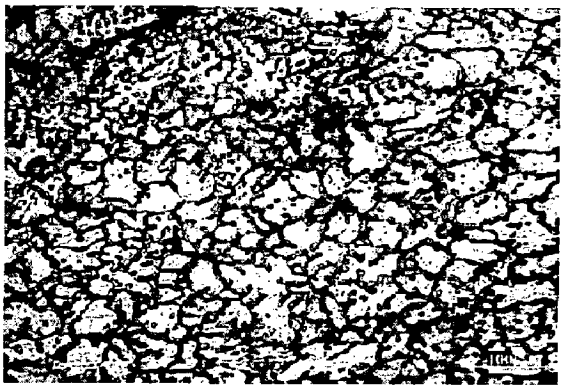

(c) HAZ region

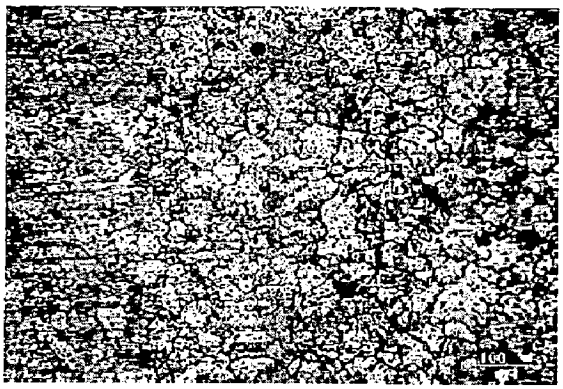

(d) Base metal region

Figure 49: Microstructures of the welded sections of BM-5(3) specimen using continuous current GMAW, 10.53 kJ/cm

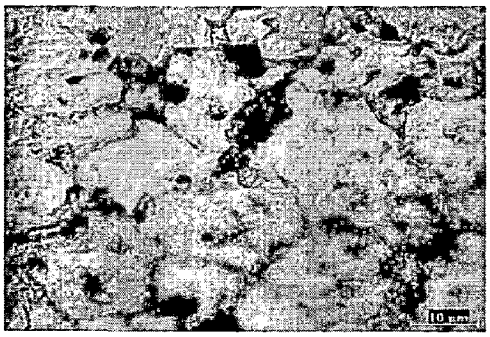

(a) HAZ region

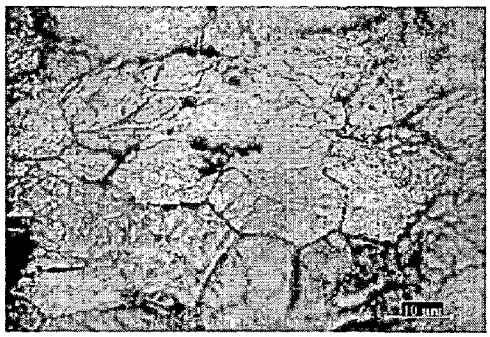

(b) Base metal region

Figure 50: Microstructure of post weld aged specimen at 124 °Cof pulse GMA welded BM-2(1) plate

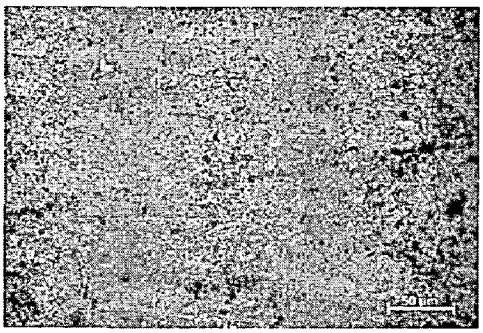

(a) HAZ region

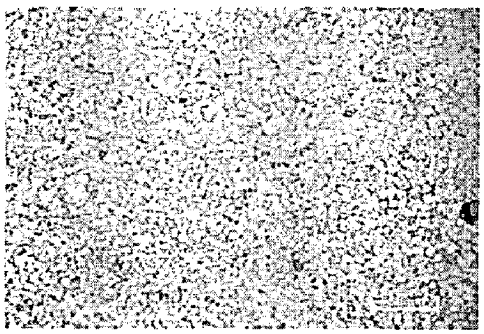

(b) Base metal region

Figure 51: Microstructure of post weld aged specimen at 124 °Cof pulse GMA welded BM-3(1) plate

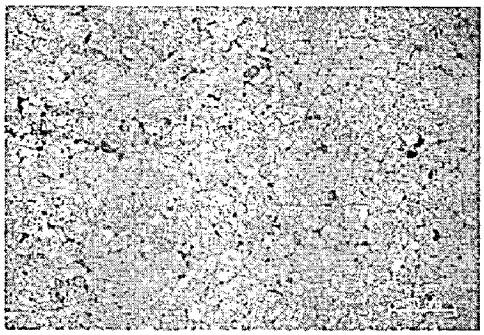

(a) HAZ region

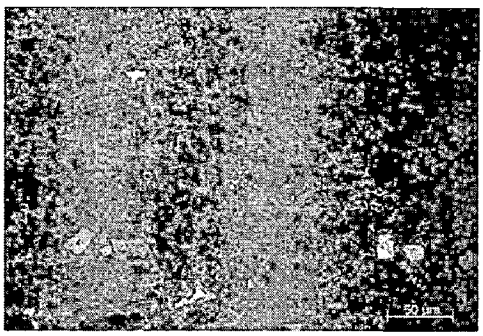

(b) Base metal region

Figure 52: Microstructure of post weld aged specimen at 124 °Cof pulse GMA welded BM-4(1) plate

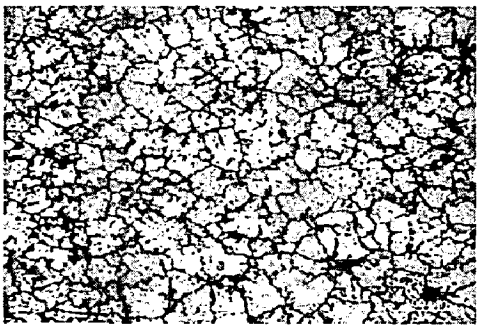

(a) HAZ region

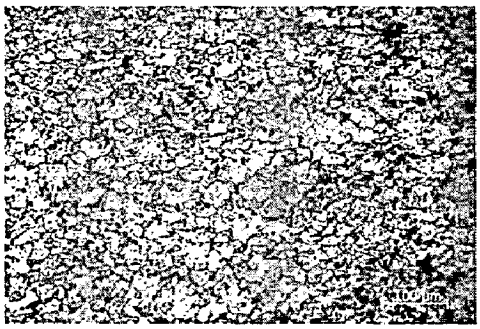

(b) Base metal region

Figure 53: Microstructure of post weld aged specimen at 124 °C of pulse GMA welded BM-5(1) plate

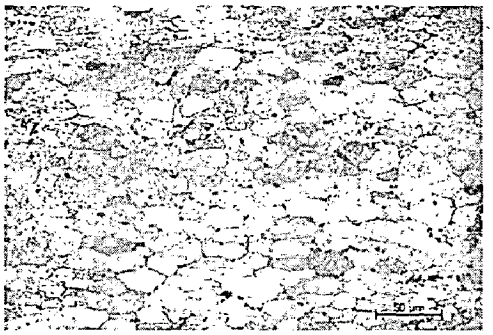

(a) HAZ region

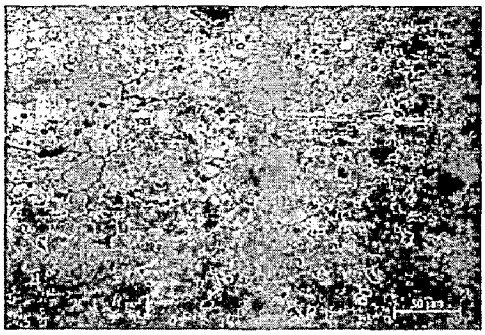

(b) Base metal region

Figure 54: Microstructure of post weld aged specimen at 145 °Cof pulse GMA welded BM-2(2) plate

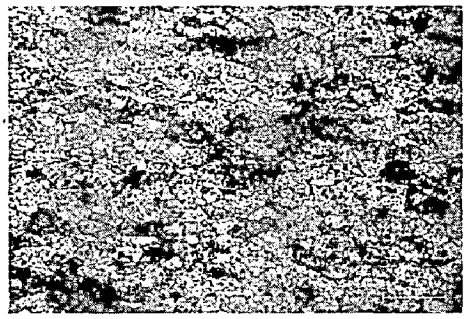

(a) HAZ region

(b) Base metal region

Figure 55: Microstructure of post weld aged specimen at 145 °Cof pulse GMA welded BM-3(2) plate

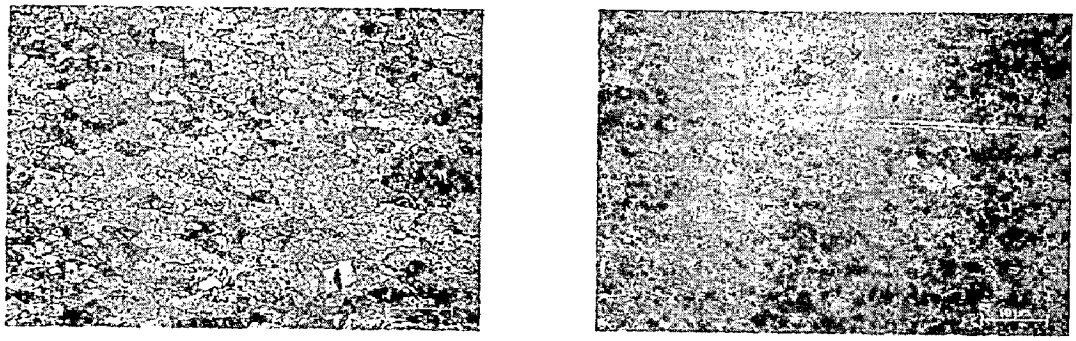

(a) HAZ region (b) Base metal region

Figure 56: Microstructure of post weld aged specimen at 145 °Cof pulse GMA welded BM-4(2) plate

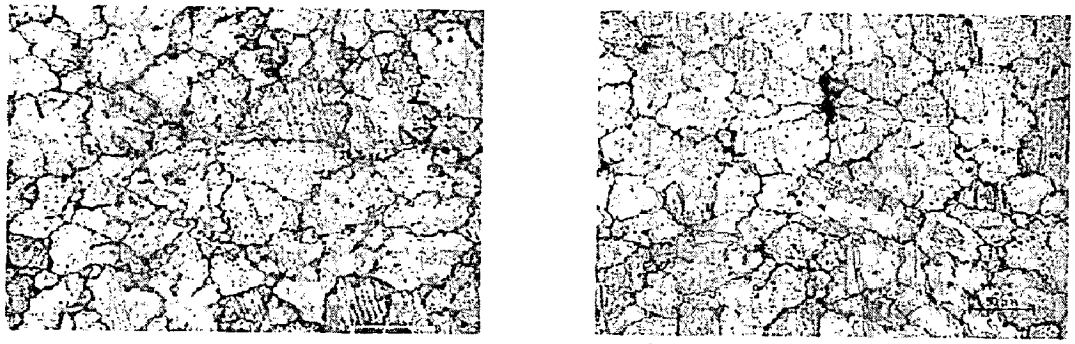

(a) HAZ region (b) Base metal region

Figure 57: Microstructure of post weld aged specimen at 145 oCof pulse GMA welded BM-5(2) plate

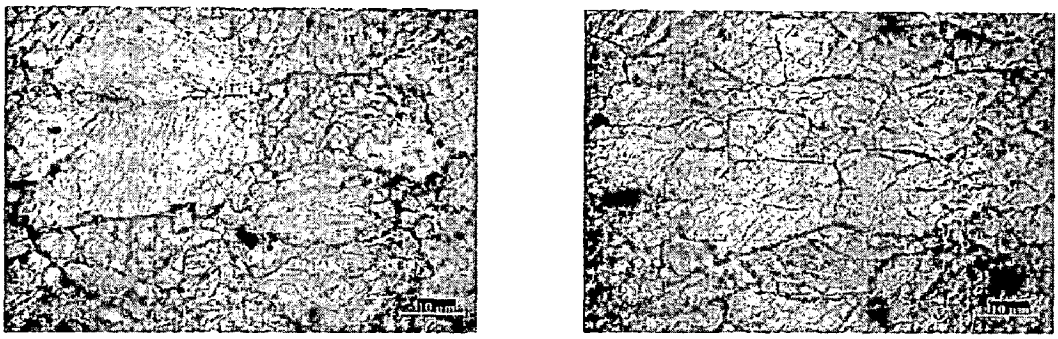

(a) HAZ region (b) Base metal region

Figure 58: Microstructure of post weld aged specimen at 170 oCof pulse GMA welded BM-2(3) plate

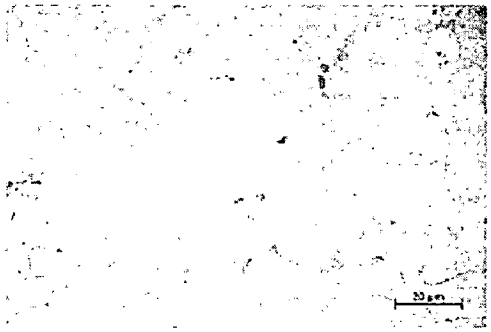

(a) HAZ region

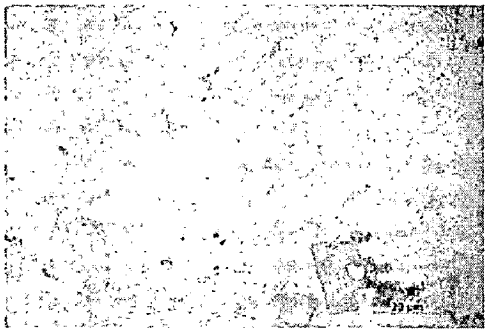

(b) Base metal region

Figure 59: Microstructure of post weld aged specimen at 170 °Cof pulse GMA welded BM-3(3) plate

(a) HAZ region

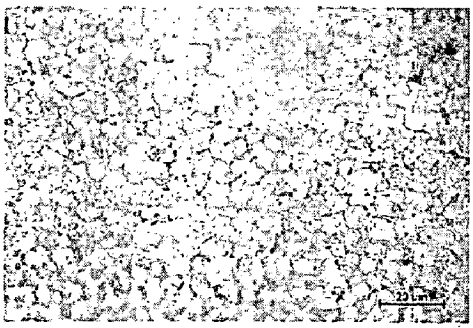

(b) Base metal region

Figure 60: Microstructure of post weld aged specimen at 170 oCof pulse GMA welded BM-4(3) plate

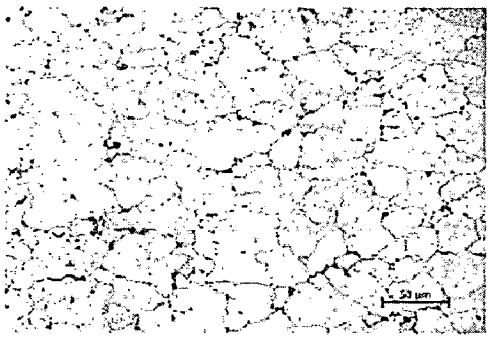

(a) HAZ region

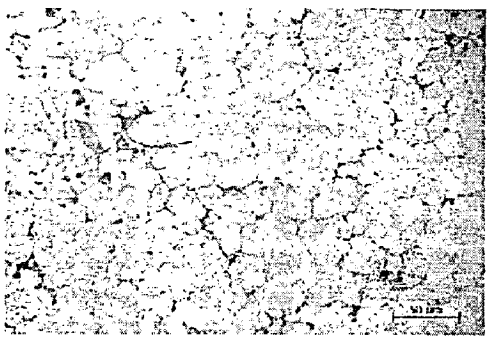

(b) Base metal region

Figure 61: Microstructure of post weld aged specimen at 170 °Cof pulse GMA welded BM-5(3) plate

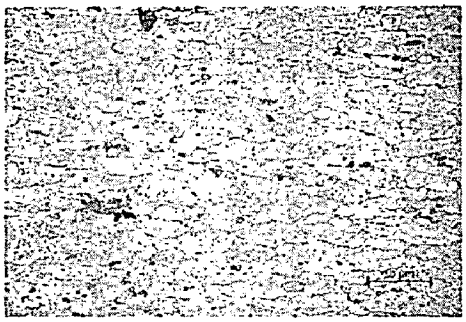

(a) HAZ region

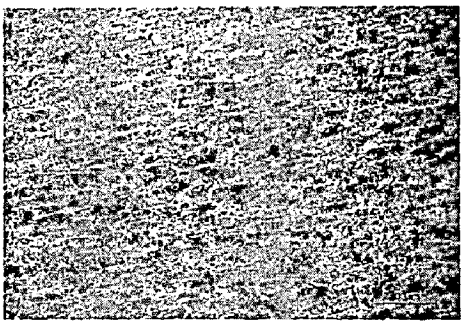

(b) Base metal region

Figure 62: Microstructure of post weld aged specimen at 200 oC of continuous GMA welded BM-2(4) plate

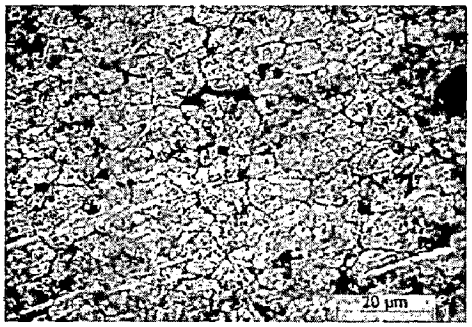

(a) HAZ region

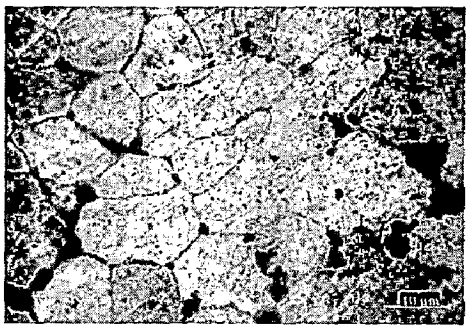

(b) Base metal region

Figure 63: Microstructure of post weld aged specimen at 200 °C of continuous GMA welded BM-3(4) plate

(a) HAZ region

(b) Base metal region

Figure 64: Microstructure of post weld aged specimen at 200 oC of continuous GMA welded BM-4(4) plate

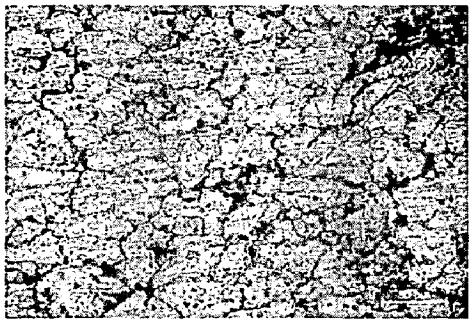

(a) HAZ region

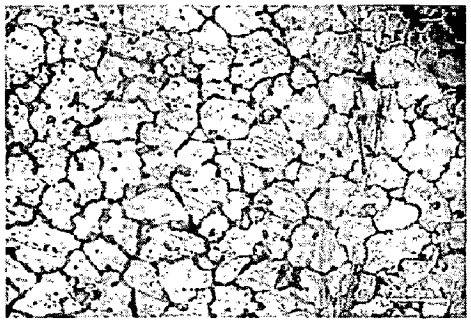

(b) Base metal region

Figure 65: Microstructure of post weld aged specimen at 200 oCof continuous GMA welded BM-5(4) plate

Table 7: Data of amount of filler metal deposited in both continuous and pulse current GMA welds

Sample Designation	Heat Input(kJ/cm)	Filler metal added (gm/cm)
BM-2(1)	7.1919	19.598
BM-2(2)	8.173	24.2731
BM-2(3)	8.939	25.36
BM-2(4)	11.389	32.037
BM-3(1)	10.562	30.783
BM-3(2)	10.273	28.996
BM-3(3)	10.397	29.334
BM-3(4)	18.725	51.029
BM-4(1)	11.372	32.991
BM-4(2)	10.684	31.1161
BM-4(3)	11.559	35.5007
BM-4(4)	10.315	28.1105
BM-5(1)	9.431	27.701
BM-5(2)	10.48	29.1155
BM-5(3)	10.934	32.797
BM-5(4)	10.53	28.696

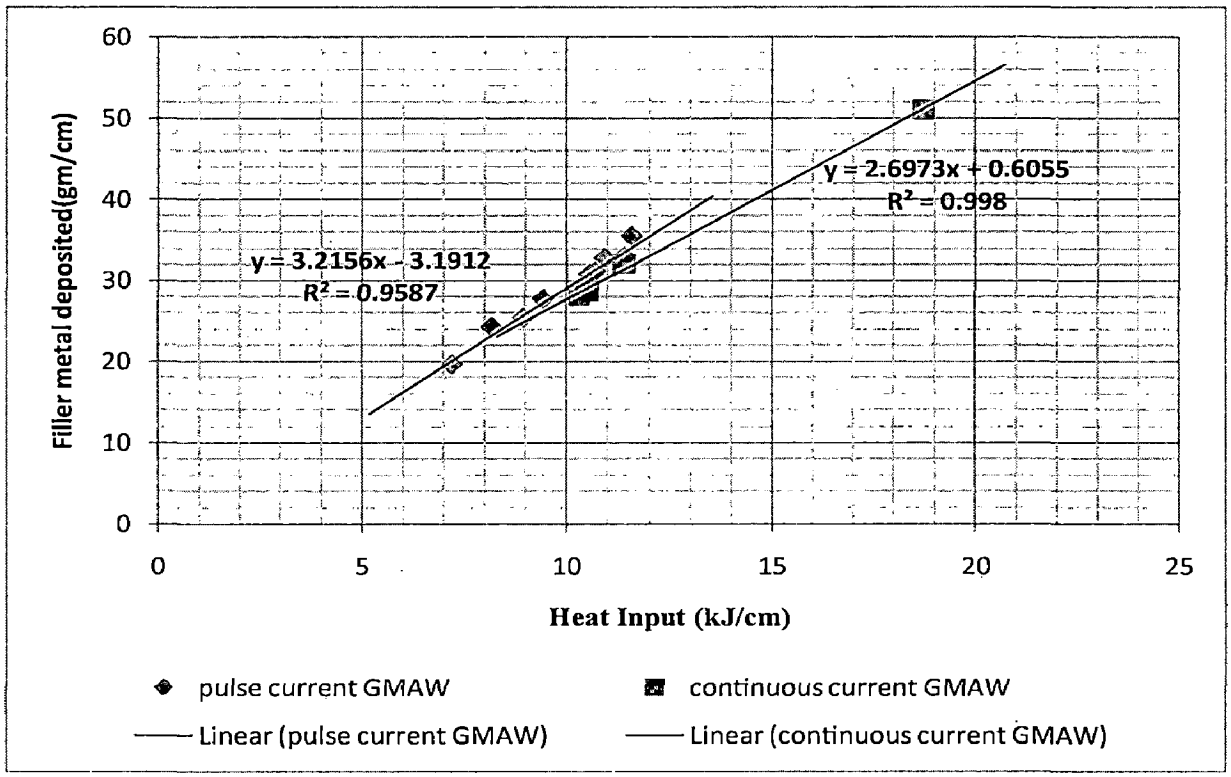

Figure 66: Graph shows the effect of heat input on filler metal deposition

Chapter 6: Conclusion

In the present study, the weldability of the Scandium inoculated Al-Zn-Mg alloy was studied by using the pulse current GMAW welding process and continuous current GMAW process. The effects of heat input and welding parameters on the mechanical and metallurgical properties of the alloy were studied and compared. The following conclusions were drawn based upon the results:

1. The weld zone showed considerable porosity at the bead top and to some extent around the fusion line and least near root. It showed lower hardness compared to the hardness in the HAZ and base material indicating the weld is ductile which is obliviously desirable. But the presence of the porosity in the area like fusion line and bead root makes it vulnerable for early failure.
2. The combined effect of forging and the heat treatments- Annealing, W-tempering and T73, had significant effect on the hardness of the alloy. As the wt% scandium addition increased from 0.11 % to 0.74%, aged hardening characteristics of the alloy showed improvement in the same proportion.
3. Sc has the highest inoculation effect on the aluminum alloys. Significant amount of grain refinement in the weld fusion zone by hampering the coarse columnar grain formation at the fusion line was observed and could only be attributed to this inoculation characteristic of Scandium.
4. The HAZ showed significant improvement in the hardness after the welding process. Normally, in HAZ of Al-Zn-Mg alloys, it takes upto 12 days to reach its peak hardness but the increase in the hardness of the HAZ was observed after 24 hours post welding, indicating that the scandium must have accelerated the natural aging tendency of the Al-Zn-Mg alloy. No grain coarsening of the HAZ was observed which could be attributed to the Sc anti-recrystallization effect. Its a common notion that the HAZ is weak compared to the base material and weld zone but the strengthening of the HAZ observed in above study suggest need for amendments to this notion.
5. Pulse parameters had considerable effects on the weld zone's characteristics like weld bead geometry, microstructure and hardness. Pulse GMAW allows for use of low heat

inputs as compared to continuous current GMAW. HAZ width increased in proportion to the heat input. For the same amount of heat inputs, the filler metal deposition in case of pulse GMAW was more as compared to the continuous current GMAW. The porosity distribution in case of the weld obtained using synergic mode-continuous current GMAW was uniform as compared to that in case of pulse GMAW. The dilution of the weld bead is directly dependent upon the heat input and the filler metal deposition rate which suggests that the dilution due to pulse GMAW is lesser compared to the continuous current GMAW.

6. Post weld aging significantly affected the microstructure of the HAZ and Base material at all the aging temperatures used in the study which showed grain coarsening and loss of hardness along with segregation of the precipitates with higher scandium percentage at the grain boundaries. A nearly equilibrated condition in terms of hardness was observed in few cases where hardness in HAZ and the base material was nearly same. The optimized post weld aging process can be used to stabilize the hardness of the base material and HAZ to an optimum value i.e. decreasing the considerable physical heterogeneity observed in the three regions that is weld zone, HAZ and base material. The severe heterogeneity may increase the stress corrosion of the alloy which is a prominent drawback among the Al-Zn-Mg alloys.

Chapter 7: Suggestions for the future work

1. Study can be carried out pertaining to optimization of the scandium in the Al-Zn-Mg alloys of different grades from the point of view of their weldability under Pulse GMAW and continuous GMAW processes.
2. A detailed study pertaining to the fatigue behavior and impact energy absorption characteristics of the Sc inoculated Al-Zn-Mg alloys of different grades and their characterization could help in understanding its practicality in critical applications especially in aerospace industries.
3. Corrosion study should be done on welded joints of the Scandium inoculated Al-Zn-Mg alloy and compared with the data available on Al-Zn-Mg alloys especially to understand their stress corrosion susceptibility and find a optimum solution for the same.
4. Simulation study related to the failure of the welds joints of Sc inoculated Al-Zn-Mg alloys under different virtual working conditions and comparing its data with the experimental data, can help in predicting the properties of the weld joint under extreme working conditions and thereby reducing the cost of experimentation and weld inspection.

References

1. The Military Uses of Aluminium, ed. G.W. Budd, Alcan Booth, Kitts Green,Birmingham, England, 1973, p.41.
2. Ibid, p.19.
3. Mondolfo, L.F., Metallurgical Reviews, 16, 1971, p.95.
4. Eger, G., Z. Metallkunde, 4, 1913, p.29.
5. Sander, W. and Meissner, K.L., Z. Metalkunde, 15, 1923, p.180, 16, 1926, p.12.
6. Ryii, N., Z. Metallkunde, 66(7), 1975, p. 377.
7. Inque, H. et al., Metallurgical Trans. A., 12A(8), 1981, p. 1 4 2 9
8. Mulhern, J.H. and Rosenthal, H., Metallurgical Trans. 2, 1971, p.427.
9. Thompson, D.S., Metallurgical Trans. A., 6A (4), 1975, p.671.
10. Thompson, D.S., Therm. Anal. Proc. Int. Conf. 2nd, Vol. 2, R.F. Schwenker and P.D. Garn, eds., Academic Press, New York, 1968, published 1969.
11. Metals Handbook Ninth Ed. Vol 4, A.S.M., Metals Park Ohio, p.688
12. Lamikhov L. K., Samsonov G. V., Tsvetn. Met., No. 8, 79 – 82 (1964).
13. Elagin V. I., Metallurgiya, Moscow (1975).
14. Elagin V. I., Zakharov V. V., and Rostova T. D., Physical Metallurgy, Casting, and Treatment of Alloys [in Russian], VILS,Moscow (1995), pp. 6 – 16.
15. Dobatkin V. I., Éskin G. I., Tsvetn. Met., No. 12, 64 – 67 (1991).
16. Drits M. E., Toropova L. S., Bykov Yu. G., et al., Izv. Akad. Nauk SSSR, Metally, No. 1, 179 – 182 (1983).
17. Hyde K. B., Norman A. F., and Prangell P. B., Mater. Sci. Forum, 331 – 337, 1013 – 1018 (2000).
18. Zakharov V. V., Translated from Metallovedenie i Termicheskaya Obrabotka Metallov, No. 7, pp. 7 – 15, July, 2003.
19. Zakharov V. V., Metalloved. Term. Obrab. Met., No. 2, 15 – 20 (1997).
20. Elagin V. I., Zakharov V. V., and Rostova T. D., Metalloved. Term. Obrab. Met., No. 7, 57 – 60 (1983).
21. Davydov V. G., Elagin V. I., Zakharov V. V., Rostova T. D., Metalloved. Term. Obrab. Met., No. 8, 25 – 30 (1996).

22. Elagin V. I., Zakharov V. V.,Rostova T. D., Problems of the Metallurgy of Light and Special Alloys[in Russian], VILS, Moscow (1991), pp. 114 – 129.
23. Drits M. E., Toropova L. S., Bykov Yu. G., et al., Izv. Akad. Nauk SSSR, Metally, No. 1, 173 – 178 (1982).
24. Drits M. E., Toropova L. S., Bykov Yu. G., Izv. Vuzov, Tsvetn. Met., No. 4, 80 – 84 (1985).
25. Chernyshev E. M., Bakanova L. N., Zakharov V. V., Rostova T. D., Tekhnol. Legk. Splavov, No. 2, 21 – 25 (1991).
26. Elagin V. I., Zakharov V. V., Rostova T. D., Tekhnol. Legk. Splavov, No. 2, 17 – 20 (1991).
27. Devletian J.H., Wood W.E., Welding Research Council, Bulletin, 290,1983.
28. D'Annessa A.T., Welding Journal, Vol. 46, 1967, pp. 491s-499s.
29. Talbot D.E.J., Proc. 3rd Int. Solidification Processing Conf., Institute of Metals, 1987, pp 29-31.
30. Field D.J., Treatise Material Science Technology, Vol. 31, 1987, pp 29-31.
31. Howden D.G., Milner D.R., Brit. Weld. J., Vol 10, 1963, p 304
32. Saperstein Z.P., Prescott G.R., Monroe E.W., Weld. J., Vol 43 (No. 10), 1964, p 443-s.
33. Ransley C., Neufeld J., J. Inst. Met., Vol 74, 1948, p 617
34. Uda M., Ohno S., TranS. Natl. Res. Inst. Met. (JPN), Vol 16, 1974, p 2
35. Martukanitz R.P., Alcoa Laboratories, Unpublished Research, 1986
36. Martukaniz R.P., Michnuk P.R., Aluminium, Vol. 58(No. 5), 1982, pp.276-279.
37. Kramer L.S., Heubaum F.H. Pickens J.R., Proceedings of the 5th International Al-Li Conference, Williamsburg, Virginia, March 27-31,1989, pp 1415-1424.
38. Pumphrey W.I., Moore D.C., J. Inst. Met., Vol 74, 1948, P 425.
39. Dawson J.K., MET. PROG., Vol 76 (No.1), 1959, P 116.
40. Meister R.P., Martin D.C., Defense Metals Information Center, Battelle Memorial Institute, 1967, P 51.
41. Kou S., Welding Metallurgy and Weldability of high strength Aluminum alloys, Weld. Res. Counc. Bull., No. 320, Welding research council, 1986.
42. Lytte A., Welding Journal, March 1983, pp.15-23
43. Cornu Jean, Weston John, IFS Publication, Vol. 2,1988, pp. 22-50.

44. Needham J.C., Carter A.W., BMRA Report, British Welding Journal, May 1965, pp. 229-241.
45. Jackson C.E., Shrubsall A.E., Welding Journal, 32,1953, pp. 172s-178s
46. Cornu Jean, Weston John, IFS Publication, Vol. 1,1988, pp. 14-38.
47. Lesnewich A., Welding Journal, Vol. 343, 1958, pp.343s-353s.
48. Gallerma Mike, Prentice Hall Publication, 1999, pp. 3-134
49. Parmar R.S., 2' edition, Khanna publications, 1997, pp. 258-262.
50. Giachino J.W., Weeks.W,5th edition, American Technical society, 1976, pp. 208-210.
51. S Kim I, H Kwon W, Siores E, Canadian Metallurgical quarterly, vol. 35(4), 1996, pp. 385-392
52. Doumanidis G., Hale M., Hart D.E., Proceedings of an International Conference on trends in welding research, Gatlinburg, USA, 18-22, 1986, pp. 449-457.
53. Jeongick Lee, Kiwoan Urn, Optics and Lasers in Engineering, Vol. 34, 2000, pp. 149-158.
54. Essers W.G., Vangompel I.F., Welding Journal, June 1984, pp. 26-32.
55. Amin M., Metal Construction , May 1983, pp 272-278.
56. Demals P., A report on pulsed MIG welding, April 1970.
57. Vagner F.A., Stepanaon V.V., Svar Proiz, 1968, no.5, pp.14-16.
58. Gupta P.C., Ghosh P.K., Jam N.K., Indian Welding Journal, Feb. 1989, p. 550.
59. Gupta P.C., Ghosh P.K., Int. Conf. on Welding Tech., Sep. 26-28, University of Roorkee, Roorkee, 1988, p. 1-71.
60. Ghosh P.K., Gupta S.R., Gupta P.C., and Rathi R., Practical metallography, 1990.
61. Goyal V.K., Ghosh P.K., Saini J.S., Journal of Materials Processing Technology, 209(2009), pp 1318-1336.
62. The Basic Metallurgy of Welding, Brazing, and Soldering, Chapter 9,pp 447-500
63. Goyal V.K., Ghosh P.K., Saini J.S., Metallurgical and Materials Transactions A Vol. 38A, Aug. 2007, pp. 1794-1805.
64. Ghosh P.K., et.al., Journal of Materials Processing Technology, 194 (2007), pp. 163-175.
65. Randhawa H.S., Ghosh P.K., Gupta S.R., ISIJ International, Vol. 40(2000), pp. 71-75.
66. Metals Handbook 10th edition, Vol. 2, Metals park Ohio, pp. 64-70.
67. AWS welding Handbook, 8th edition, vol.2, p.120.

68. AWS welding Handbook, 8th edition, vol.2, p.112.
69. AWS welding Handbook, 8th edition, vol.2, p.116.
70. RATHI R., ME Dissertation, University of Rorrkee, India (1988).
71. Ghosh P.K., Journal of Materials Science, Vol. 26(1991), pp.61614-6170.
72. Ghosh P.K., Gupta S. R., Gupta P.C., Rathi R. Trans. JIM, Vol. 31,1990.
73. Idem, Practical Metallogr., 1990.
74. S. Kou and Y. Le, Weld J (1986), pp. 65–70.
75. T. Mohandoss and G. Madhusudhan Reddy, J. Mater. Sci. Lett., Vol. **15** ,1996, pp. 626–628.
76. D.A. Shelwatker, G. Madhusudhan Reddy and A.A. Gokhale, Sci. Technol. Weld Joining, 2002, pp. 352–361.
77. Ryum, N., Z. Metallkunde, 66(7), 1975, p.377.
78. Royset J., Ryum N., Mater. Rev., Vol. 50, 2005, pp.19-44.
79. Bartle, P.M., ibid, paper 3, p. 24
80. Metals Handbook 9th edition, Vol. 4, Metals park Ohio, p.684
81. Rogerson, J.H., British Welding J., 11(1), 1964, p.12